APPENDIX

APPENDIX A

Details of boundary condition and numerical modeling in
proton exchange membrane fuel cell

Proton Exchange Membrane Fuel Cell Modeling

Generic conditions

In its geometry setup fully follows typical structure of the fuel cell. Geometry contains anode (hydrogen) and cathode (air) flow channels. Each channel is embodied into solid plate that neighbors with a collector plate. Generic fuel cell "sandwich" has collector plates on top and bottom. One plate (anode side) is maintained at ground conditions (zero potential) and another plate (cathode) side is typically maintained at -0.1 or -0.9 Volts depending on specific design. Channel plate/layer follows by porous diffusion layer, which follows by porous catalyst layer. Cathode side layers are called cathode diffusion and cathode catalyst layers correspondingly. Catalyst layer follows by porous membrane. Geometry structure is symmetrical around membrane layer. After membrane we have anode catalyst, anode diffusion and anode channel and anode collecting plates respectively. Each layer consists of several grid nodes in vertical direction and thus is resolved computationally.

In user must supply corresponding properties for each layer. Most critical properties are permeability and porosity, electrical conductivities of fluid and solid phases, tortuosity and surface to volume ratio (for catalyst only). Electro-chemical reaction mechanisms and associated kinetic constants must be specified, and heat conductivity of fluid and solid phases must be assigned.

Physics and Parameters

To study electrochemistry of a fuel cell user is required to Flow, Heat, Chemistry, and Electric module. Membrane conductivity model and electrochemistry surface reactions capability. We set reference pressure for cell operation. This pressure is used to define other pressure boundary conditions, which are gage pressures in such situations. Usually reference pressure is 3 atm (anode channel) and then cathode channel may have inlet pressure (gage) of 2 atm, which means that cathode channel has 5 atm (gage+reference) static pressure at the inlet. Electric field is solved using DC (direct current) conduction option with solid DC conduction option for porous media electrochemistry. We then set volume conditions VC properties for each volume/layer and they consist of "Properties" and "Porous properties" menus. In properties section we set "fluid" related properties, which are: density, viscosity, electrical conductivity, (relative electrical permittivity and permeability are all unit values), Thermal conductivity, specific heat and mass diffusion coefficients. Fuel cell calculations require that we use solid conditions for collector plates, solid conditions (optional) for channel plates, and fluid conditions for membrane, catalyst and diffusion layers. However, for the three layers we use not just fluid conditions, but porous fluid conditions. Porous part is activated in Porous Media properties menu for each specific volume condition (VC). If it is activated, then corresponding porous models for heat, chemistry and flow resistance are being activated in the code to properly tackle corresponding volumes. Porous media conditions offer variety of options, we utilize isotropic linear resistance model

(Darcy) with porosity and permeability, constant heat conductivity for solid phase, constant electrical conductivity for solid phase and porous chemistry is described via surface reactions (yes or no) with surface to volume ratio, tortuosity and average pore size. Chemical reactions are prescribed for catalyst layer only, where typical surface to-volume ratio is between 1000 to 5000. Effective diffusivity model for porous layers follow Bruggman or Dagan models. While for all fluid layers fluid electrical conductivity is set as constant for membrane it is calculated following special membrane model, which takes into account membrane temperature and H_2O (moisture) content. User can use mechanism of user defined subroutines UDS, (UECOND template) to create his own models for membrane electrical conductivity or other fluid volume conditions.

After we complete our volume condition setup we then proceed with boundary conditions BC setup. Key boundary conditions are cathode (O_2) and anode (H_2) inlets and outlets. We set inlet velocities (usually are around 200 to 500 cm^3/min) and inlet pressures. Such settings clearly define corresponding mass flow rates for given cross sectional area. Inlet pressure is used to calculate inlet flow density. For anode inlet pressure is usually zero (With ref. Pressure of 3 atm) and for cathode it is 5 atm (with reference pressure of 2 atm). Outlet conditions can follow default values. Boundary conditions on the sides of the cells usually are symmetric or wall conditions with zero chemical and electrical fluxes (Currents). Temperatures can be isothermal or be calculated as adiabatic or for convection/radiation heat transfer. Most importantly user must set potentials (ground and negative) on the external surfaces of collector plates. Zero potential (ground conditions) are set on anode side and negative potential (often –0.1. –0.9V) is set on cathode collector plate. To obtain polarization curve user must change value of negative potential, then run case for convergence, obtain electric current on collector plate.

Initial conditions and Flow Solvers

It is possible to set (by default) same solvers and initial conditions for all volumes. For fuel cell calculations we suggest for user to specify reasonable initial temperatures flow velocities and pressures separately for each volume or for groups of volumes. This will provide better convergence. User should utilize AMG Algebraic Multi-Grid solver for pressure equation. CGS-Pre Conjugate Gradient with pre-conditioning solver works badly when used for straight or curved channel flow, especially if block-constant inlet conditions are set. AMG solver provides much better convergence in all cases we studied (with or without chemical reactions).

Typical Property values

We here present most typical property values. User can set their problems using these values and adjust them as requiredfor their applications. Membrane Solid sigma 1E-20 1/Om-m, S/V ratio = 0, no surface chemistry, diffusivity = Bruggman model, Tortuosity = 5, average pore size = 1.E-6, heat conductivity solid = 200 W/mK, Porosity 0.28, permeability 1E-18 m^2, linear resistance, fluid electrical conductivity = out of membrane model = f(H2O, T). Membrane model is described in detail by Springer et al, JECS vol 138, p. 2334 (1991). Catalyst Layer – cathode or

anode chemical reaction, Surface to Volume Ratio = 1000 Tortuosity = 1.5, sigma solid = 53, Average pore size = 1.E-6, Heat conductivity solid = 200, Porosity=0.4 and permeability 1E-11, linear resistance Fluid Electrical conductivity = 4.2 Diffusion Layer – same as catalyst layer, but S/V = 0 and no reactions, fluid electrical conductivity =1E-20 Fluid Properties – density is calculated out of ideal gas law, inlet mixtures define mass fractions of chemicals (H_2, O_2, N_2, H_2O) at inlets. Chemicals usually come fully saturated by water (to enhance membrane moist and conductivity). Model requires chemical mass fractions to be defined in mixtures for boundary conditions. Data is available for saturation pressure for various gases. Such pressure defines partial pressure of H_2O in a particular mixture, its molar fraction and correspondingly mass fraction.

For anode (H_2) saturated with H_2O at 3 atm mass fraction of H_2 is around 1.3% and for cathode (O_2) saturated with H_2O at 5 atm water mass fraction it is 25-30%.Fluid viscosity is calculated using mixture kinetic theory, specific heat via JANNAF tables for mixtures and thermal conductivity is calculated for const Prandtl number or out of kinetic theory for a given mixture. Finally transport and diffusion coefficients are calculated using multi-component diffusion using corresponding Lennard-Jones parameters for chemical species.

Initial mixtures and Inlets. Mixtures are based on H_2O saturation properties calculations at 50 ^{o}C. Fuel: H_2O – 0.27%, $H_2 = 0.73$%, Inlet velocity = 0.2 m/s, Area = 1.4E-5 m^2, P = 3atm, T = 323K, Humid air: $H_2O = 0.015$, $N_2 = 0.75$, $O_2 = 0.235$ %, inlet velocity = 0.3 m/s, Area = 1.4E-5 m^2, T = 323 K, P = 5 atm

For inlets at T = 80 ^{o}C (often case for PEM Fuel Cells) Mass fractions are: saturated air: H_2O 0.05921, N_2 0.72158 O_2 0.21921. Saturated fuel: H_2O 0.61856 H_2 0.38144.

Instructions for Simple Proton Exchange Membrane Fuel Cell model.

1: Specify the Problem types.
- Flow
- Heat transfer
- Chemistry
- Electric
- Specify the mixtures
  - Tools
    - Database
      - Chemistry
        - Mixtures
      - New mixture
        - Name
          - Fuel_50C
        - Species Mass fraction/Concentration
          - H2 0.73
          - H2O 0.27
        - Name
          - HumidAir_50C
        - Species Mass fraction/Concentration

 - H2O 0.015
 - N2 0.75
 - O2 0.235
• Name
 - N2
• Species Mass fraction/Concentration
 - N2 1.00

• Specify the surface reaction
 ☐ Tools
 o Database
 ☐ Chemistry
 • Surface Reactions
 ☐ Mechanism name
 • Anode_Reaction
 ☐ Bulk species
 • H (L)
 ☐ Density=1
 ☐ Equation
 • 0.5H2->H (L)
 • J0 = 9.2272E+08
 • Alpha (a) = 0.5
 • Alpha(c) = 0.5,
 • Concentration exponents = 0.5
 • Notes = Ber&Ver at353 K
 ☐ Mechanism name
 • Cathode_Reaction
 ☐ Bulk species = H (L)
 • Density = 1
 ☐ Equation
 • 0.25O2+H (L)->0.5H2O
 • J0 = 1.05E+06
 • Alpha (a) = 1.5
 • Alpha(c) = 1.5,
 • Concentration exponents = 1, 0
 • Notes = Ber&Ver at353 K

2: Specify the Model Options.
 • MO Tab
 ☐ Simulation Properties
 o Title
 ☐ PEM Fuel Cell
 ☐ Shared tab
 o Transient conditions
 ☐ Time dependence
 • Steady

☐ Flow tab
  o Reference Pressure = 300000N/m^2

☐ Heat Tab
 o Default
☐ Chem. tab

 o Chemistry media
  ☐ Gas phase
 o Gas phase
  ☐ Solve for
   • Species mass fractions
  ☐ Reaction source
☐ Elect tab
 o Electric field options
  ☐ DC Conduction
  ☐ Check Solid DC Cond. box

3: Specify the Volume Conditions.
 • VC Tab
  ☐ Group Volume names Anode_Catalyst_Layer (Solid VC).
  ☐ Group Volume names Anode_Channel (Fluid VC)
  ☐ Group Volume names Anode_Collector (Solid VC)
  ☐ Group Volume names Anode_Diffusion_Layer (Fluid VC)
  ☐ Group Volume names Cathode_Catalyst_Layer (Fluid VC)
  ☐ Group Volume names Cathode_Channel (Fluid VC)
  ☐ Group Volume names Cathode_Collector (Solid VC)
  ☐ Group Volume names Cathode_Diffusion_Layer (Fluid VC)
  ☐ Group Volume names Membrane
 • Specify the volume conditions named Anode_catalyst_layer
  ☐ Phys tab
   o Density
    ☐ Ideal Gas Law
  ☐ Fluid tab
   o Viscosity
    ☐ Mix Kinetic Theory
    ☐ Mass Diffusion
    ☐ Schmidt Number 0.7
  ☐ E/M tab
   o Relative Permittivity = 1
   o Relative Permeability = 1
   o Electrical Conductivity = 4.2 1/Ohm-m
  ☐ Electrical Conductivity
   o Isotropic
  ☐ Therm tab
   o Specific heat
    ☐ Mixed JANNAF Method

o Thermal Conductivity
    ☐ Prandtl number Pr = 0.707

Switch Properties selector to Porous Media
    ☐ Flow tab
        o Resistance Model
            ☐ Isotropic Resistance
        o Isotropic Resistance
            ☐ Porous media
                • Linear resistance from the drop down menu
                    − Porosity = 0.4
                    − Permeability = 1E-11 m^2
    ☐ Heat tab
        o Solid thermal conductivity
            ☐ Constant
                • K (solid) = 200 W/m-K
    ☐ Chem. tab
        o Reaction Type
            ☐ Electrochemical
                • Surface Reaction Name
                    − Anode_Reaction
        o Surface to Volume Ratio
            ☐ Constant = 1000 1/m
        o Effective Diffusivity Model
            ☐ Bruggman Model
                • Tortuosity = 1.5
        o Average pore size Value
            ☐ Constant = 1.5E-6 m
    ☐ Electr tab
        o Solid Electrical Conductivity Sigma (solid) = 53 1/Ohm-m
  • Specify the volume conditions named Anode_Channel
    ☐ Phys tab
        o Density
            ☐ Ideal Gas Law
            ☐ Gas Phas->Mass diffusion
                • Schmidt Number = 0.7
    ☐ Fluid tab
        o Viscosity
            ☐ Mix Kinetic Theory
    ☐ E/M tab
        o Relative Permittivity=1
        o Relative Permeability=1
        o Electrical Conductivity =1E-020 1/Ohm-m
        o Electrical Conductivity
            ☐ Isotropic

- Therm tab
  - o Specific heat
    - Mixed JANNAF method
  - o Thermal Conductivity
    - Prandtl number Pr = 0.707
- Chem. tab
  - o Select Multi-component diffusion option
- Electra tab
  - o Not applicable
- Specify the volume conditions named Anode_Collector
  - Phys tab
    - o Density = 2698.9 Kg/m^3
  - E/M tab
    - o Electrical conductivity
    - o Isotropic
    - o Relative Permittivity = 1
    - o Relative Permeability = 1
    - o Electrical Conductivity = 0.00027 1/Ohm-m
  - Therm tab
    - o Specific heat = 900 J/Kg-K
    - o Thermal Conductivity = 210 W/m-K
- Specify the volume conditions named Anode_Diffusion_Layer
  - Phys tab
    - o Density
      - Ideal Gas Law
  - Fluid tab
    - o Gas Phase->Mass diffusion
      - Schmidt Number 0.7
    - o Viscosity
      - Mix Kinetic Theory
  - E/M Tab
    - o Relative Permittivity = 1
    - o Relative Permeability = 1
    - o Electrical conductivity =1E-020 1/Ohm-m
    - o Electrical conductivity
    - o Isotropic
  - Therm tab
    - o Specific heat
      - Mixed JANNAF method
    - o Thermal Conductivity
      - Prandtl number Pr = 0.707

Switch Properties selector to Porous Media

    ☐ Flow tab

        o Resistance Model

            ☐ Isotropic Resistance

        o Isotropic Resistance

            ☐ porous media

                • Linear resistance from the drop down menu

                    − Porosity = 0.4

                    − Permeability = 1E-11 m^2

    ☐ Heat tab

        o Solid Thermal Conductivity

            ☐ Constant

                • K (solid) = 200 W/m-K

    ☐ Chem. tab

        o Reaction Type

            ☐ Neutral

        o Surface Reaction Name = none

        o Surface to Volume Ratio

            ☐ Constant = 0 1/m

        o Effective Diffusivity Model

            ☐ Bruggman Model

                • Tortuosity = 1.5

        o Average pore size Value

            ☐ Constant = 1E-6 m

    ☐ Elec tab

        o Solid Electrical Conductivity Sigma (solid)=53

  • Specify the volume conditions named Membrane

    ☐ Phys tab

        o Density

            ☐ Ideal Gas Law

    ☐ Fluid tab

        o Gas Phase ->Mass diffusion

            ☐ Schmidt Number = 0.7

        o Viscosity

            ☐ Mix Kinetic Theory

    ☐ E/M tab

        o Electrical Conductivity

            ☐ Isotropic

        o Relative Permittivity = 1

        o Relative Permeability = 1

        o Electrical conductivity

            ☐ Membrane Model (Fuel cell)

    ☐ Therm tab

        o Specific heat

            ☐ Mixed JANNAF method

o Thermal Conductivity
    □ Prandtl number Pr = 0.707)

Switch Properties selector to Porous Media
    □ Flow tab
        o Resistance Model
            □ Isotropic Resistance
        o Isotropic Resistance
            □ Porous media
                • Linear resistance from the drop down menu
                    − Porosity = 0.28
                    − Permeability = 1E-18 m^2
    □ Heat tab
        o Solid Thermal Conductivity
            □ Constant
                • K (solid) = 200 W/m-K
    □ Chem. tab
        o Reaction Type
            □ Neutral
        o Surface Reaction Name
            □ None
        o Surface to Volume Ratio
            □ Constant = 0 1/m
        o Effective Diffusivity Model
            □ Bruggman Model
                • Tortuosity = 5
        o Average pore size Value
            □ Constant = 1E-06 m
    □ Elec tab
        o Solid Electrical Conductivity Sigma (solid) = 1E-20 1/Ohm-m
  • Specify the volume conditions named Cathode_Catalyst_Layer
    □ Phys tab
        o Density
            □ Ideal Gas Law
    □ Fluid tab
        o Gas Phase->Mass diffusion
            □ Schmidt Number = 0.7
        o Viscosity
            □ Mix Kinetic Theory
    □ E/M tab
        o Electrical Conductivity
            □ Isotropic
        o Relative Permittivity = 1

o Relative Permeability = 1
o Electrical conductivity = 4.2 1/Ohm-m
☐ Heat tab
o Specific heat
☐ Mixed JANNAF method
o Thermal Conductivity
☐ Prandtl number Pr = 0.707

Switch Properties selector to Porous Media
☐ Flow tab
o Resistance Model
☐ Isotropic Resistance
o Isotropic Resistance
☐ Porous media
• Linear resistance from the drop down menu
− Porosity = 0.4
− Permeability = 1E-11 m^2

☐ Heat tab
o Solid Thermal Conductivity
☐ Constant
• K (solid) = 200 W/m-K
☐ Chem. tab
o Reaction Type
☐ Electrochemical
o Surface Reaction Name
☐ Cathode_Reaction
o Surface to Volume Ratio
☐ Constant = 1000 1/m
o Effective Diffusivity Model
☐ Bruggman Model
• Tortuosity = 1.5
o Average pore size Value
☐ Constant = 1.5E-6 m
☐ Elec tab
o Solid Electrical Conductivity Sigma (solid) = 53 1/Ohm-m
• Specify the volume conditions named Cathode_Channel
☐ Phys tab
o Density
☐ Ideal Gas Law
☐ Fluid tab
o Gas Phase ->Mass diffusion
☐ Schmidt Number = 0.7
o Viscosity

             ☐ Mix Kinetic Theory
       ☐ E/M tab
          o Electrical conductivity
             ☐ Isotropic
          o Relative Permittivity = 1
          o Relative Permeability = 1
          o Electrical conductivity =1E-020 1/Ohm-m
       ☐ Therm tab
          o Specific heat
             ☐ Mixed JANNAF method
          o Thermal Conductivity
             ☐ Prandtl number Pr = 0.707

• Specify the volume conditions named Cathode_Collector
       ☐ Phys tab
          o Density = 2698.9 Kg/m^3
       ☐ E/M tab
          o Electrical conductivity
             ☐ Isotropic
          o Relative Permittivity =1
          o Relative Permeability =1
          o Electrical conductivity = 0.00027 1/Ohm-m
       ☐ Therm tab
          o Specific heat = 900 J/Kg-K
          o Thermal Conductivity = 210 W/m-K

• Specify the volume conditions named Cathode_Diffusion_Layer
       ☐ Phys tab
          o Density = Ideal Gas Law
       ☐ Fluid tab
          o Gas Phase->Mass diffusion
             ☐ Schmidt Number 0.7
          o Viscosity = Kinetic Theory
       ☐ E/M tab
          o Electrical Conductivity
             ☐ Isotropic
          o Relative Permittivity = 1
          o Relative Permeability = 1
          o Electrical conductivity =1E-020 1/Ohm-m
       ☐ Heat tab
          o Specific Heat
             ☐ Mixed JANNAF method
          o Thermal Conductivity
             ☐ Prandtl number Pr = 0.707
       ☐ Chem. tab
          o Select Multi-component diffusion option

Electr tab
  o Not applicable

Switch Properties selector to Porous Media
  Flow tab
   o Resistance Model
    Isotropic Resistance
   o Isotropic Resistance
    Porous media
     • Linear resistance from the drop down menu
      − Porosity = 0.4
      − Permeability = 1E-11 m^2
  Heat tab
   o Solid Thermal Conductivity
    Constant
     • K (solid) = 200 W/m-K

  Chem. tab
   o Reaction Type
    Neutral
   o Surface Reaction Name = none
   o Surface to Volume Ratio
    Constant = 0 1/m
   o Effective Diffusivity Model
    Bruggman Model
     • Tortuosity=1.5
   o Average Pore Size Value
    Constant = 1E-6 m
  Elec tab
   o Solid Electrical Conductivity Sigma (solid) = 53 1/Ohm-m

4: Specify the Boundary Conditions.
 • Cathode_Channel_Inlet
  Boundary conditions for inlet
  Flow tab
   o Sub Type
    Fixed Velocity Cartesian
   o U = 0 m/s
   o V = 0.3 m/s
   o W = 0 m/s
   o Pressure = 200000 N/m^2
   o Temperature T = 323 K
  Chem. tab
   o Mixture Specification
    Species Mass Fraction

• Constant
o Mixture name
  ☐ HumidAir_50C
☐ Electr tab
  o Check Electric Potential box
    ☐ Fixed Current
      • J = 0 A/m^2
  o Porous Media Electrochemistry
    ☐ Check Electric Potential box
      • Fixed Current
        − Current density
        − Constant = 0 A/m^2
• Boundary conditions for outlet (Cathode_Channel_Outlet)
  ☐ Flow tab
    o Subtype
      ☐ Fixed Pressure
    o Pressure = 200000 N/m^2
    o Temperature T = 323 K
  ☐ Chem. tab
    o Backflow Mixture Specification
      ☐ Species mass fraction
      ☐ Constant
    o Mixture name
      ☐ HumidAir_50C
  ☐ Electr tab
    o Check Electric Potential box
      ☐ Fixed Current
        • J = 0 A/m^2
    o Porous Media Electrochemistry
      ☐ Check Electric Potential box
        • Fixed Current
          − Current density
          − Constant = 0 A/m^2

5:Specify the Boundary Conditions.
• Anode_Channel_Inlet
• Boundary conditions for inlet
  ☐ Flow tab
    o Sub Type
      ☐ Fixed Velocity Cartesian
    o U = 0 m/s
    o V = 0.2 m/s
    o W = 0 m/s
    o Pressure = 0 N/m^2

o Temperature T = 323 K

☐ Chem. tab

o Mixture Specification

☐ Species Mass Fraction

• Constant

o Mixture Name

☐ Fuel_50C

☐ Electr tab

o Check Electric Potential box

☐ Fixed Current

• J = 0 A/m^2

o Porous Media Electrochemistry

☐ Check Electric Potential box

• Fixed Current

− Current density

− Constant = 0 A/m^2

Boundary conditions for outlet (Anode_Channel_Outlet)

☐ Flow tab

o Subtype

☐ Fixed Pressure

o Pressure = 0 N/m^2

o Temperature T = 323 K

☐ Chem. tab

o Backflow Mixture Specification

☐ Species mass fraction

• Constant

o Mixture name

☐ Fuel_50C

☐ Electr tab

o Check Electric Potential box

☐ Fixed Current

o J = 0 A/m^2

o Porous Media Electrochemistry

☐ Check Electric Potential box

• Fixed Current

− Current density

− Constant = 0 A/m^2

• Collector Plate Boundary Conditions − Anode_Collector_Top [Zero potential/Ground]

Select all walls on top of the cell (anode side, Z=Zmax) and group them. Specify following conditions for the group:

☐ Flow tab

      o All velocity components in x, y, z directions = 0 m/s
     ☐ Heat tab
      o Isothermal
       ☐ T=323 K
      o Wall Heat Source
       ☐ None (leave unmarked)
     ☐ Chem. tab
      o Zero flux = 0
     ☐ Electr tab
      o Check Electric Potential box
       ☐ Fixed Current
        • $J = 0$ A/m^2
      o Porous Media Electrochemistry
       ☐ Check Electric Potential box
        • Fixed Current
         − Current density
         − Constant = 0 A/m^2
 • Collector Plate Boundary Conditions −Cathode [Negative Potential]
  [Cathode_Collector _Bottom]

Select all walls on the bottom of the cell (Z = 0, Cathode side)
    ☐ Flow tab
     o All velocity components in x, y, z directions = 0 m/s
    ☐ Heat tab
     o Isothermal
      ☐ T = 323 K
     o Wall Heat Source
      ☐ None (leave unmarked)
    ☐ Chem. tab
     o Zero flux = 0
    ☐ Electr tab
     o Check Electric Potential box
      ☐ Fixed Current
       • $J = 0$ A/m^2
     o Porous Media Electrochemistry
      ☐ Check Electric Potential box
       • Fixed Current
        − Current density
        − Constant = 0 A/m^2
 • Side Wall Boundary Conditions

Select and group all the sidewalls on the inlet side and specify following conditions for
the entire group:
    ☐ Flow tab

    o All velocity components in x, y, z directions = 0 m/s
   ☐ Heat tab
    o Isothermal
     ☐ T = 323 K
    o Wall Heat Source
     ☐ None (leave unmarked)
   ☐ Chem. tab
    o Zero flux = 0
   ☐ Electr tab
    o Check Electric Potential box
     ☐ Fixed Current
      • $J = 0$ A/m^2
    o Porous Media Electrochemistry
     ☐ Check Electric Potential box
      • Fixed Current
       − Current Density
       − Constant = 0 A/m^2
• Then select all walls on the opposite side (outlet side), group them and specify same
 conditions again or group walls on both sides and specify same conditions as above.
• Symmetry Boundary conditions – select and group all BC's named 'Sym' on the
 sides that do not have inlets or outlets (i.e. sides perpendicular to Side Walls
 Boundary Conditions that we just set). Specify SYMMETRY boundary conditions
 for all BC's in this group.

6: Specify the initial conditions.
 • IC Tab
  ☐ IC Sources
   o Constant
 • Cathode_Collector (group all)
  ☐ Flow tab
   o Velocities
    ☐ U = 0 m/s
    ☐ V = 0 m/s
    ☐ W = 0 m/s
    ☐ Pressure = 0 N/m^2
  ☐ Heat tab
   o T = 323 K
  ☐ Chem. tab
   o Species mass fractions
    ☐ Constant
   o Mixture name
    ☐ N2

    □ Elec tab
     o Electric Potential
      □ Voltage = 0 V
     o Solid Electric Potential
      □ Voltage = 0 V
• Cathode_Channel (group all)
  □ Flow tab
   o Velocities
    □ U = 0.0001 m/s
    □ V = 0.0001 m/s
    □ W = 0.0001 m/s
    □ Pressure = 200000 N/m^2
  □ Heat tab
   o T = 323 K
  □ Chem. tab
   o Species mass fractions
    □ Constant
   o Mixture name
    □ Humidair_50
  □ Elec tab
   o Electric Potential
    □ Voltage = 0 V
   o Solid Electric Potential
    □ Voltage = 0 V
• Cathode_Diffusion_Layer (group all)
  □ Flow tab
   o Velocities
    □ U = 0.0001 m/s
    □ V = 0.0001 m/s
    □ W = 0.0001 m/s
    □ Pressure = 200000 N/m^2
  □ Heat tab
   o T = 323 K
  □ Chem. tab
   o Species mass fractions
    □ Constant
   o Mixture name
    □ N2
  □ Elec tab
   o Electric Potential
    □ Voltage = 0 V
   o Solid Electric Potential
    □ Voltage = 0 V

- Cathode_Catalyst_Layer (group all)
    - Flow tab
        - o Velocities
            - U = 0.0001 m/s
            - V = 0.0001 m/s
            - W = 0.0001 m/s
            - Pressure = 200000 N/m^2
    - Heat tab
        - o T = 323 K
    - Chem. tab
        - o Species mass fractions
            - Constant
        - o Mixture name
            - Humidair_50C
    - Elec tab
        - o Electric Potential
            - Voltage = 0 V
        - o Solid Electric Potential
            - Voltage = 0 V
- Membrane (group all)
    - Flow tab
        - o Velocities
            - U = 0 m/s
            - V = 0 m/s
            - W = 0 m/s
            - Pressure = 0 N/m^2
    - Heat tab
        - o T = 323 K
    - Chem. tab
        - o Species mass fractions
            - Constant
        - o Mixture name
            - N2
    - Elec tab
        - o Electric Potential
            - Voltage = 0 V
        - o Solid Electric Potential
            - Voltage = 0 V
- Anode_Catalyst_Layer (group all)
    - Flow tab
        - o Velocities

  - ☐ U = 0.0001 m/s
  - ☐ V = 0.0001 m/s
  - ☐ W = 0.0001 m/s
  - ☐ Pressure = 0 N/m^2
- ☐ Heat tab
  - o T = 323 K
- ☐ Chem tab
  - o Species mass fractions
    - ☐ Constant
  - o Mixture name
    - ☐ N2
- ☐ Elec tab
  - o Electric Potential
    - ☐ Voltage = 0 V
  - o Solid Electric Potential
    - ☐ Voltage = 0 V
- Anode diffusion (group all)
  - ☐ Flow tab
    - o Velocities
      - ☐ U = 0.0001 m/s
      - ☐ V = 0.0001 m/s
      - ☐ W = 0.0001 m/s
      - ☐ Pressure = 0 N/m^2
  - ☐ Heat tab
    - o T = 323 K
  - ☐ Chem. tab
    - o Species mass fractions
      - ☐ Constant
    - o Mixture name
      - ☐ N2
  - ☐ Elec tab
    - o Electric Potential
      - ☐ Voltage = 0 V
    - o Solid Electric Potential
      - ☐ Voltage = 0 V
- Anode_Channel (group all)
  - ☐ Flow tab
    - o Velocities
      - ☐ U = 0.0001 m/s
      - ☐ V = 0.0001 m/s
      - ☐ W = 0.0001 m/s
      - ☐ Pressure = 0 N/m^2

☐ Heat tab
   o T = 323 K
☐ Chem. tab
   o Species mass fractions
      ☐ Constant
   o Mixture name
      ☐ Fuel_50C
☐ Elec tab
   o Electric Potential
      ☐ Voltage = 0 V
   o Solid Electric Potential
      ☐ Voltage = 0 V

• Anode_Collector (group all)
☐ Flow tab
   o Velocities
      ☐ U = 0 m/s
      ☐ V = 0 m/s
      ☐ W = 0 m/s
      ☐ Pressure = 0 N/m^2
☐ Heat tab
   o T = 323 K
☐ Chem. tab
   o Species mass fractions
      ☐ Constant
   o Mixture name
      ☐ N2
☐ Elec tab
   o Electric Potential
      ☐ Voltage = 0 V
   o Solid Electric Potential
      ☐ Voltage = 0 V

7: Specify the Solver control settings.
   • SC Tab
     ☐ Iter. Tab.
       o Max. Iterations = 1000
       o Convergence = 0.0001
       o Min residual = 1E-018
     ☐ Spatial tab
       o Velocity
          ☐ Upwind

- o Density
  - ☐ Upwind
- o Enthalpy
  - ☐ Upwind
- o Species
  - ☐ Upwind
- ☐ Solver tab
  - o Velocity
    - ☐ CGS+Pre
      - • 50, 0.0001
  - o P correction
    - ☐ AMG
      - • 50, 0.1
  - o Enthalpy
    - ☐ CGS+Pre
      - • 500, 0.01
  - o Species
    - ☐ CGS+Pre
      - • 50, 0.0001
  - o Electric potential
    - ☐ CGS+Pre
      - • 500, 0.0001
- ☐ Relax tab
  - o Inertial relaxation
    - ☐ Velocities = 0.2
    - ☐ P correction = 0.2
    - ☐ Enthalpy = 0.001
    - ☐ Species = 0.001
    - ☐ Electric Potential = 0.001
  - o Spatial Relaxation.
    - ☐ Pressure = 0.2
    - ☐ Density = 0.2
    - ☐ Viscosity = 0.2
    - ☐ Temperature = 0.2
- ☐ Limits tab
  - o Temperature = 200, 1000 K
  - o Species = 0, 1
- ☐ Adv tab
  - o Viscous dissipation

8:Specify the Output settings.
- OUT Tab
  - ☐ Output tab
    - o Steady state results
      - ☐ Output results
        - Specified intervals
          - − Iteration frequency = 25
  - ☐ Print tab
    - o Mass flow summary
    - o Species summary
    - o Current summary
  - ☐ Graphic summary.
    - o Density
    - o Static Temperature
    - o Electrical conductivity
    - o Velocity vector
    - o Static pressure
    - o Species mass fraction
    - o Electric potential
    - o Conduction current density.

9:Run the Simulation.
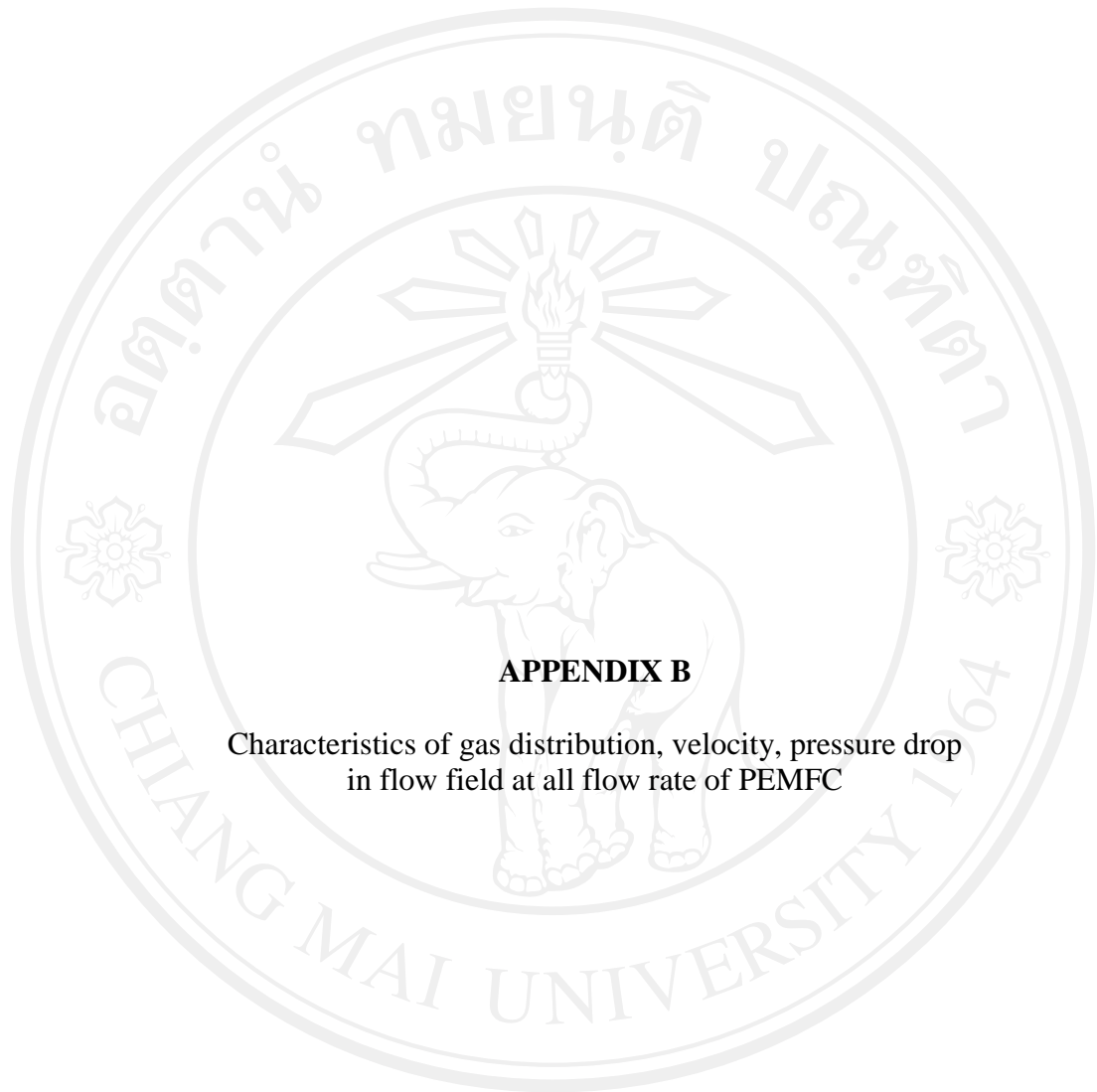
APPENDIX B

Characteristics of gas distribution, velocity, pressure drop
in flow field at all flow rate of PEMFC
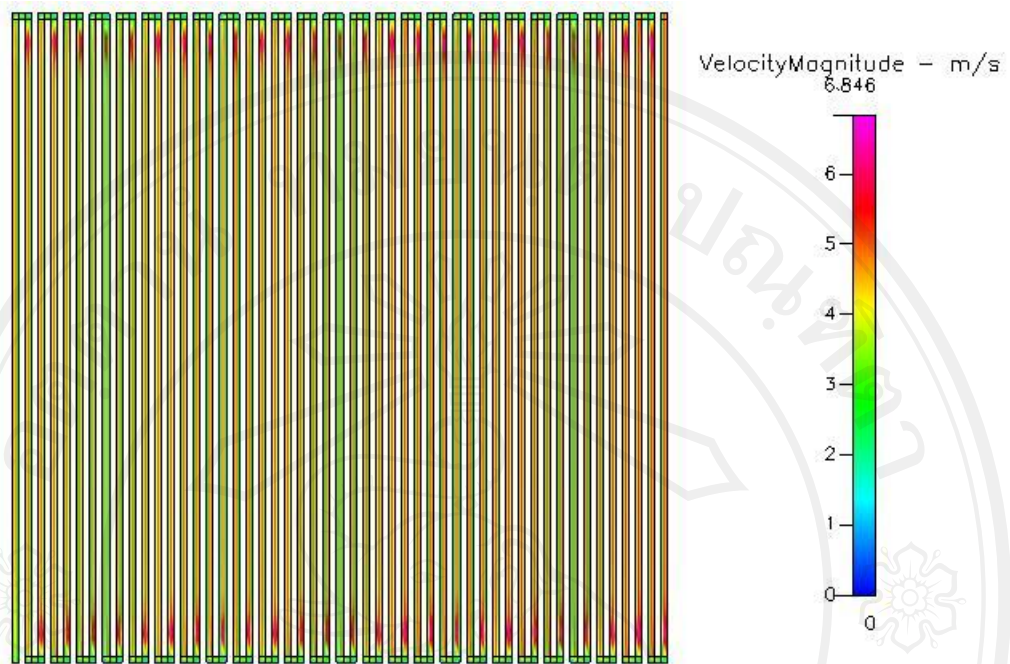
- **In non-fillet curve**

Figure B.1 Velocity distribution at 200 cm^3/min of non-fillet curve
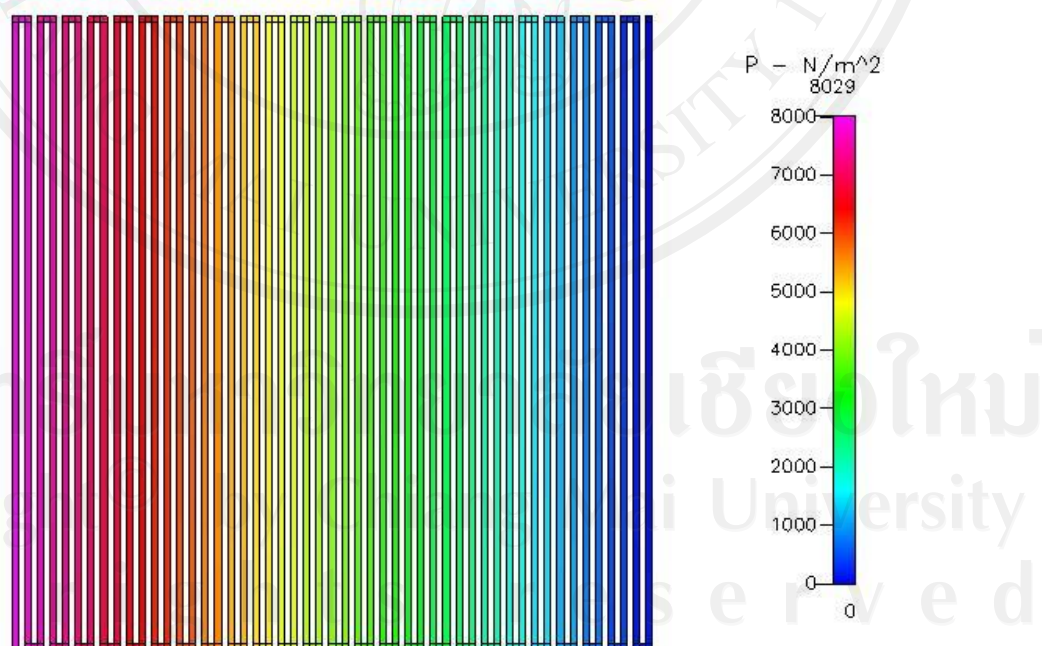
Figure B.2 Pressure distribution at 200 cm^3/min of non-fillet curve

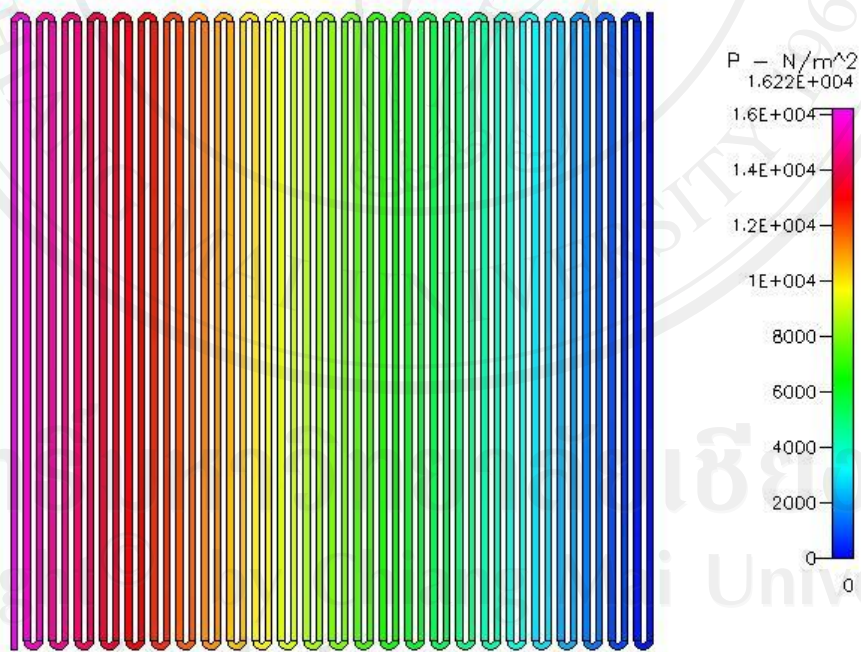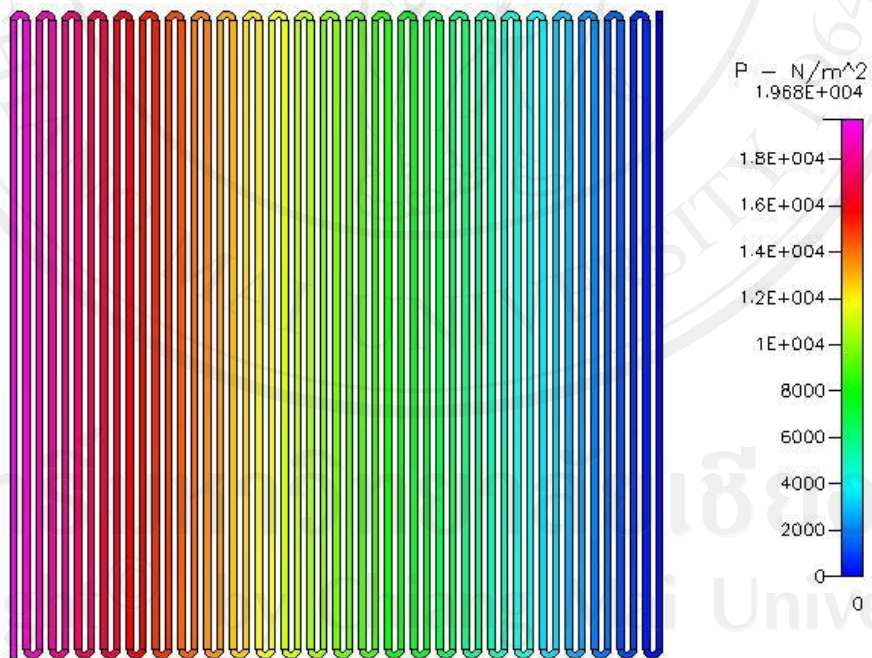Figure B.3 Velocity distribution at 400 cm^3/min of non-fillet curve
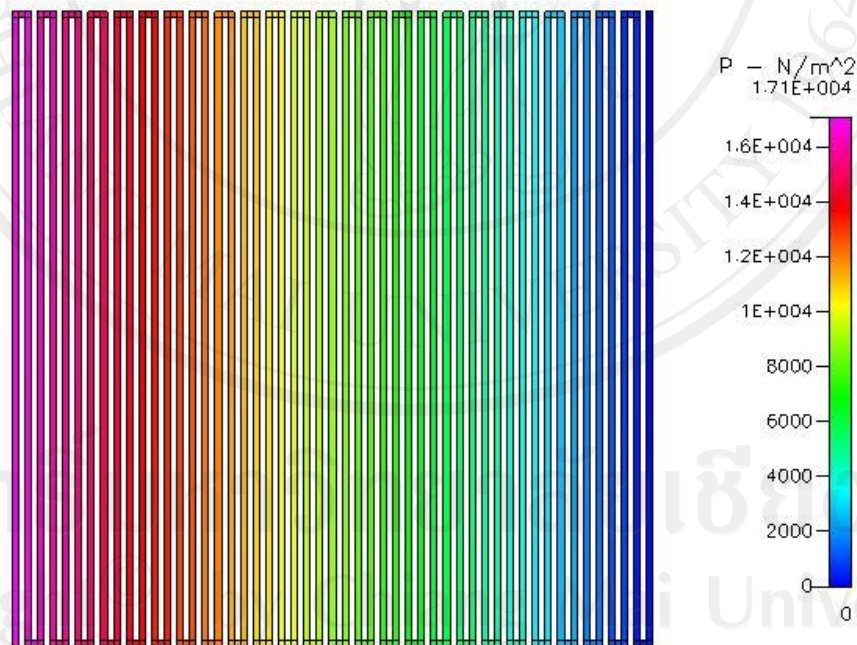
Figure B.4 Pressure distribution at 400 cm^3/min of non-fillet curve
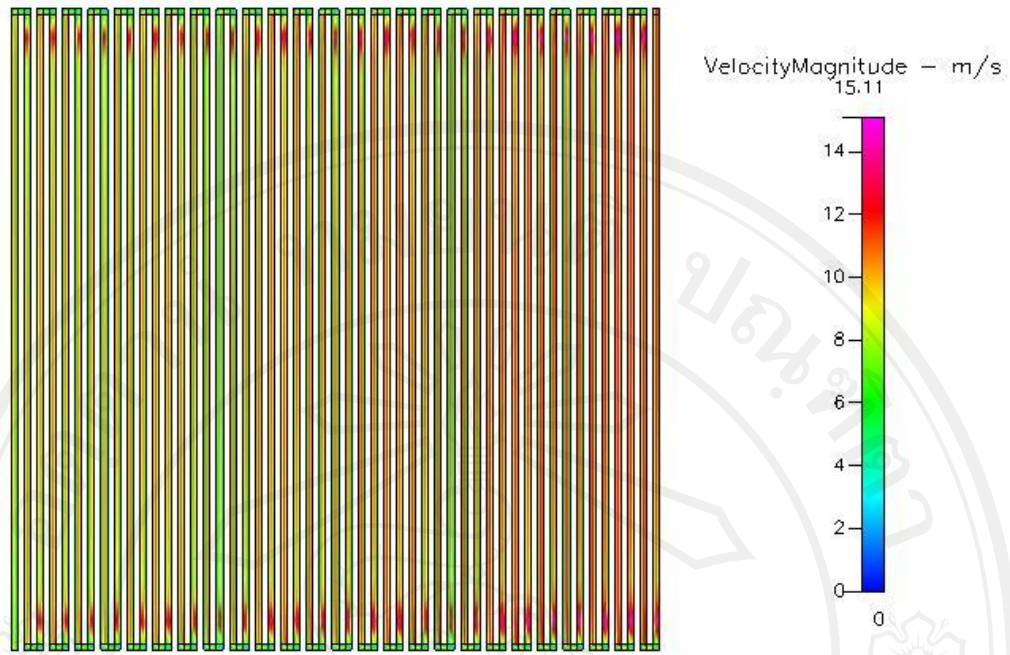
Figure B.5 Velocity distribution at 500 cm^3/min of non-fillet curve
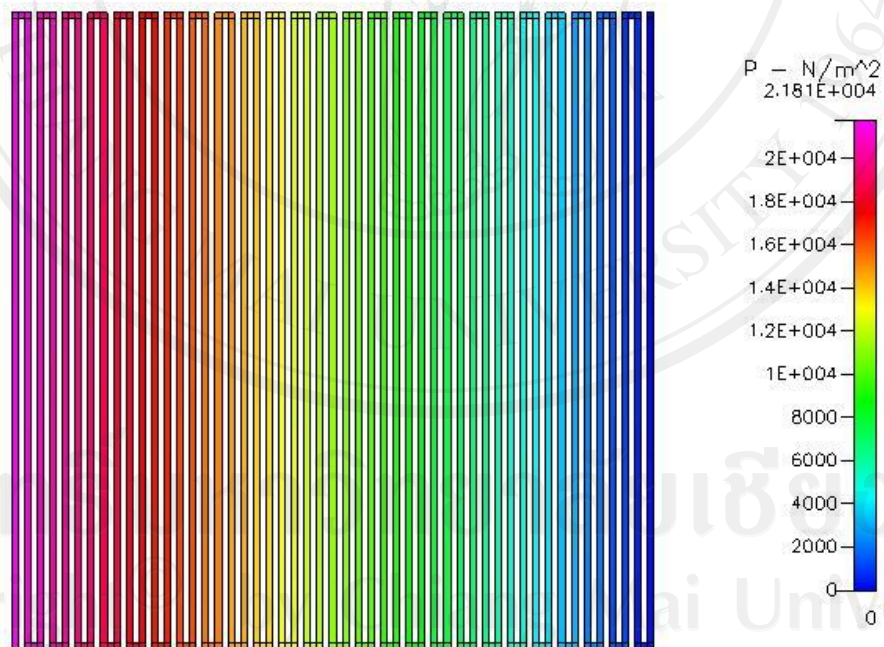
Figure B.6 Pressure distribution at 500 cm^3/min of non-fillet curve

- **In inside fillet curve**
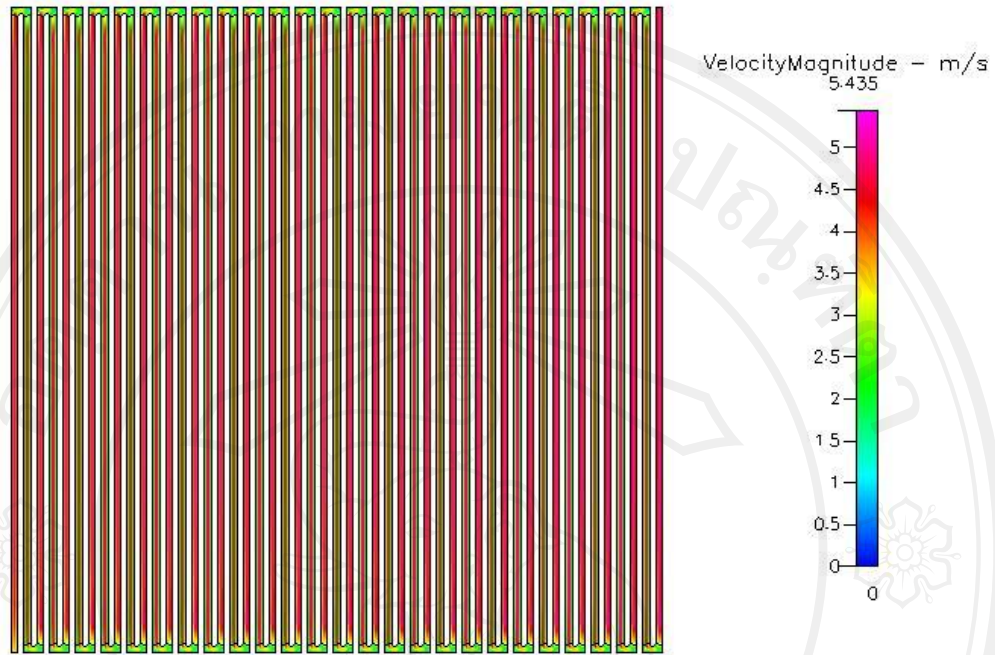
Figure B.7 Velocity distribution at 200 cm^3/min of inside fillet curve
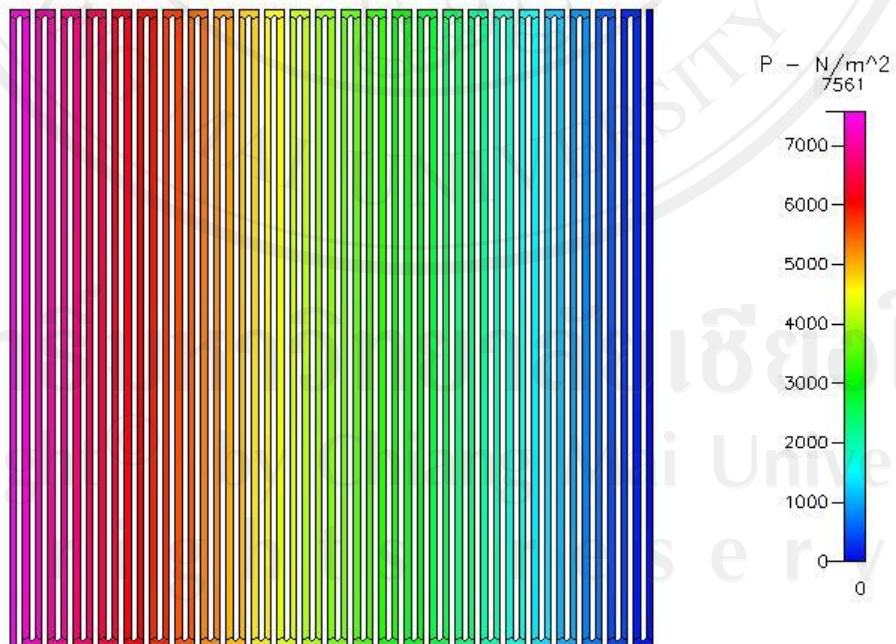
Figure B.8 Pressure distribution at 200 cm^3/min of inside fillet curve
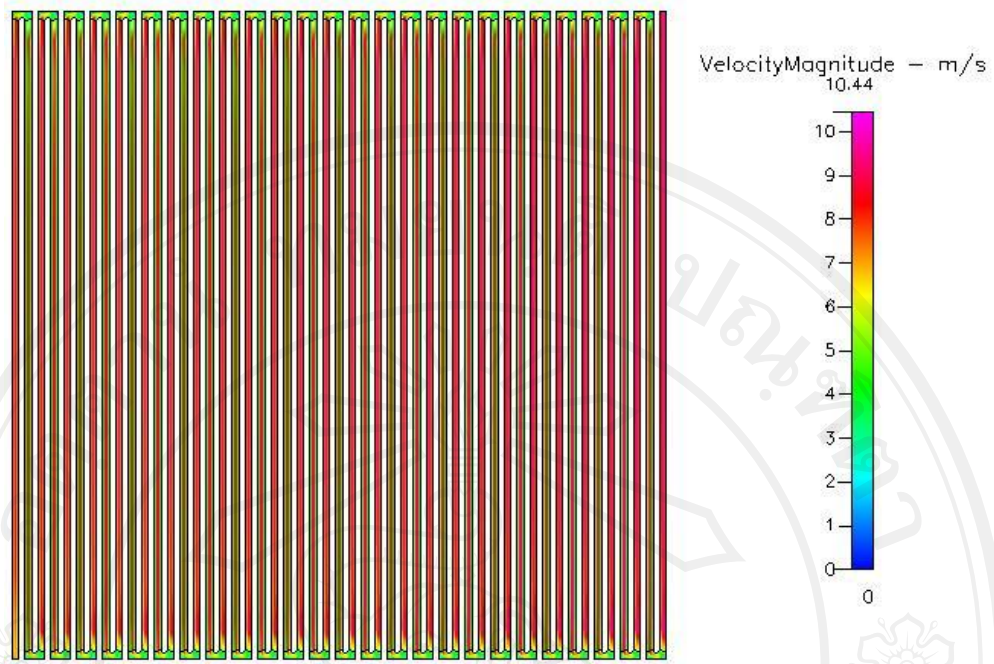
Figure B.9 Velocity distribution at 400 cm^3/min of inside fillet curve
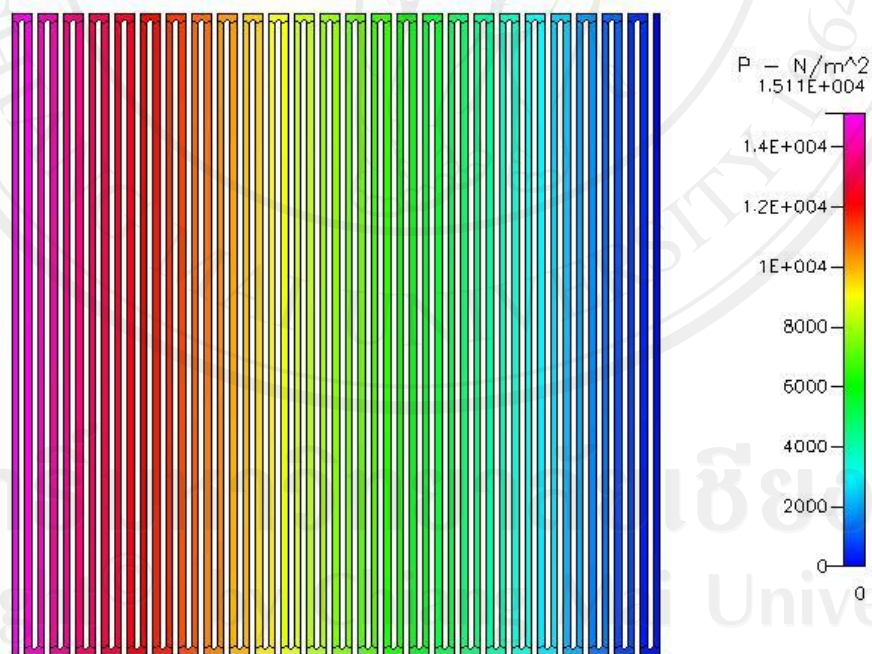
Figure B.10 Pressure distribution at 400 cm^3/min of inside fillet curve

188
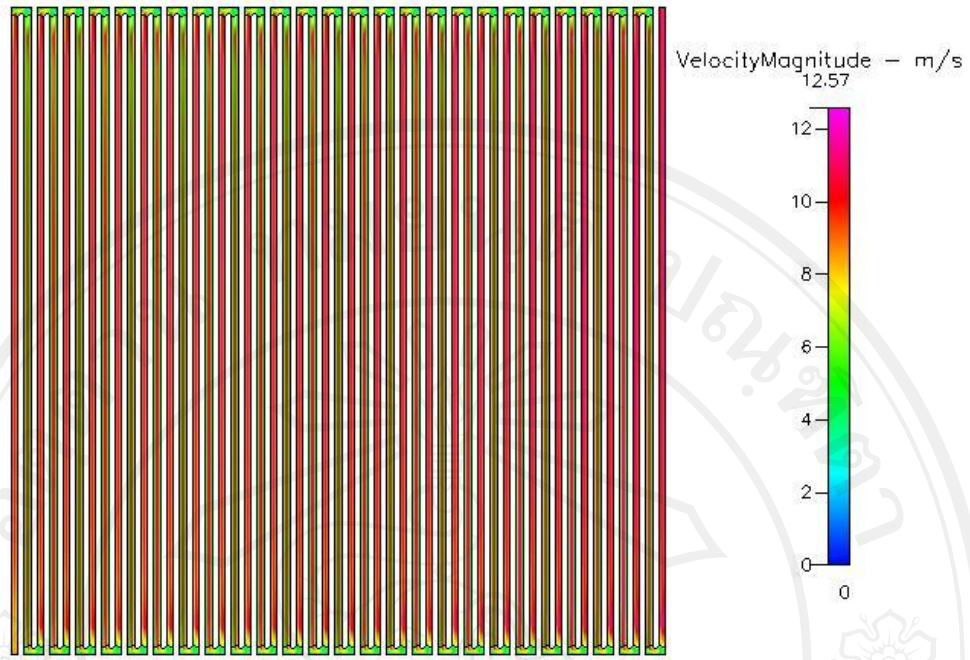
Figure B.11 Velocity distribution at 500 cm^3/min of inside fillet curve
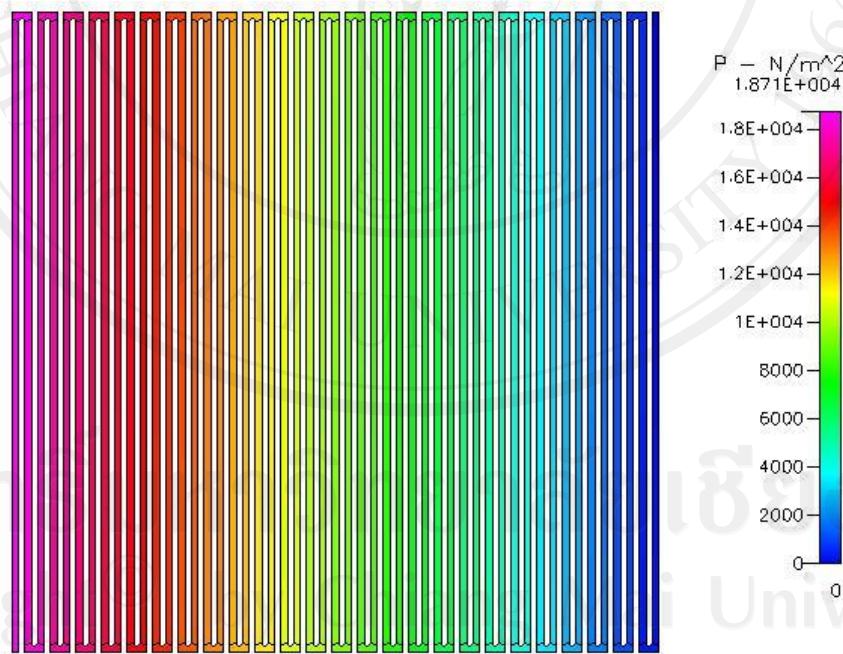
Figure B.12 Pressure distribution at 500 cm^3/min of inside fillet curve

- **In outside fillet curve**
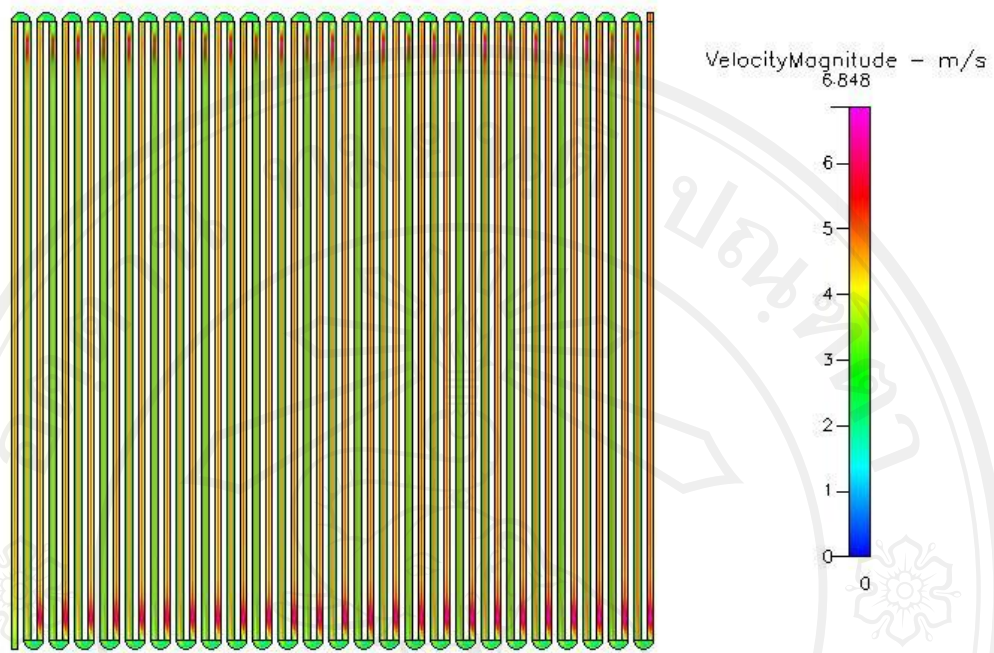
Figure B.13 Velocity distribution at 200 cm^3/min of outside fillet curve
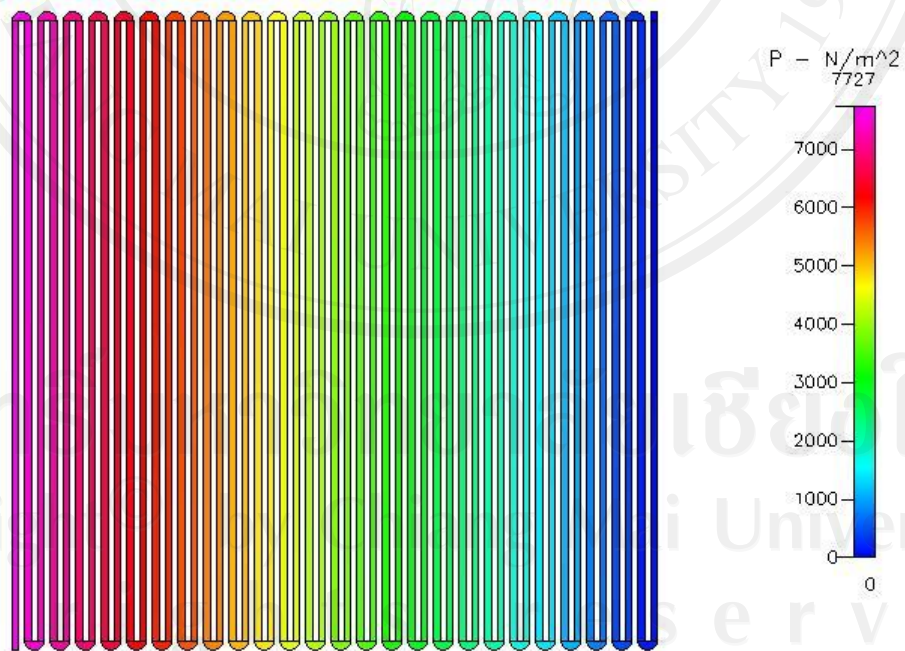
Figure B.14 Pressure distribution at 200 cm^3/min of outside fillet curve
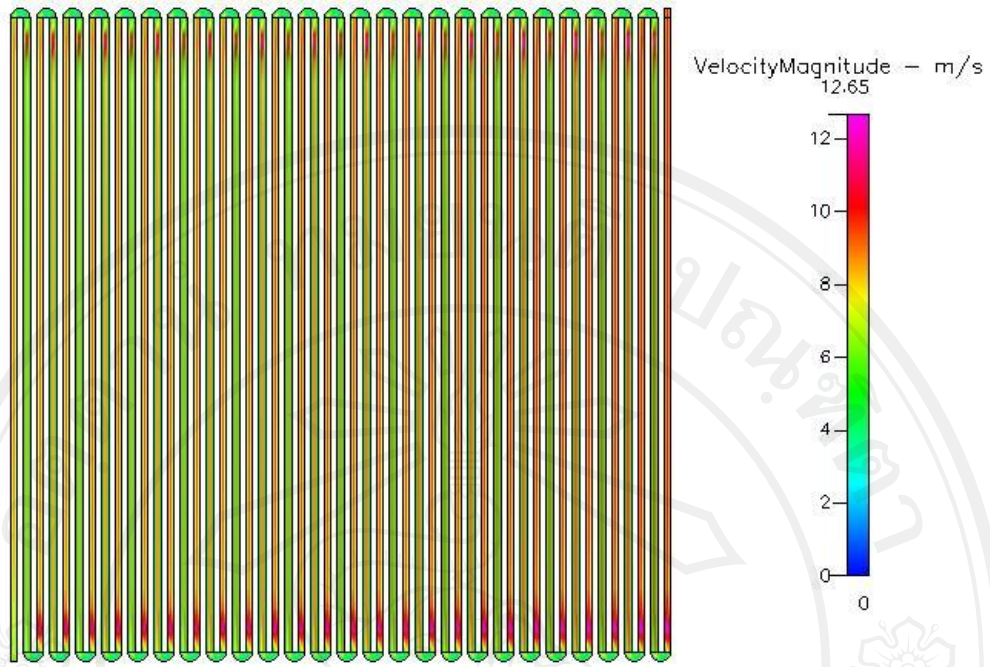
Figure B.15 Velocity distribution at 400 cm^3/min of outside fillet curve
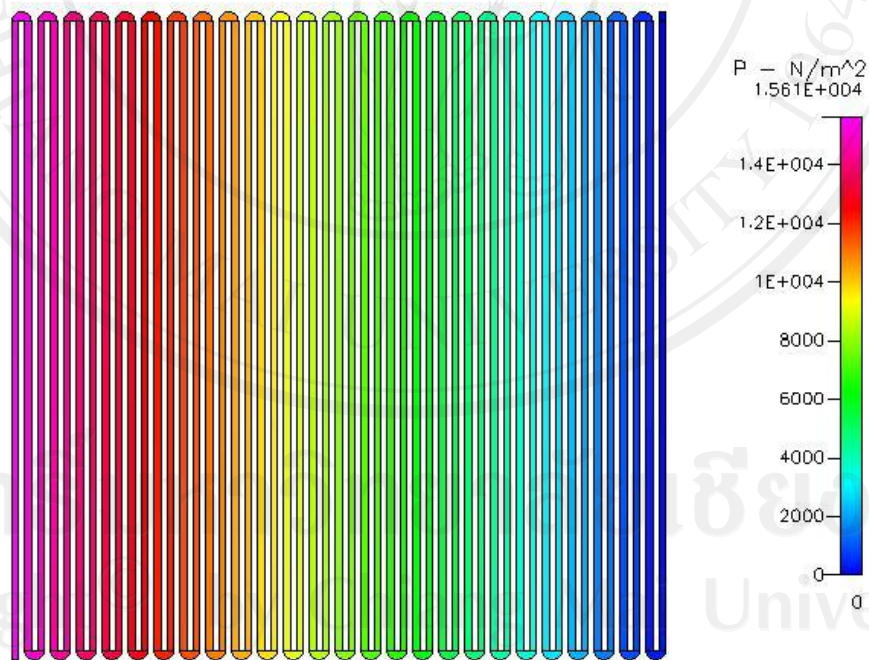
Figure B.16 Pressure distribution at 400 cm^3/min of outside fillet curve
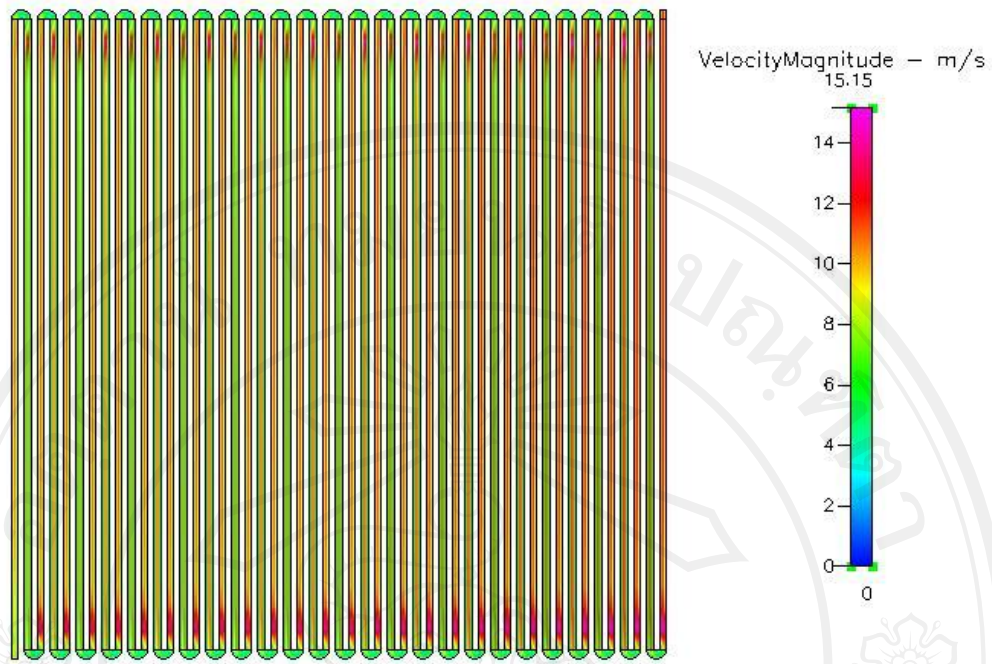
Figure B.17 Velocity distribution at 500 cm^3/min of outside fillet curve
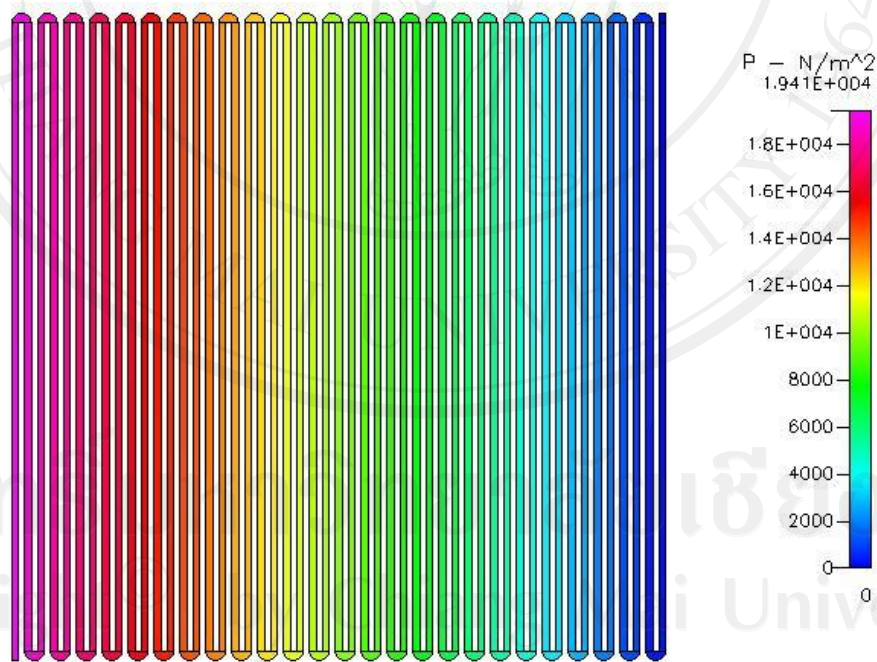
Figure B.18 Pressure distribution at 500 cm^3/min of outside fillet curve

- **In fillet curve**
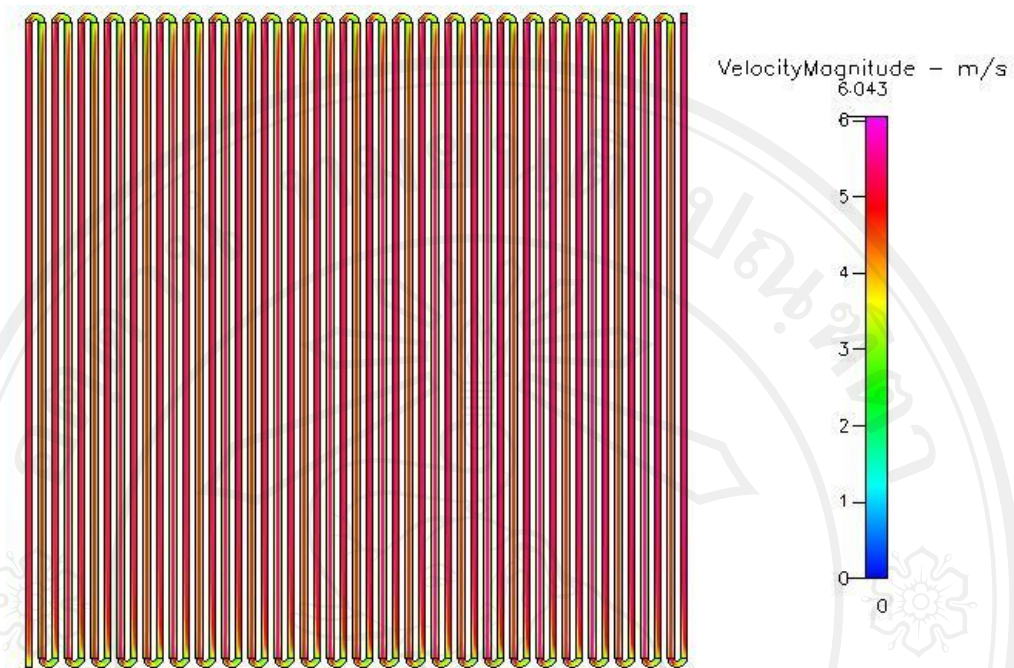
Figure B.19 Velocity distribution at 200 cm^3/min of fillet curve
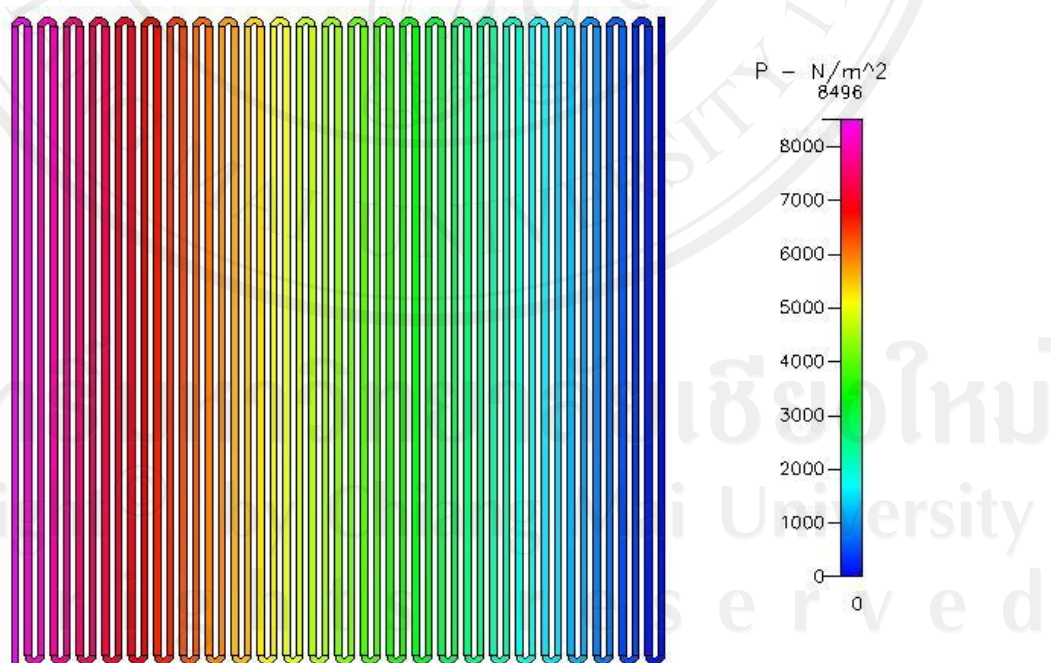
Figure B.20 Pressure distribution at 200 cm^3/min of fillet curve
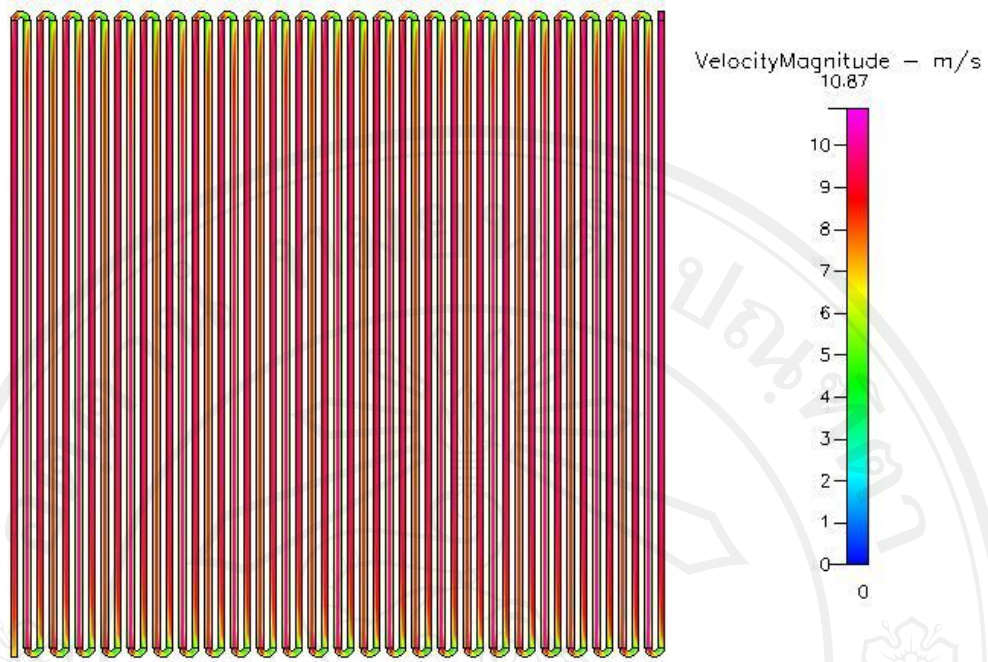
Figure B.21 Velocity distribution at 400 cm^3/min of fillet curve

Figure B.22 Pressure distribution at 400 cm^3/min of fillet curve

Figure B.23 Velocity distribution at 500 cm^3/min of fillet curve

Figure B.24 Pressure distribution at 500 cm^3/min of fillet curve

- **In 2 channels**

Figure B.25 Velocity distribution at 200 cm^3/min of 2 channels

Figure B.26 Pressure distribution at 200 cm^3/min of 2 channels

Figure B.27 Velocity distribution at 400 cm^3/min of 2 channels

Figure B.28 Pressure distribution at 400 cm^3/min of 2 channels
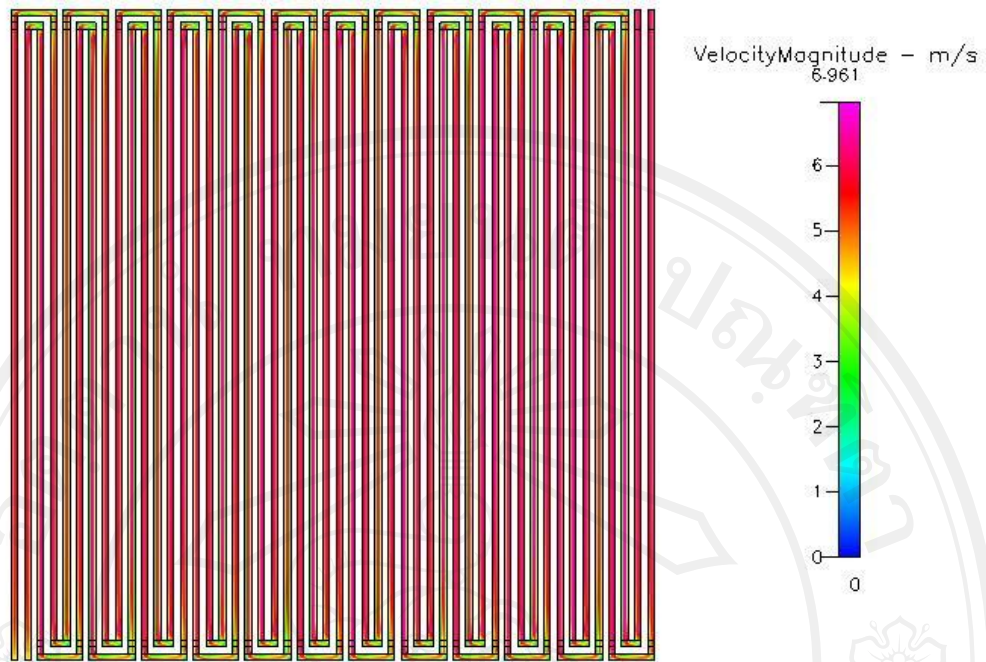
Figure B.29 Velocity distribution at 500 cm^3/min of 2 channels

Figure B.30 Pressure distribution at 500 cm^3/min of 2 channels

- **In 3 channels**
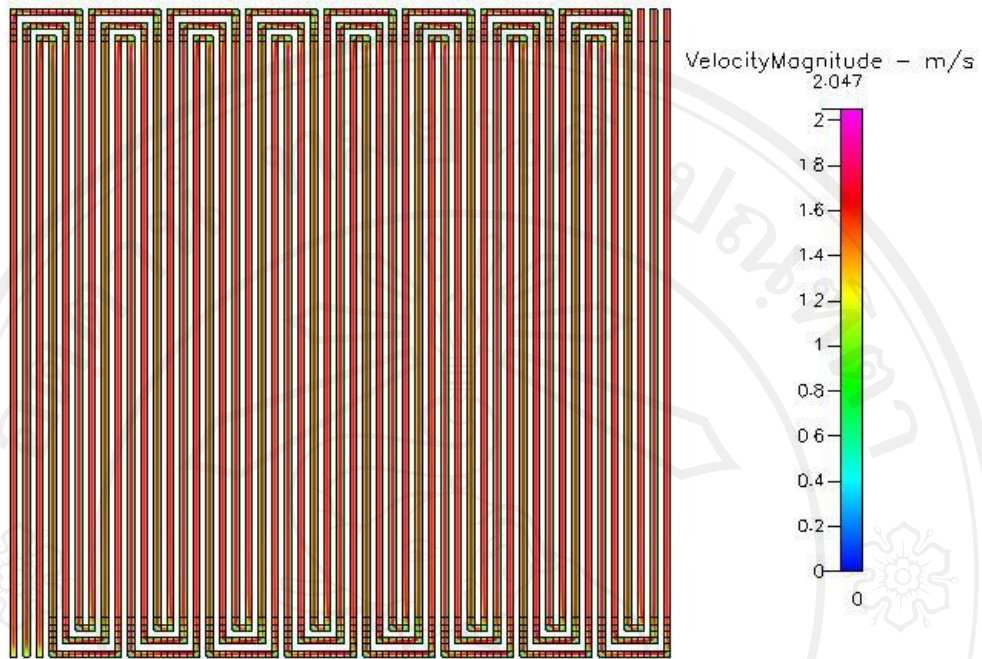
Figure B.31 Velocity distribution at 200 cm^3/min of 3 channels
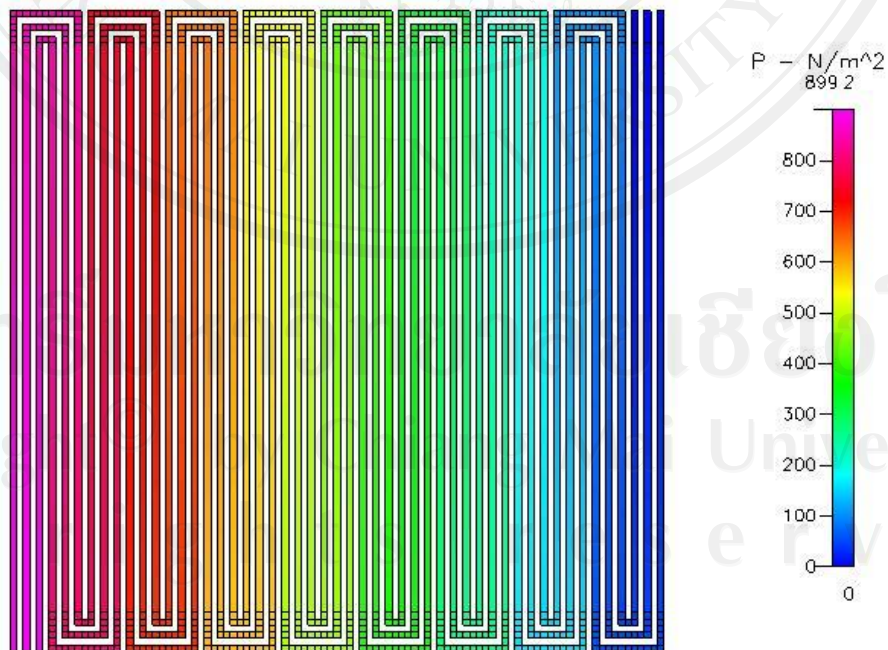
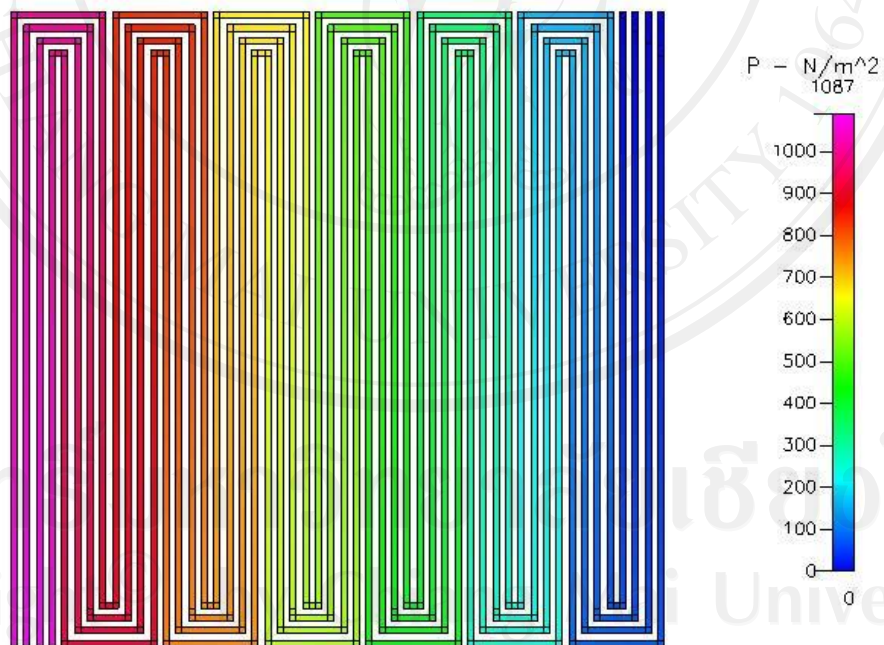Figure B.32 Pressure distribution at 200 cm^3/min of 3 channels

Figure B.33 Velocity distribution at 400 cm^3/min of 3 channels
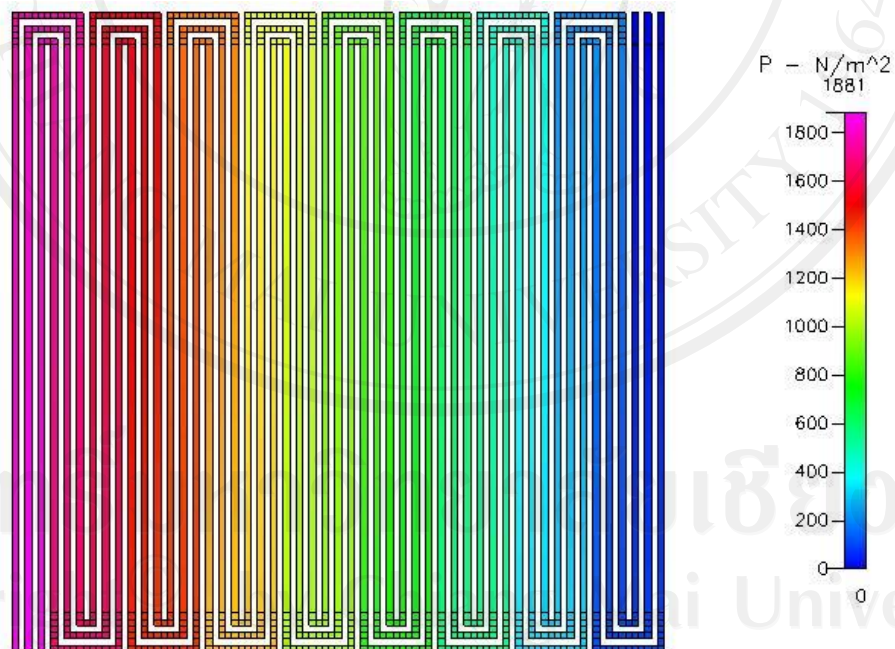
Figure B.34 Pressure distribution at 400 cm^3/min of 3 channels
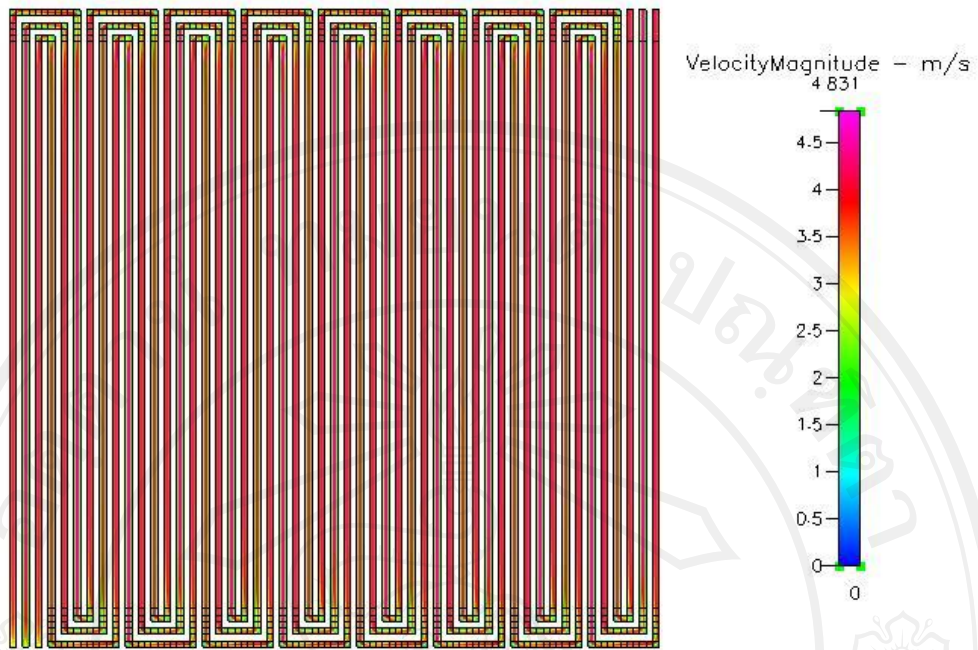
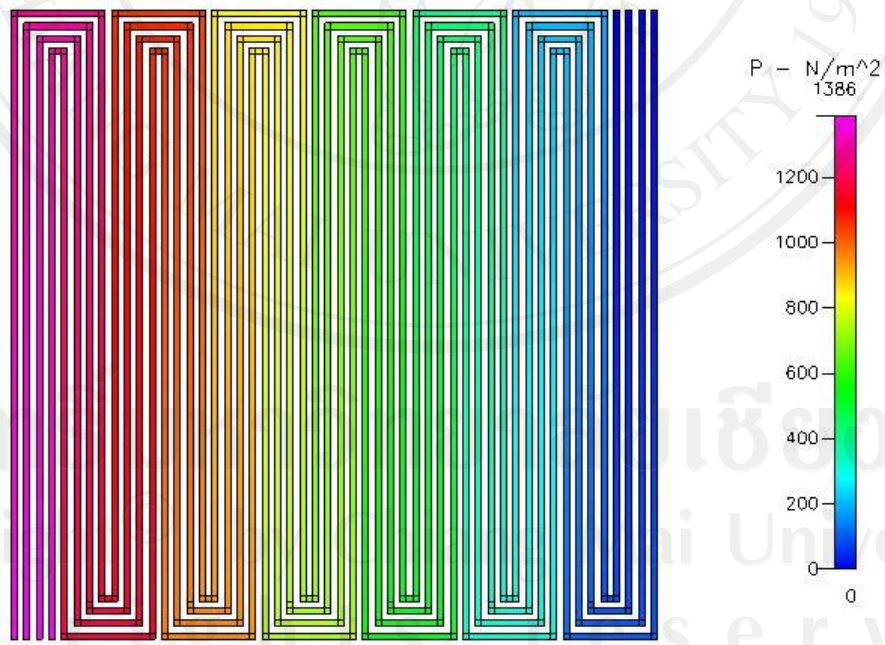Figure B.35 Velocity distribution at 500 cm^3/min of 3 channels
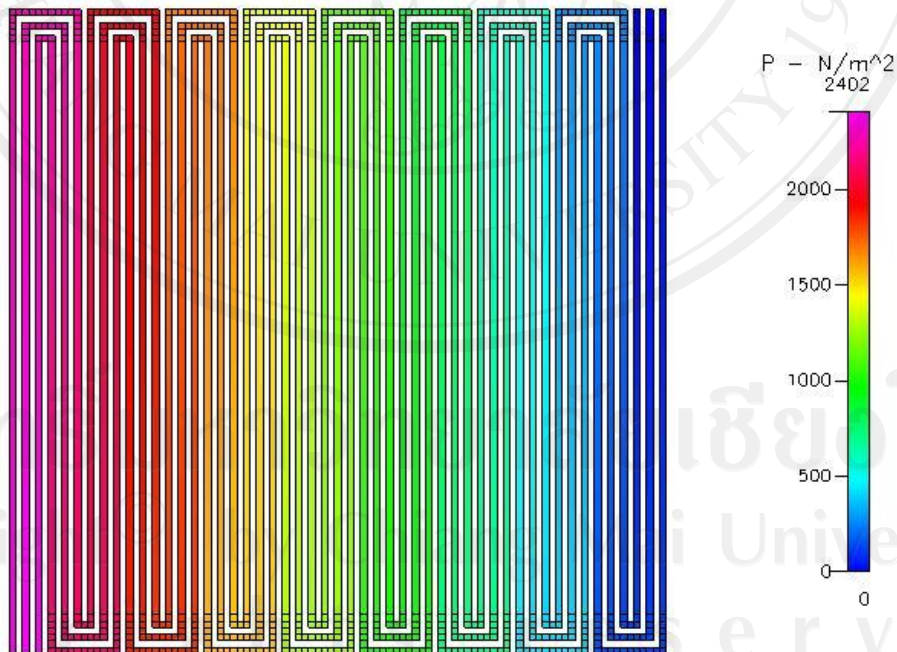
Figure B.36 Pressure distribution at 500 cm^3/min of 3 channels

- **In 4 channels**
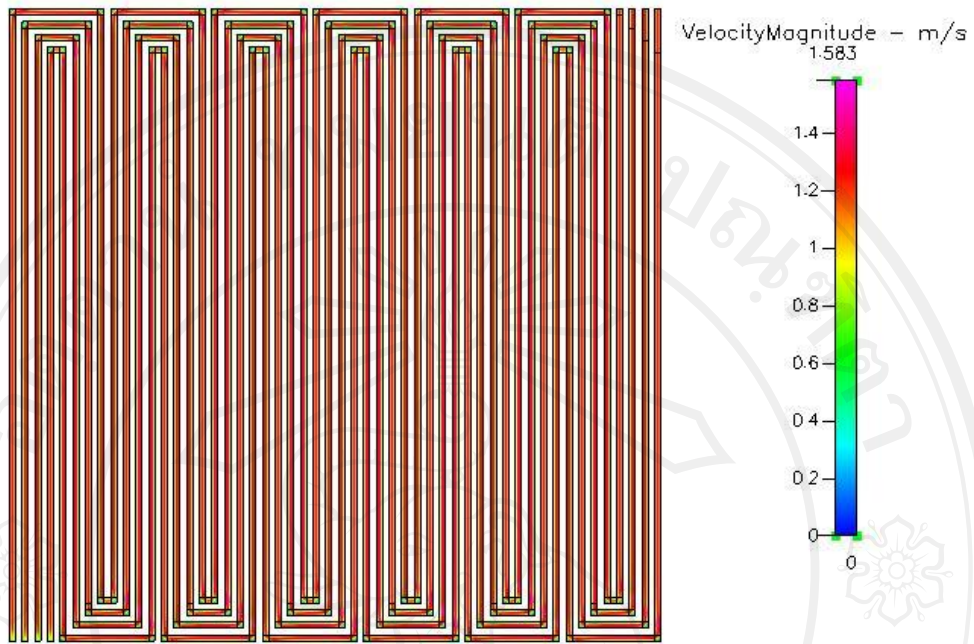
Figure B.37 Velocity distribution at 200 cm^3/min of 4 channels
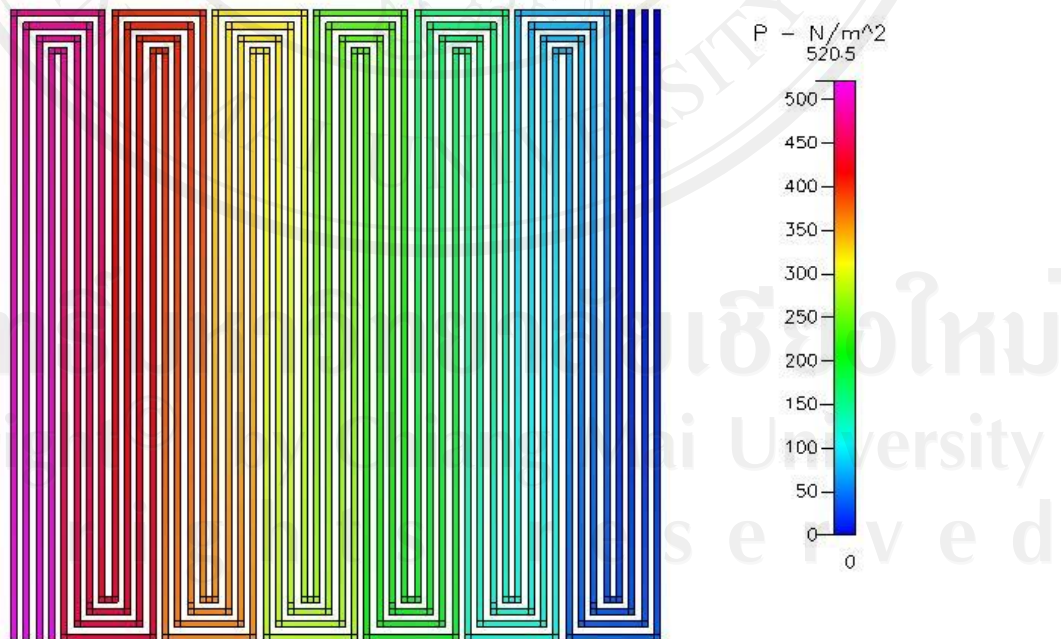
Figure B.38 Pressure distribution at 200 cm^3/min of 4 channels
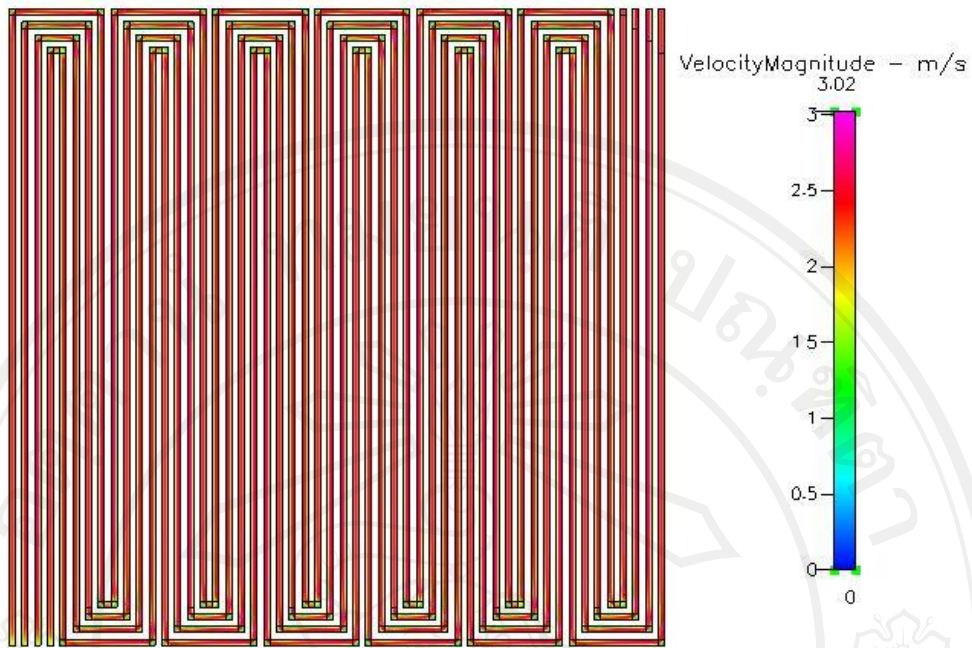
Figure B.39 Velocity distribution at 400 cm^3/min of 4 channels

Figure B.40 Pressure distribution at 400 cm^3/min of 4 channels

Figure B.41 Velocity distribution at 500 cm^3/min of 4 channels

Figure B.42 Pressure distribution at 500 cm^3/min of 4 channels
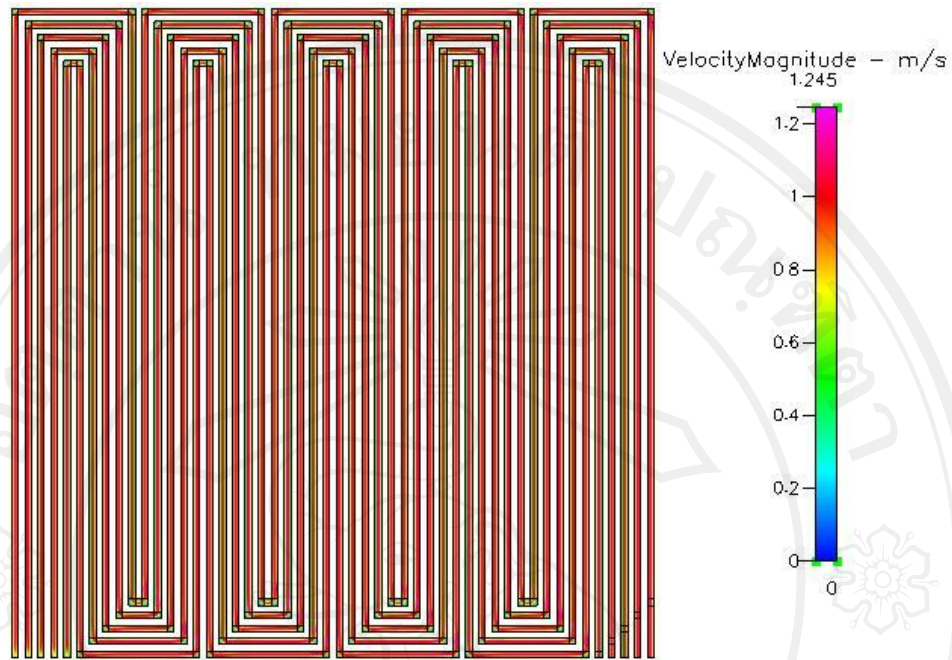
- **In 5 channels**

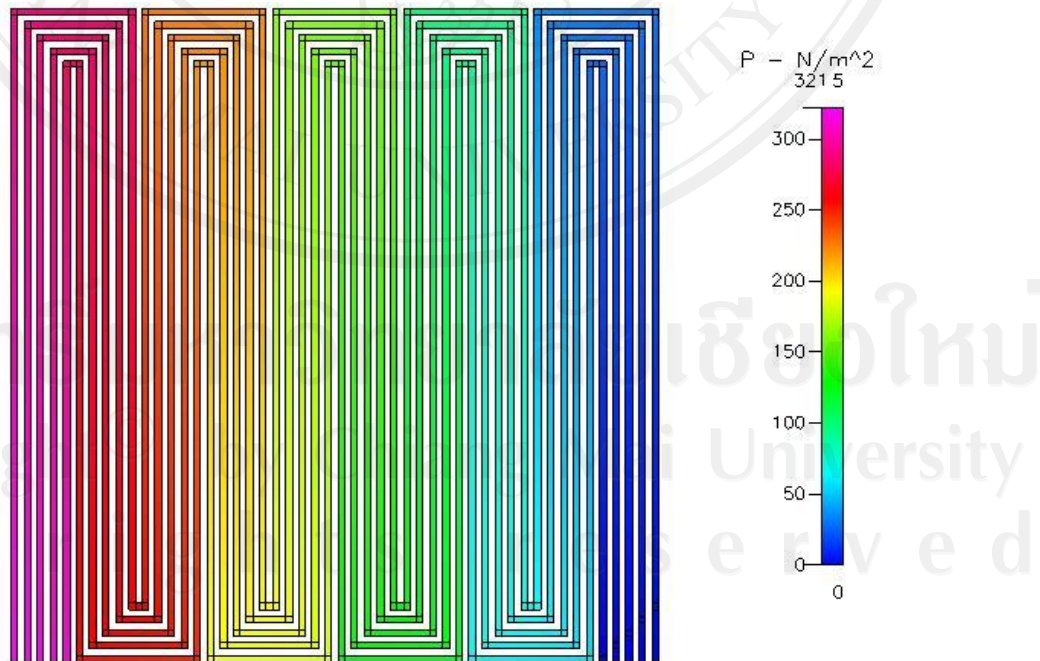Figure B.43 Velocity distribution at 200 cm³/min of 5 channels

Figure B.44 Pressure distribution at 200 cm³/min of 5 channels
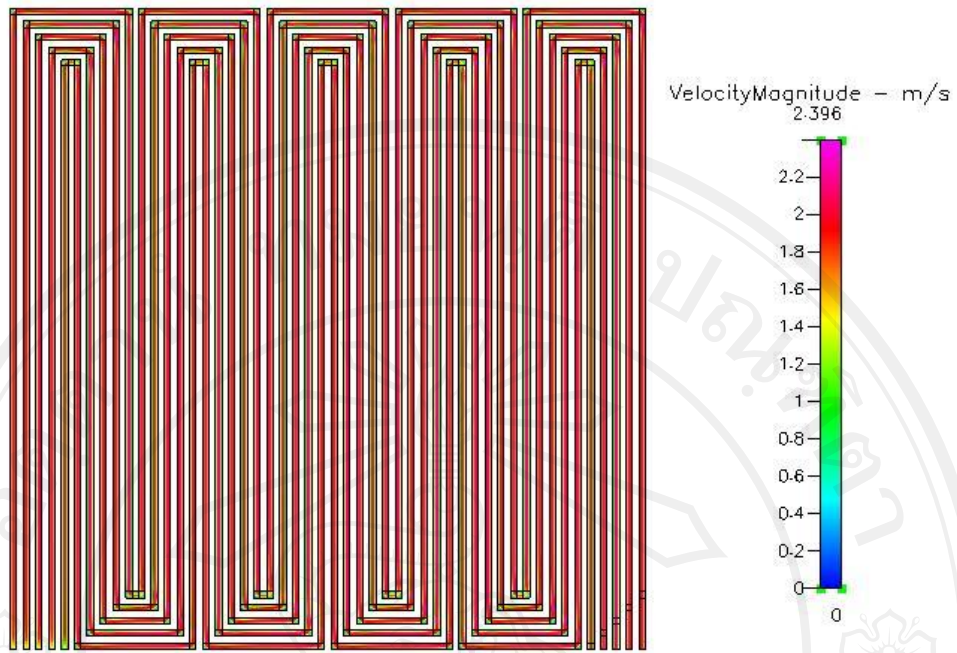
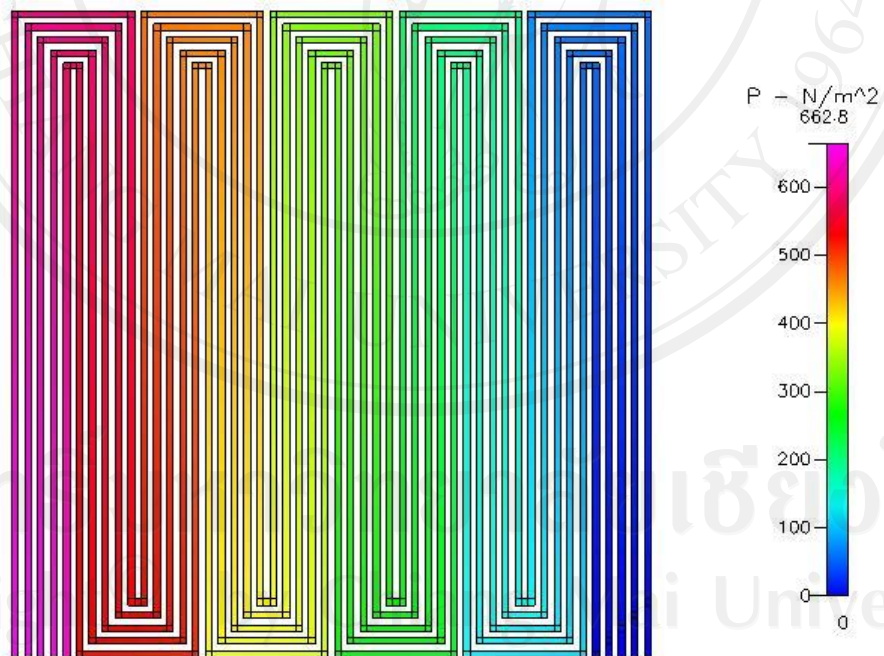Figure B.45 Velocity distribution at 400 cm^3/min of 5 channels

Figure B.46 Pressure distribution at 400 cm^3/min of 5 channels

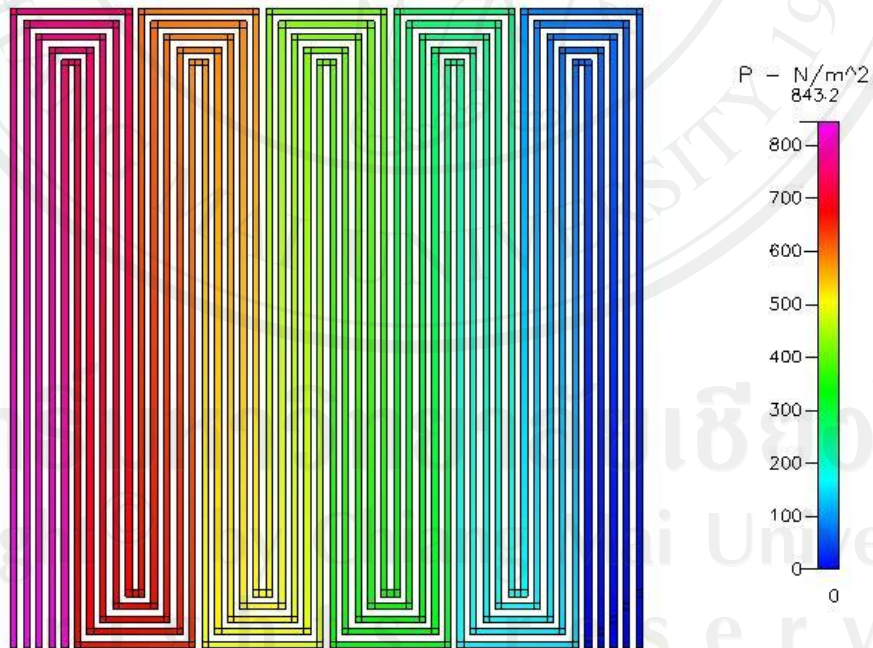Figure B.47 Velocity distribution at 500 cm^3/min of 5 channels

Figure B.48 Pressure distribution at 500 cm^3/min of 5 channels

- **In 6 channels**

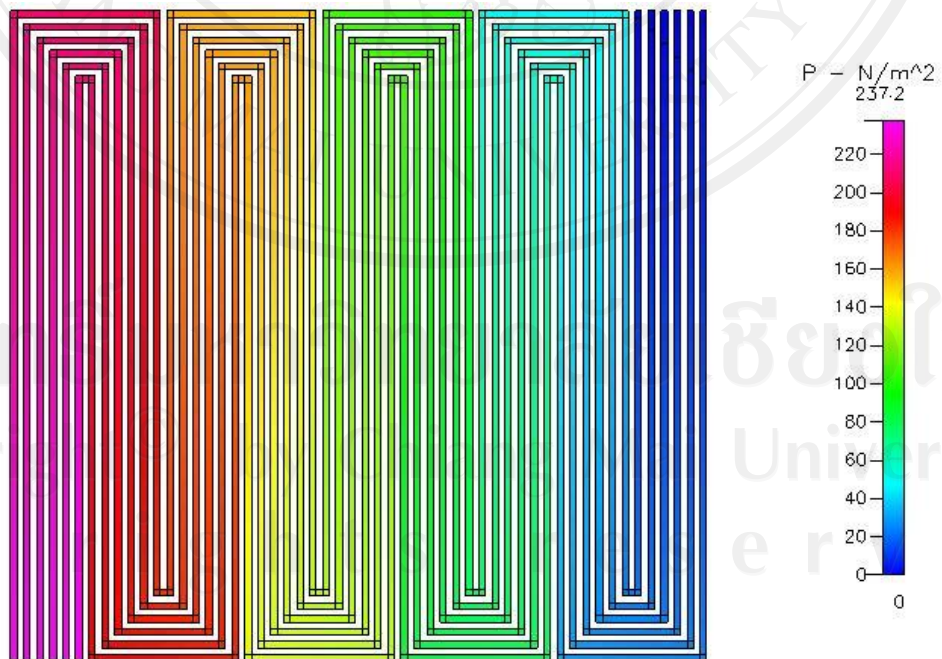Figure B.49 Velocity distribution at 200 cm^3/min of 6 channels

Figure B.50 Pressure distribution at 200 cm^3/min of 6 channels

Figure B.51 Velocity distribution at 400 cm^3/min of 6 channels
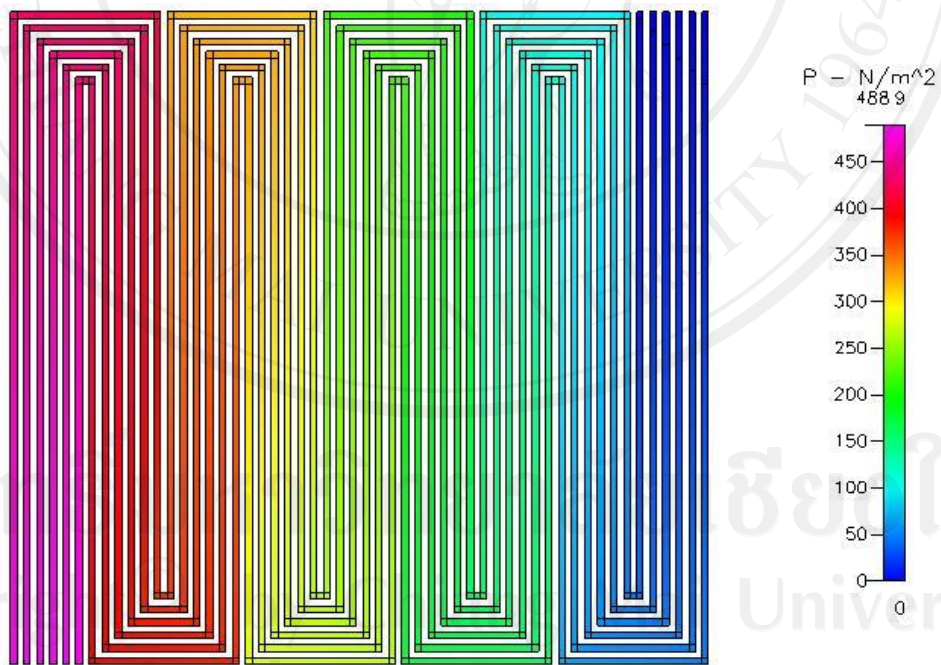

Figure B.52 Pressure distribution at 400 cm^3/min of 6 channels
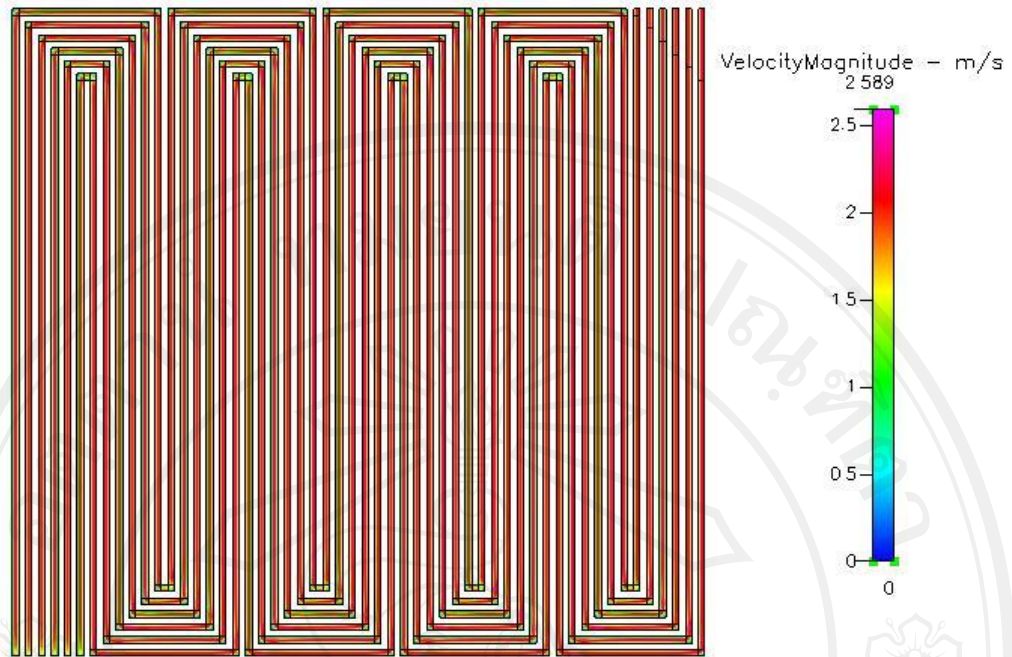
Figure B.53 Velocity distribution at 500 cm^3/min of 6 channels
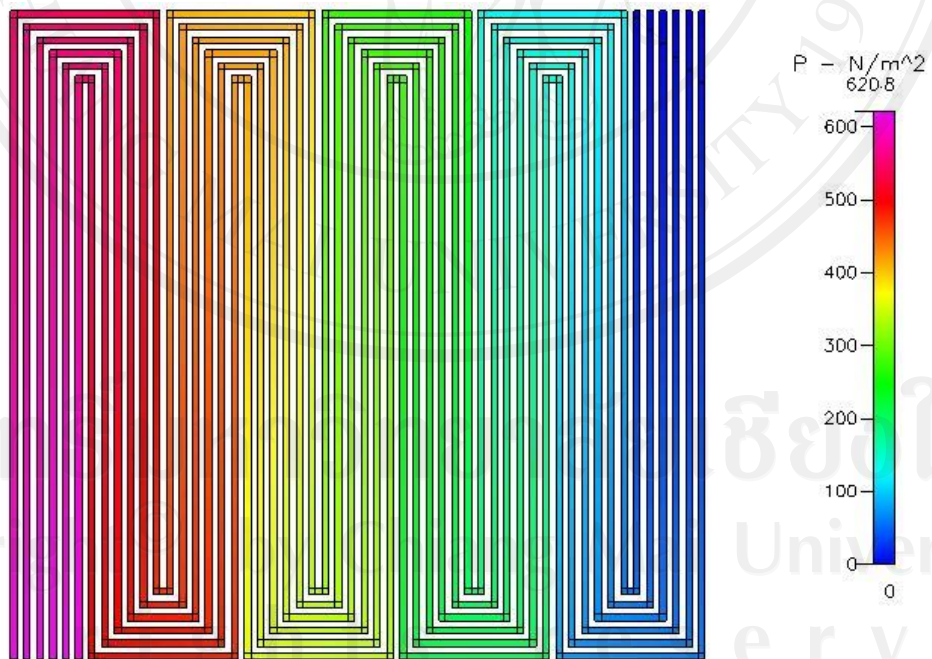
Figure B.54 Pressure distribution at 500 cm^3/min of 6 channels

- **In 0.8 mm. channel depth**

Figure B.55 Velocity distribution at 200 cm^3/min of 0.8 mm. channel depth

Figure B.56 Pressure distribution at 200 cm^3/min of 0.8 mm. channel depth

Figure B.57 Velocity distribution at 400 cm^3/min of 0.8 mm. channel depth

Figure B.58 Pressure distribution at 400 cm^3/min of 0.8 mm. channel depth

Figure B.59 Velocity distribution at 500 cm^3/min of 0.8 mm. channel depth
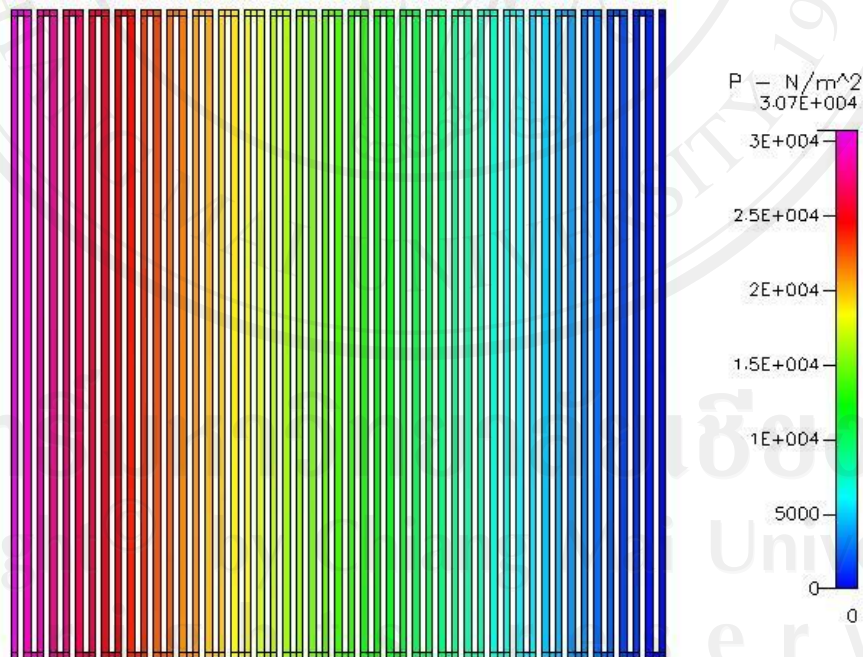
Figure B.60 Pressure distribution at 500 cm^3/min of 0.8 mm. channel depth

- **In 1.2 mm. channel depth**

Figure B.61 Velocity distribution at 200 cm^3/min of 1.2 mm. channel depth

Figure B.62 Pressure distribution at 200 cm^3/min of 1.2 mm. channel depth

Figure B.63 Velocity distribution at 400 cm^3/min of 1.2 mm. channel depth
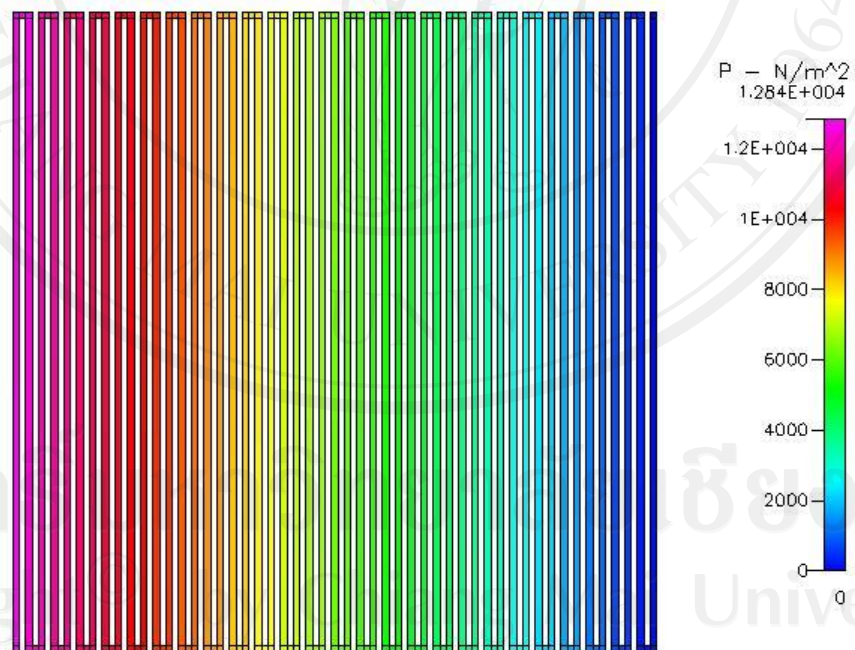
Figure B.64 Pressure distribution at 400 cm^3/min of 1.2 mm. channel depth
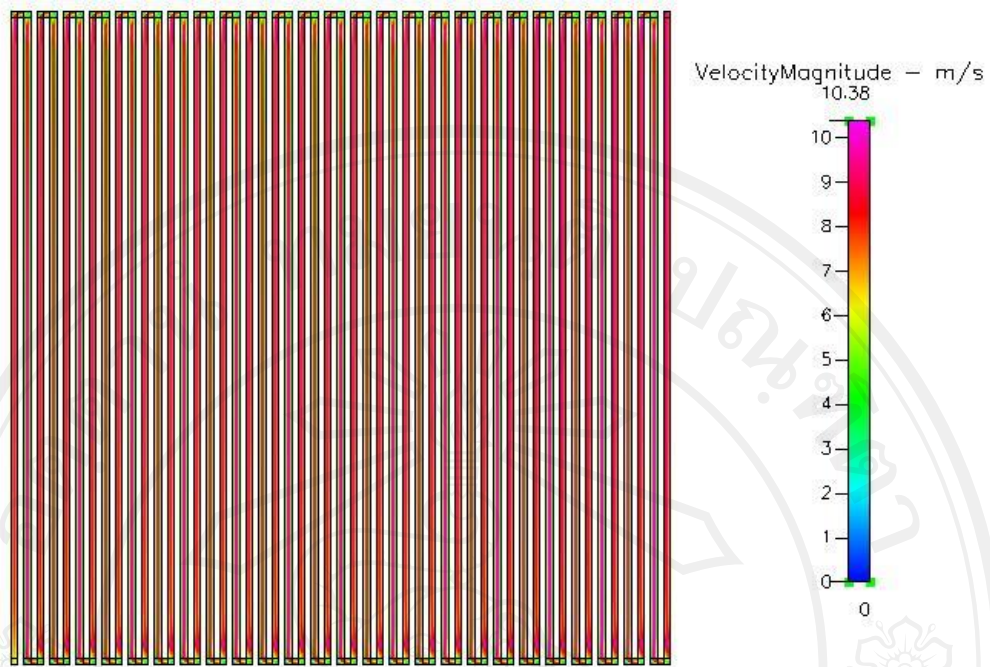
Figure B.65 Velocity distribution at 500 cm^3/min of 1.2 mm. channel depth
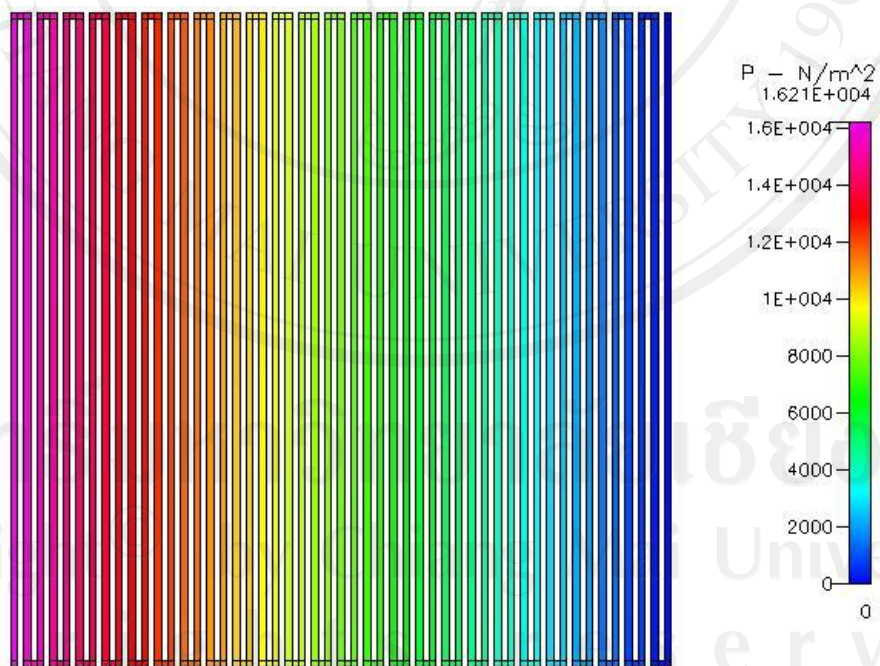
Figure B.66 Pressure distribution at 500 cm^3/min of 1.2 mm. channel depth
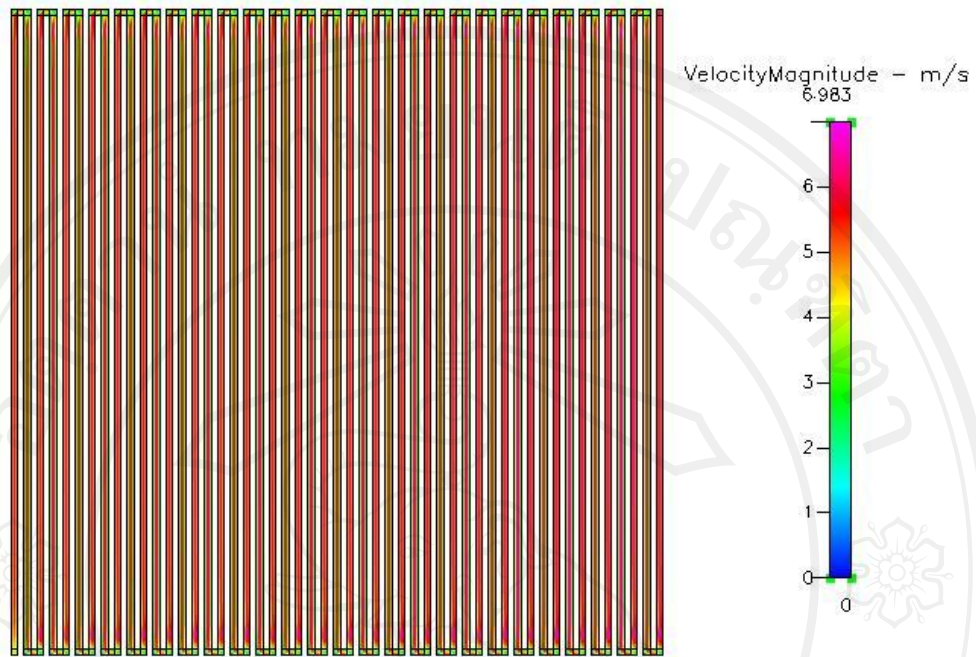
- **In 0.8 mm. channel width**
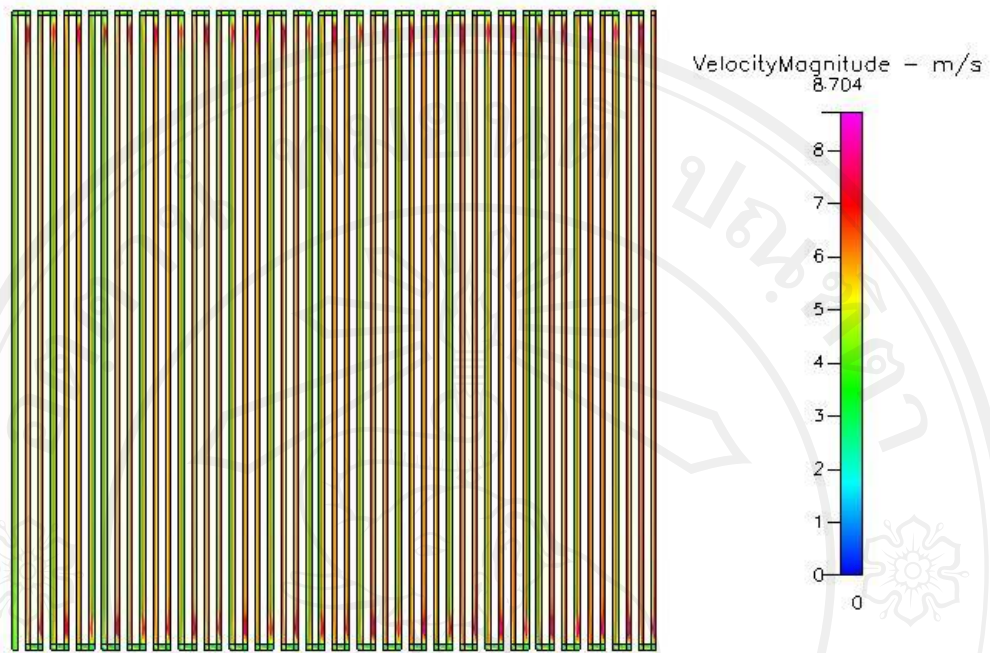
Figure B.67 Velocity distribution at 200 cm^3/min of 0.8 mm. channel width
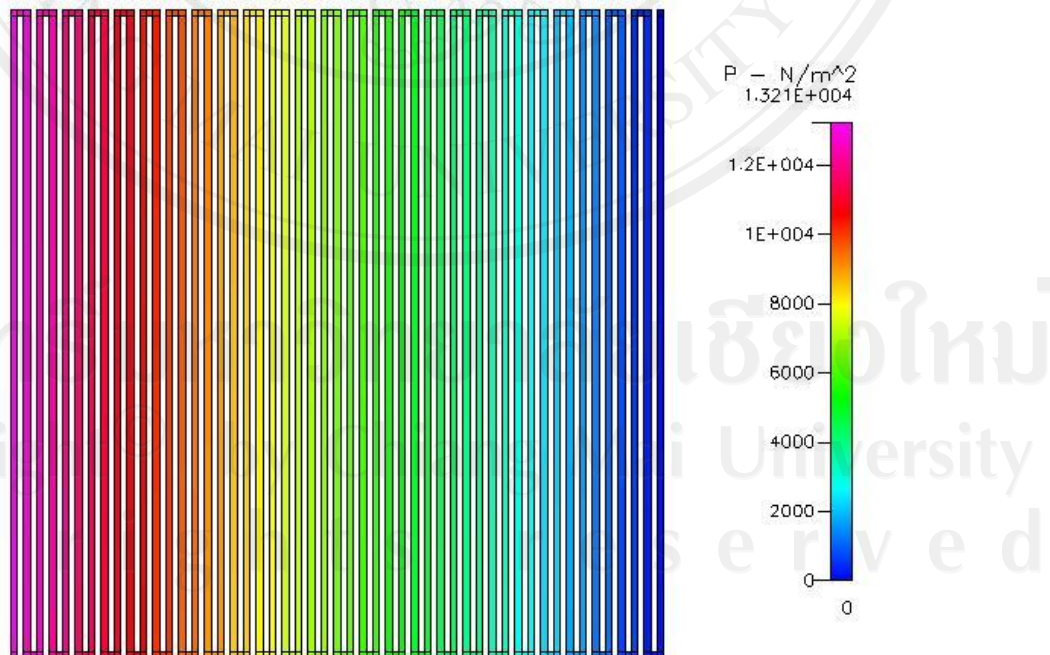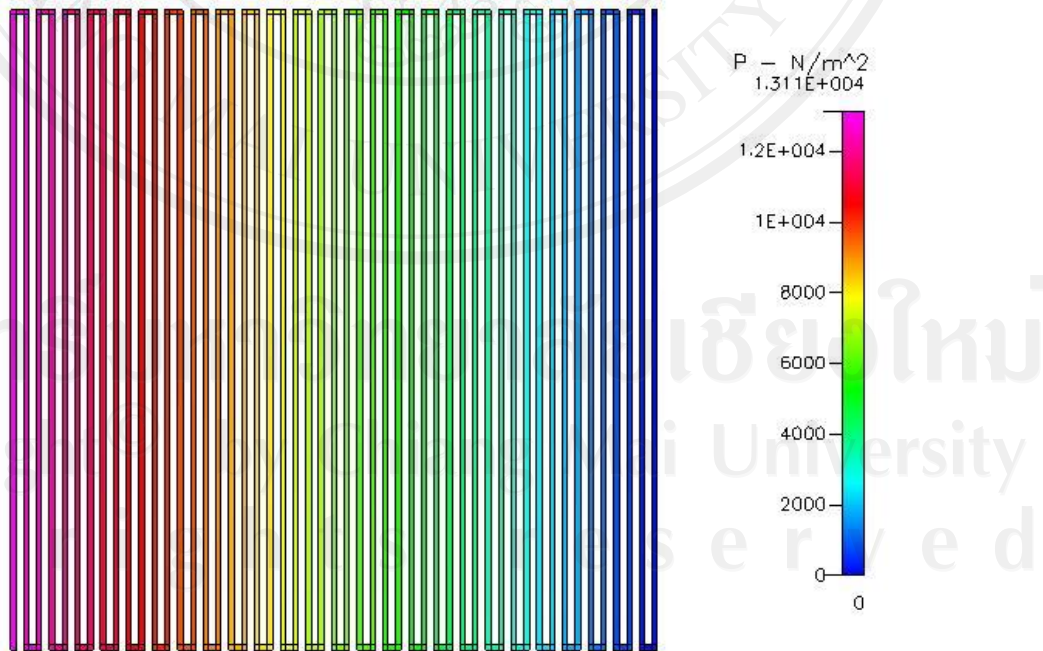

Figure B.68 Pressure distribution at 200 cm^3/min of 0.8 mm. channel width
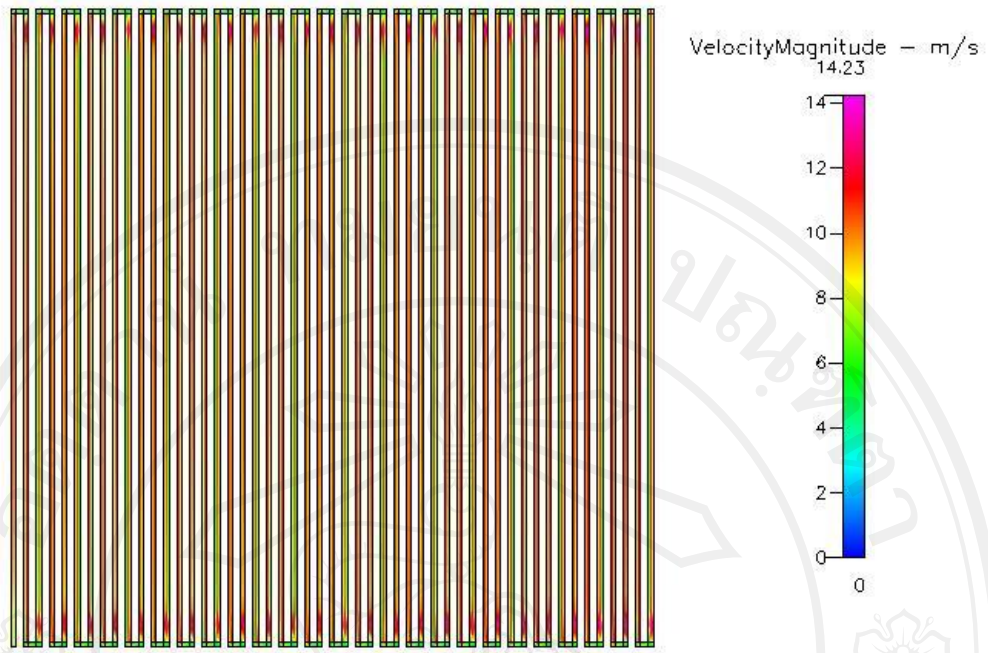
Figure B.69 Velocity distribution at 400 cm^3/min of 0.8 mm. channel width
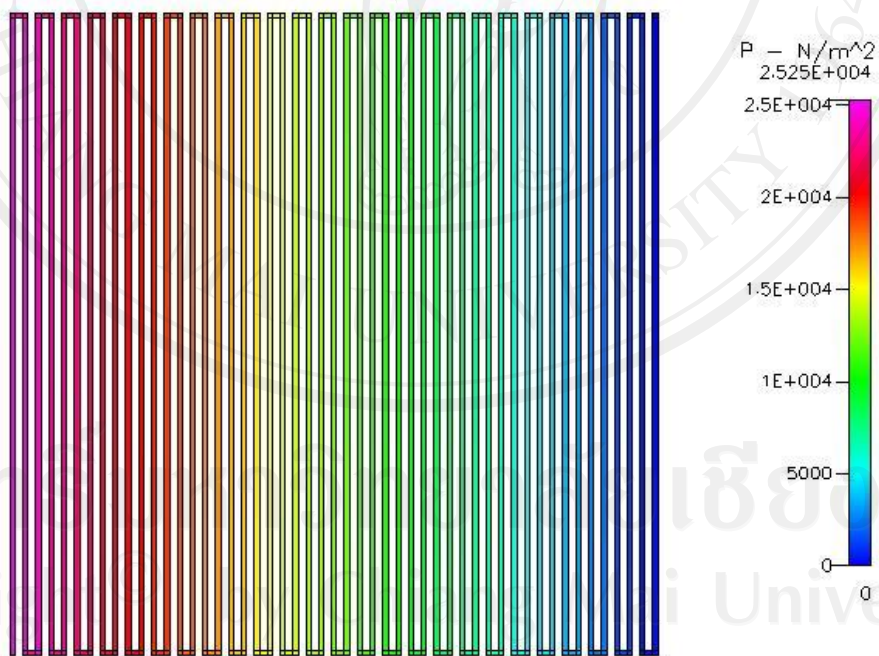
Figure B.70 Pressure distribution at 400 cm^3/min of 0.8 mm. channel width
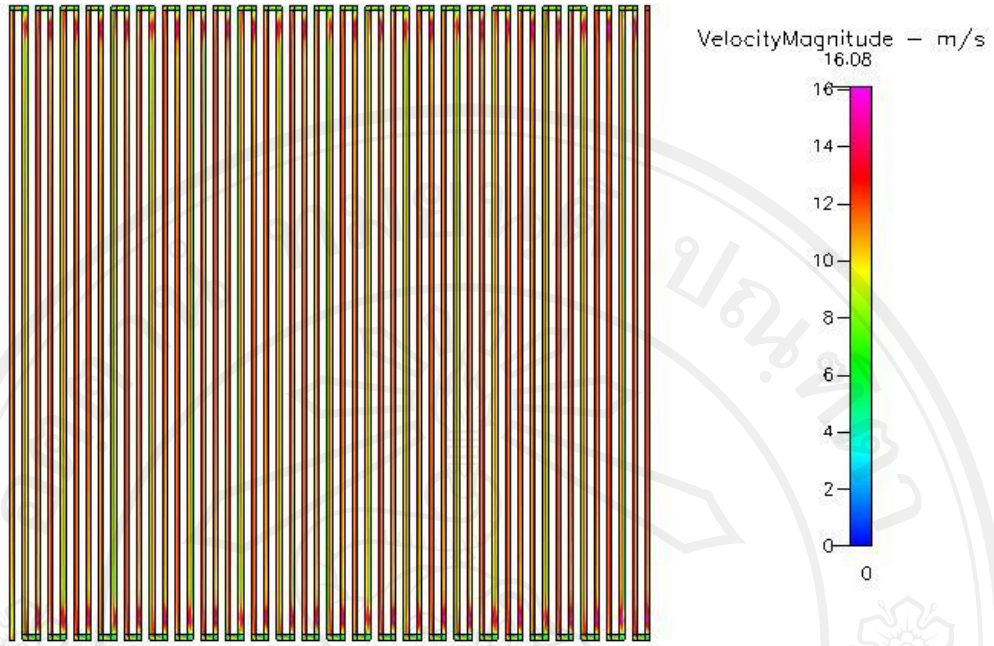
Figure B.71 Velocity distribution at 500 cm^3/min of 0.8 mm. channel width
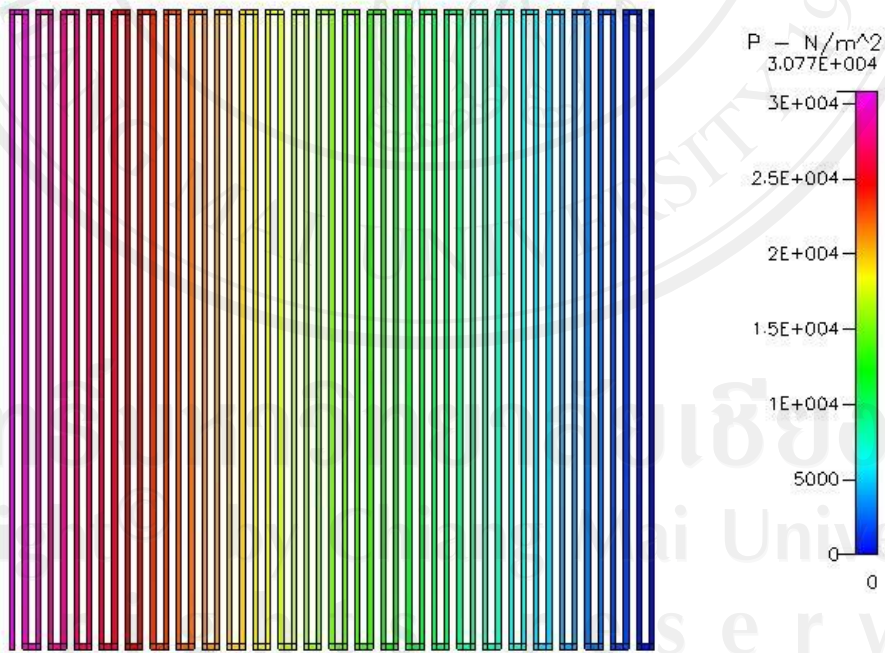
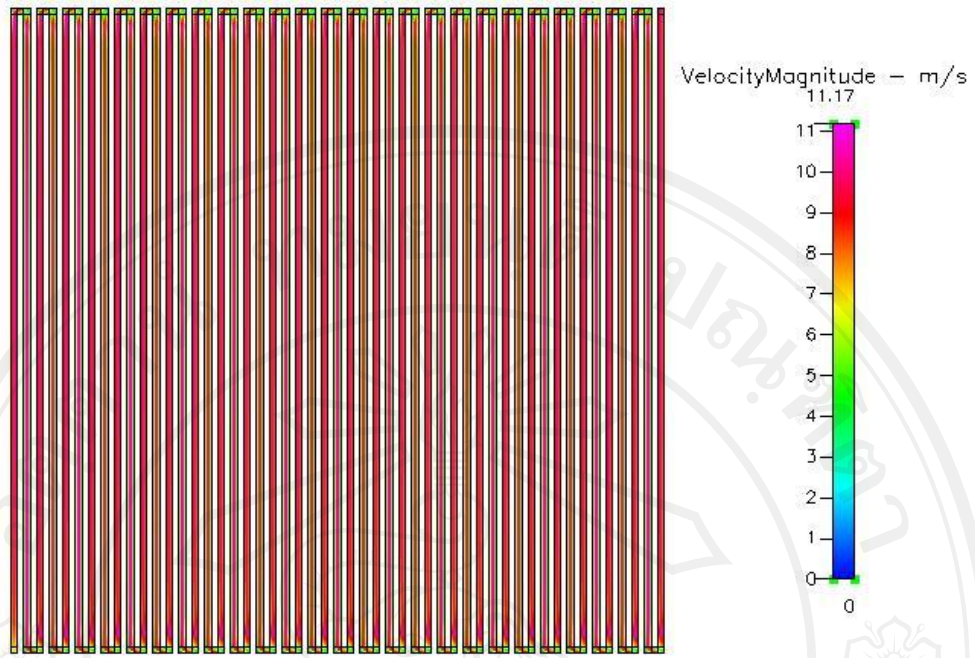Figure B.72 Pressure distribution at 500 cm^3/min of 0.8 mm. channel width

- **In 1.2 mm. channel width**
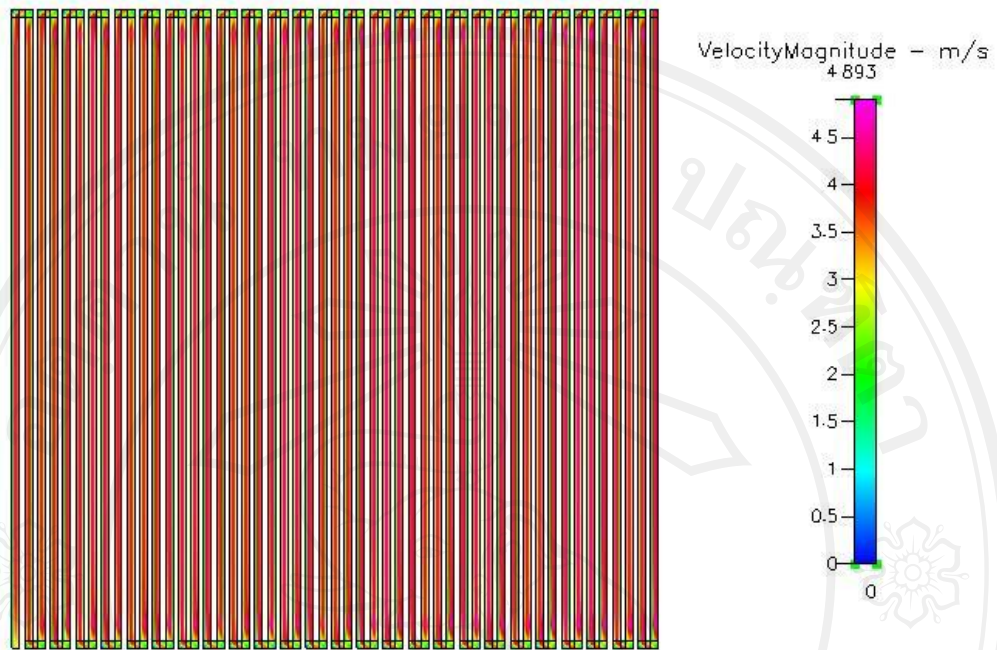
Figure B.73 Velocity distribution at 200 cm^3/min of 1.2 mm. channel width
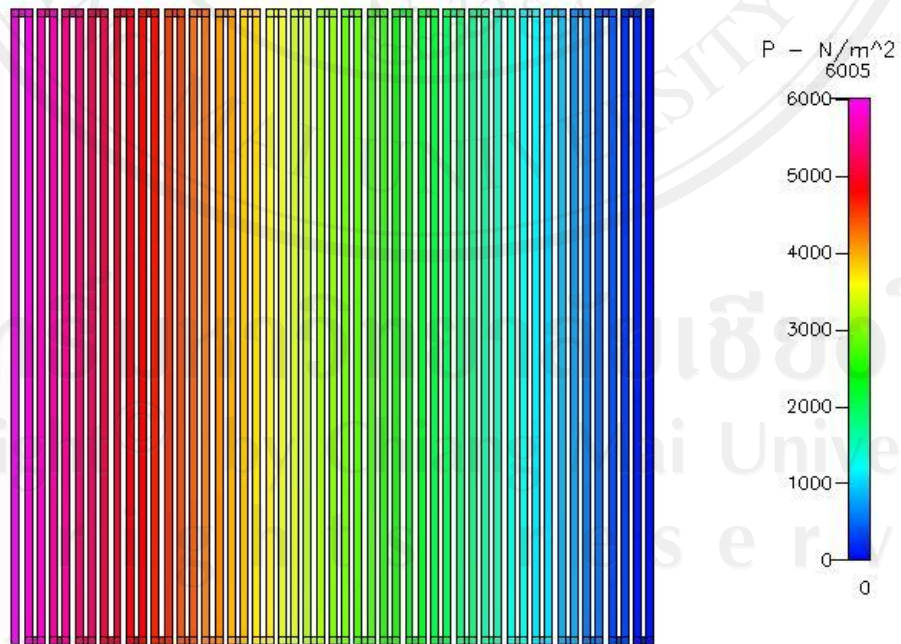
Figure B.74 Pressure distribution at 200 cm^3/min of 1.2 mm. channel width

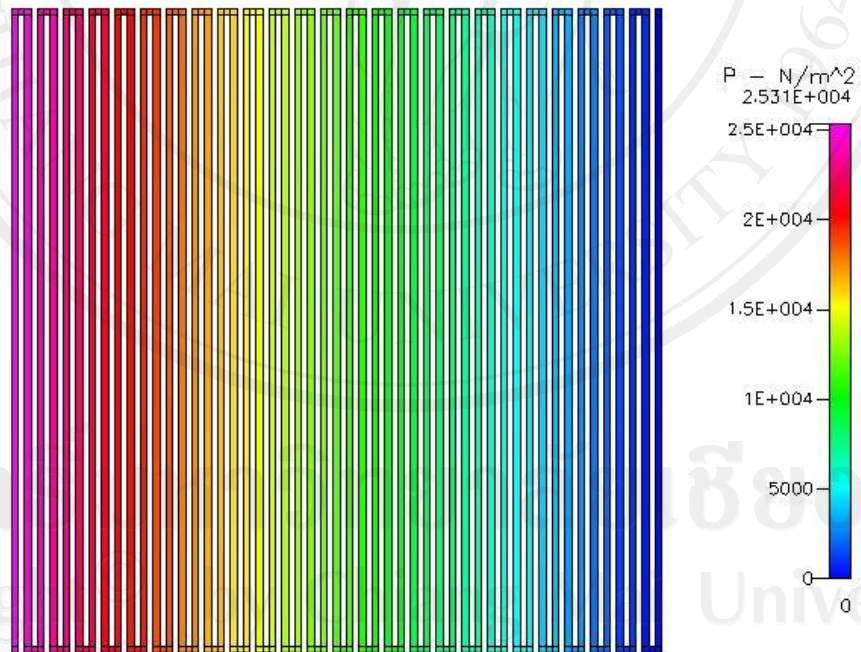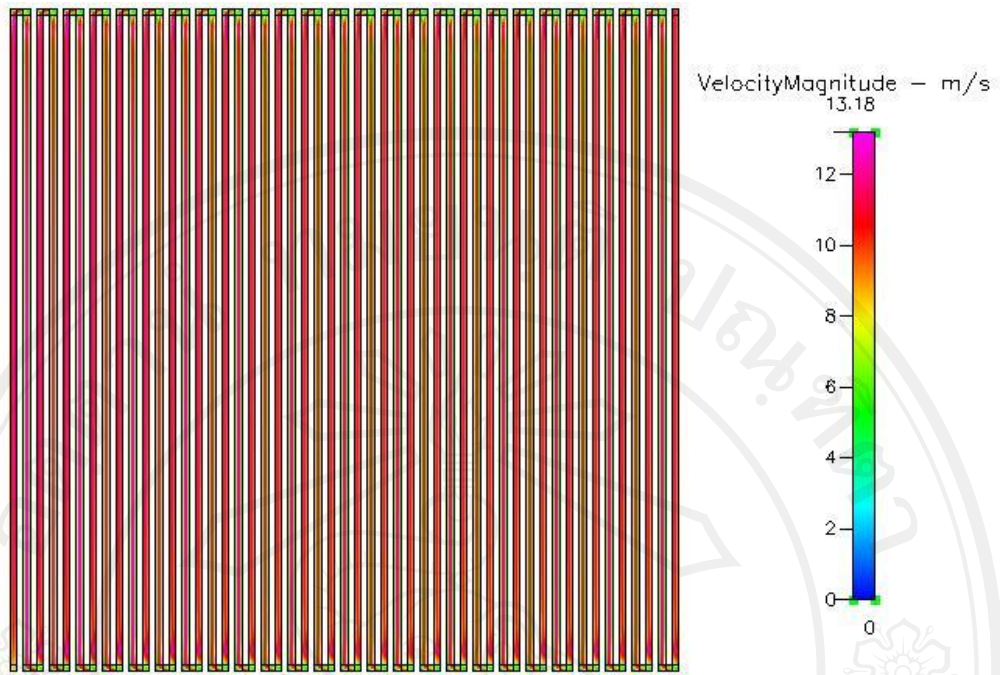Figure B.75 Velocity distribution at 400 cm^3/min of 1.2 mm. channel width
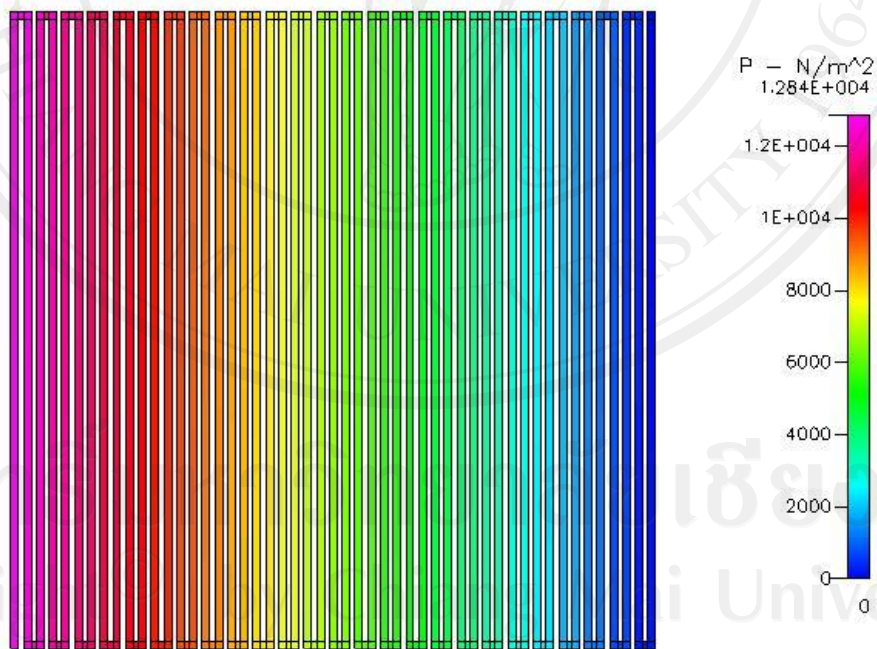
Figure B.76 Pressure distribution at 400 cm^3/min of 1.2 mm. channel width

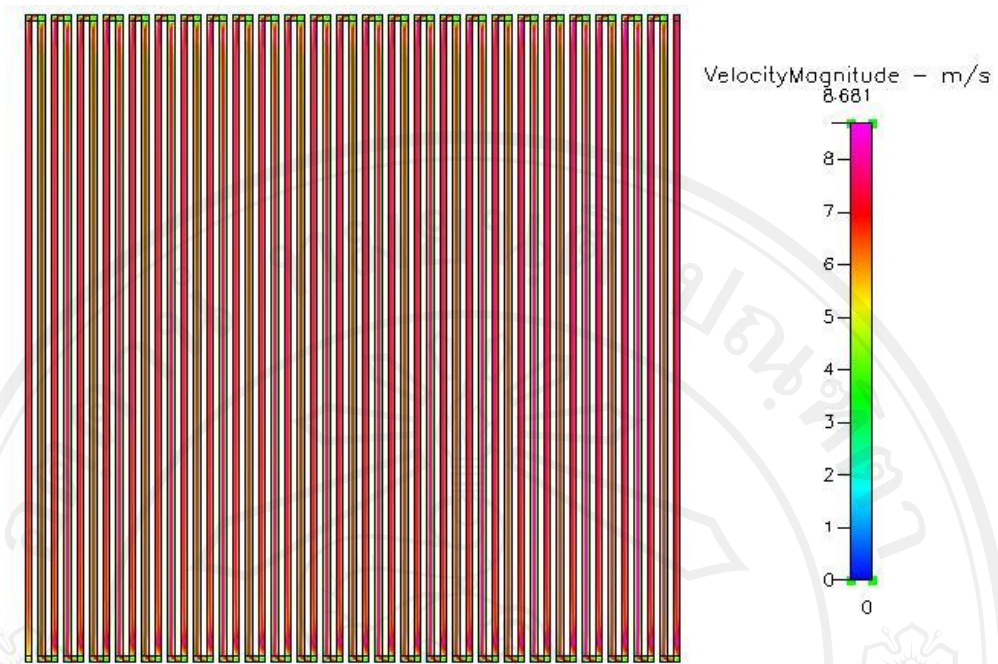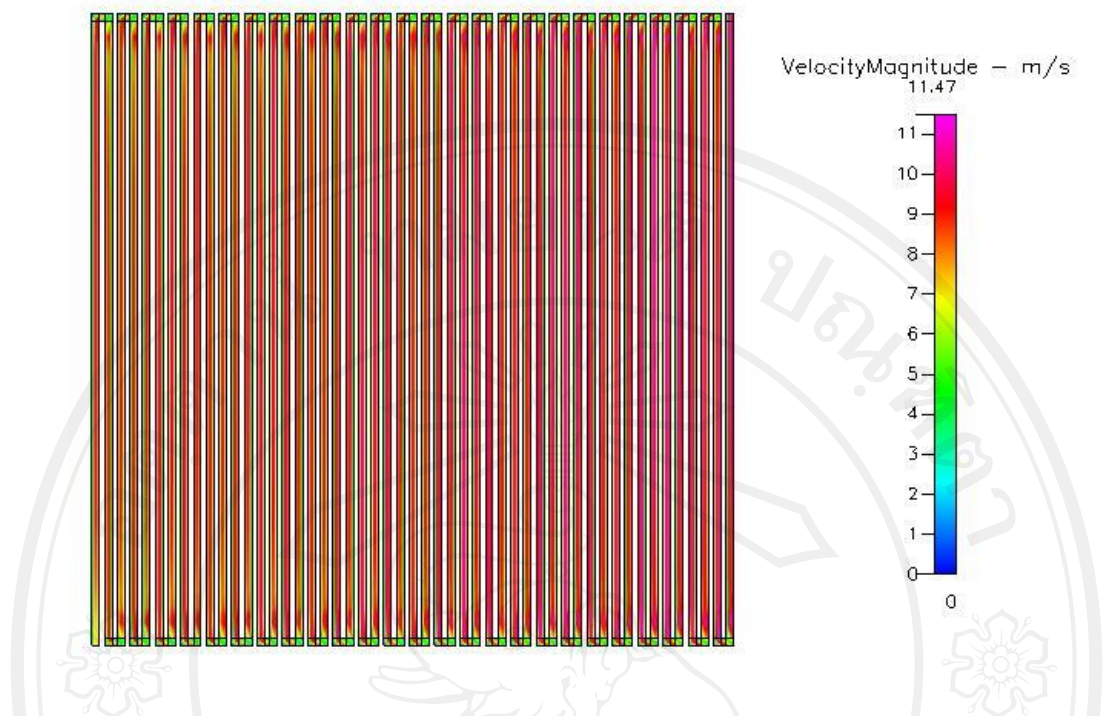Figure B.77 Velocity distribution at 500 cm^3/min of 1.2 mm. channel width

Figure B.78 Pressure distribution at 500 cm^3/min of 1.2 mm. channel width

- **In 2 channels manifold**
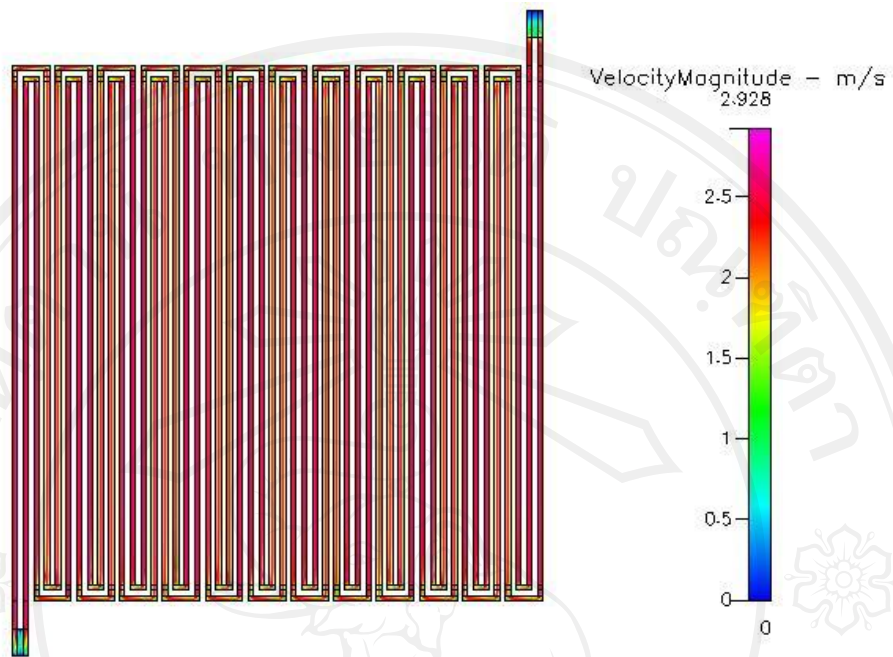
Figure B.79 Velocity distribution at 200 cm^3/min of 2 channels manifold
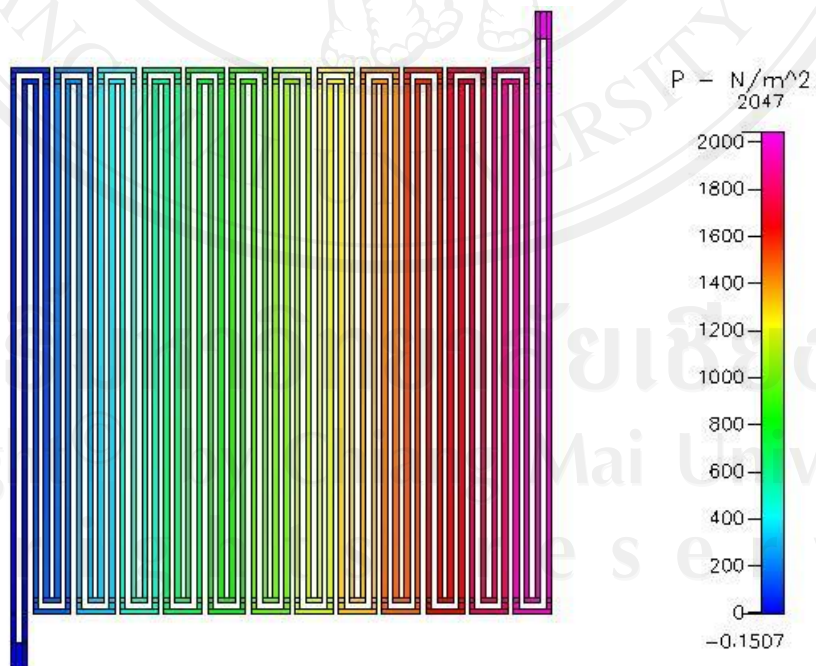
Figure B.80 Pressure distribution at 200 cm^3/min of 2 channels manifold
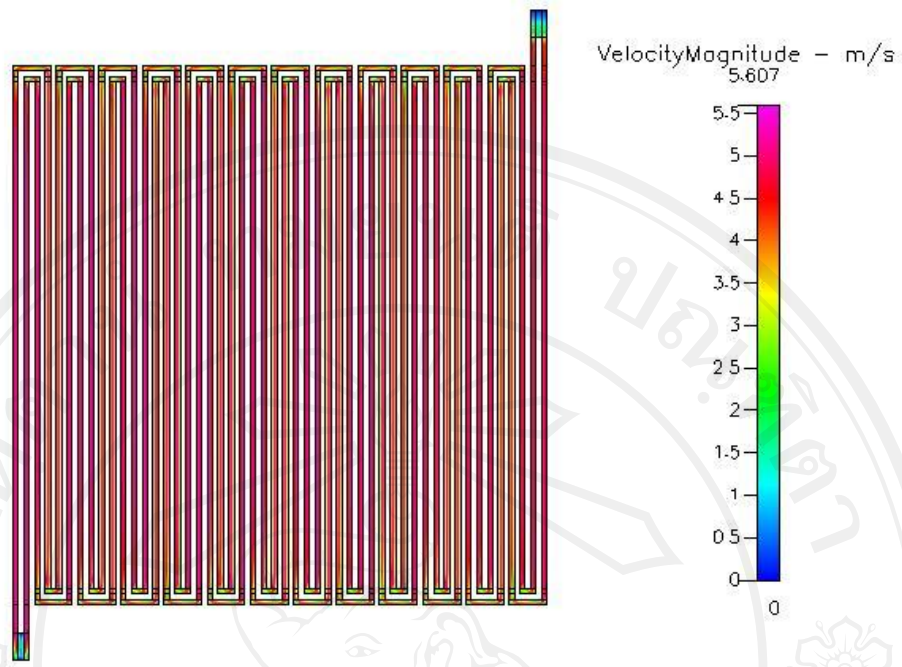
Figure B.81 Velocity distribution at 400 cm^3/min of 2 channels manifold
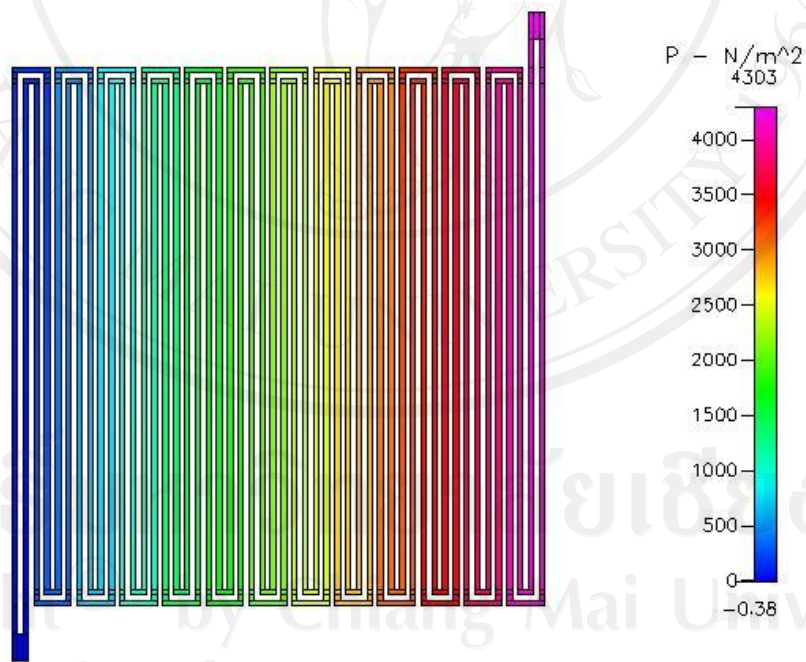
Figure B.82 Pressure distribution at 400 cm^3/min of 2 channels manifold
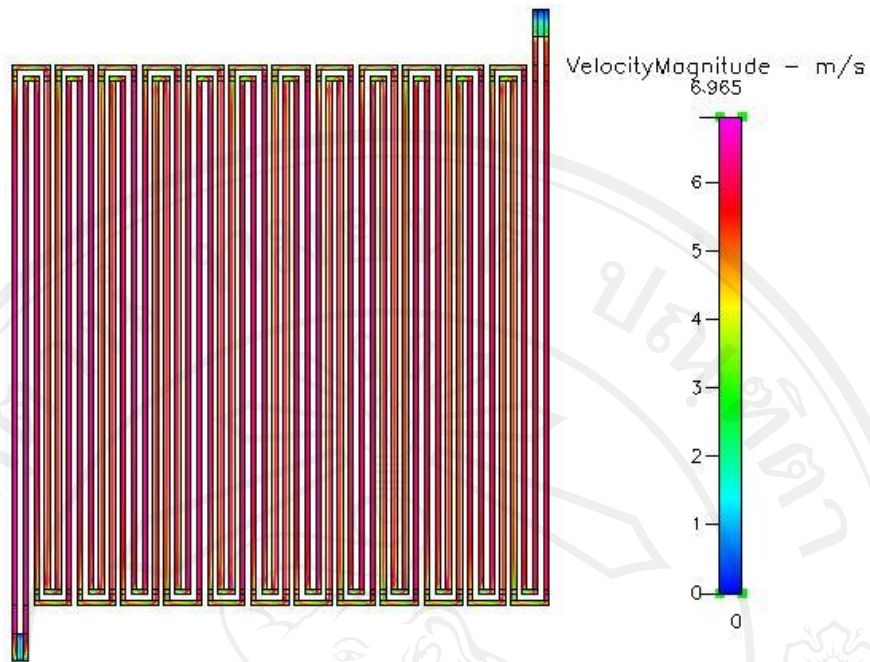
Figure B.83 Velocity distribution at 500 cm^3/min of 2 channels manifold
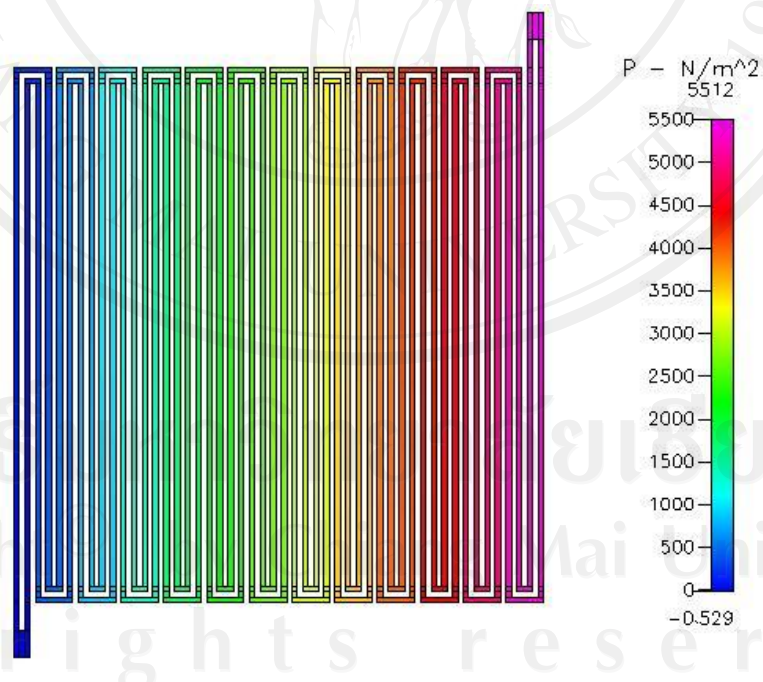
Figure B.84 Pressure distribution at 500 cm^3/min of 2 channels manifold

- **In 3 channels**
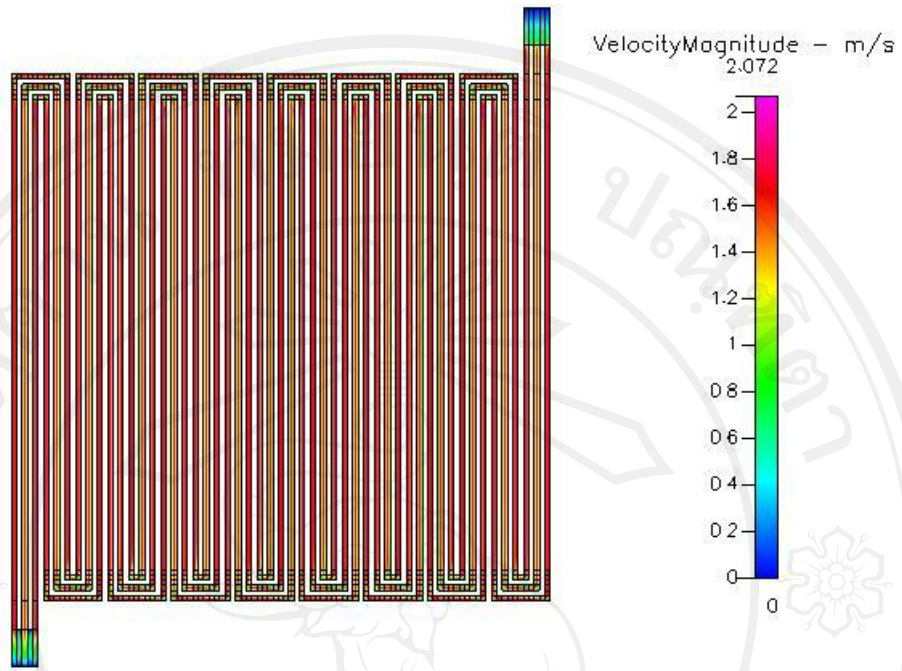
Figure B.85 Velocity distribution at 200 cm^3/min of 3 channels manifold
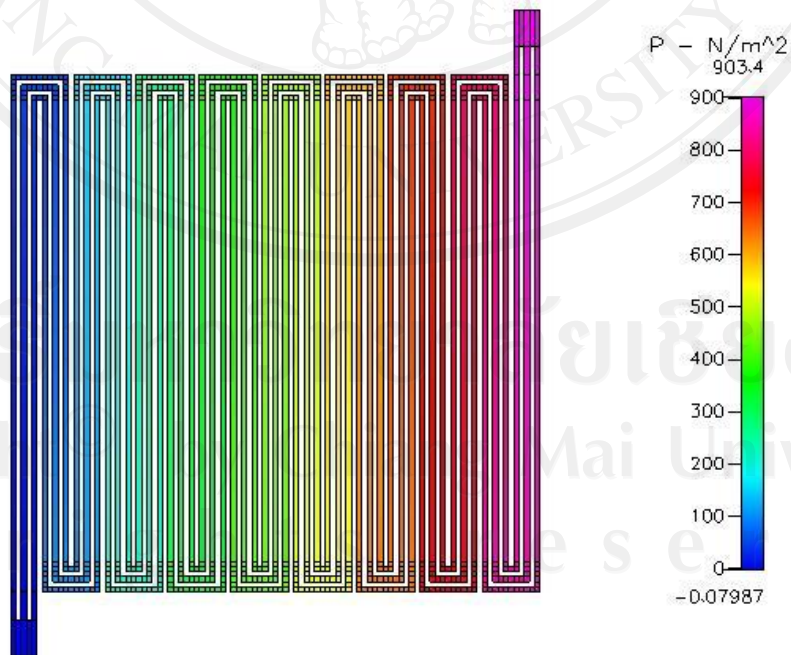
Figure B.86 Pressure distribution at 200 cm^3/min of 3 channels manifold
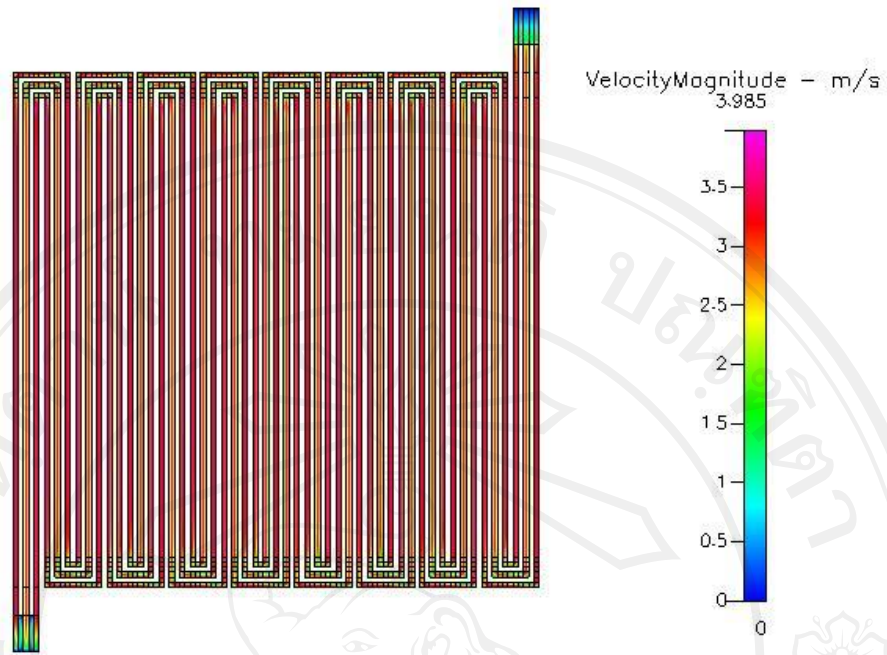
Figure B.87 Velocity distribution at 400 cm^3/min of 3 channels manifold
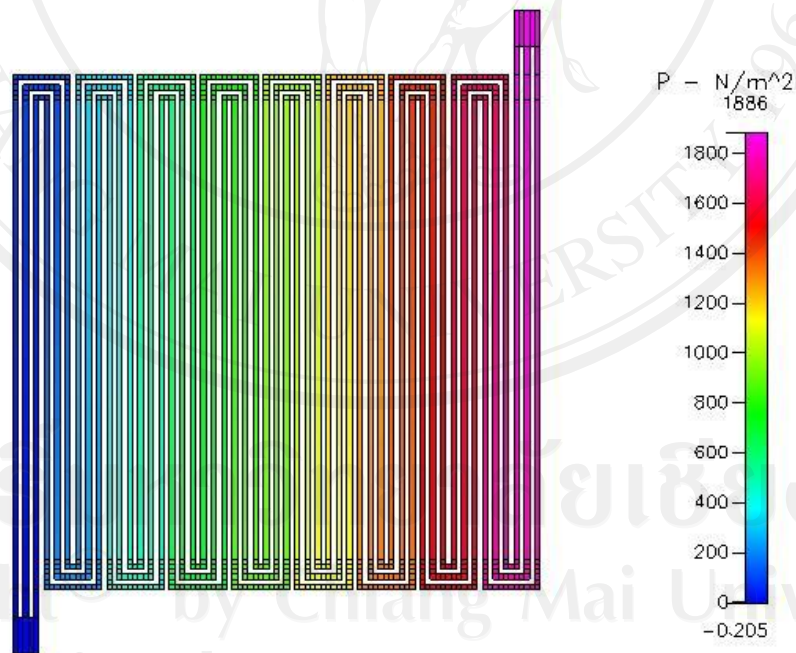
Figure B.88 Pressure distribution at 400 cm^3/min of 3 channels manifold
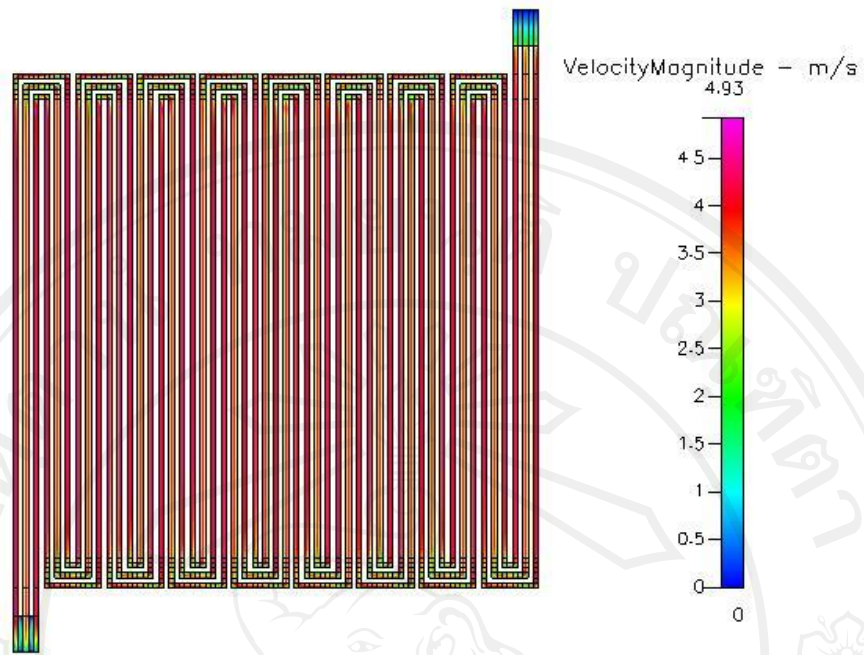
Figure B.89 Velocity distribution at 500 cm^3/min of 3 channels manifold
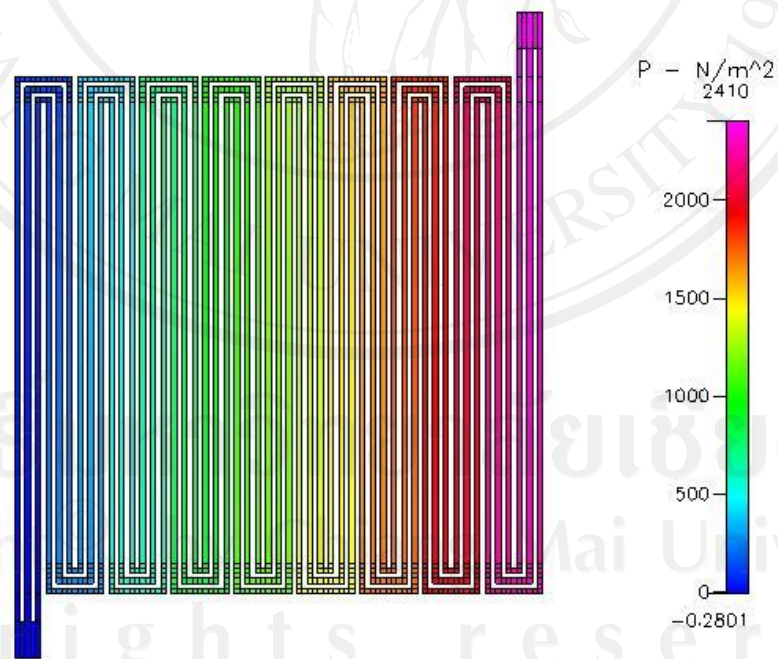
Figure B.90 Pressure distribution at 500 cm^3/min of 3 channels manifold

- **In 4 channels**
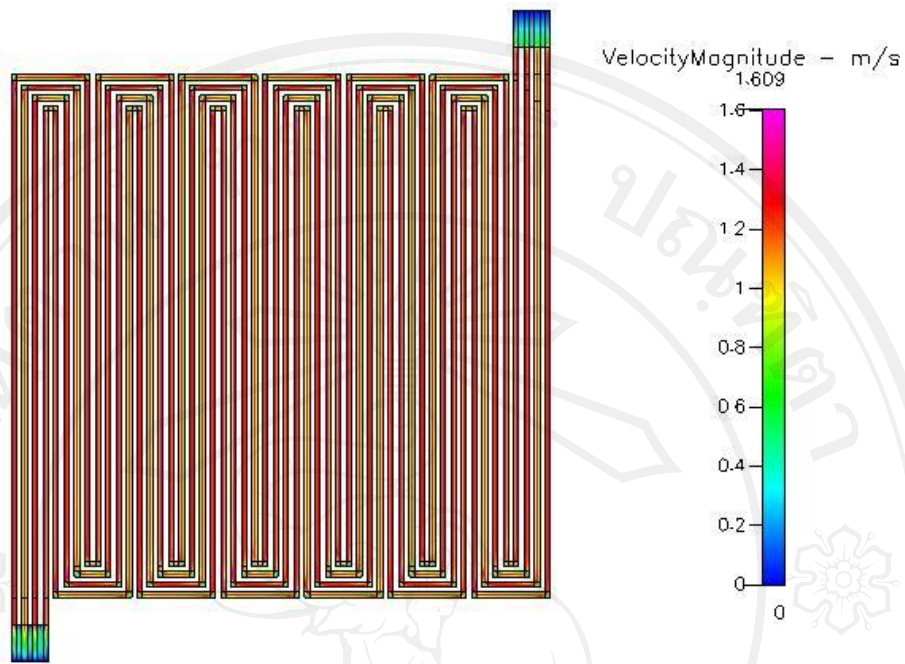
Figure B.91 Velocity distribution at 200 cm^3/min of 4 channels manifold
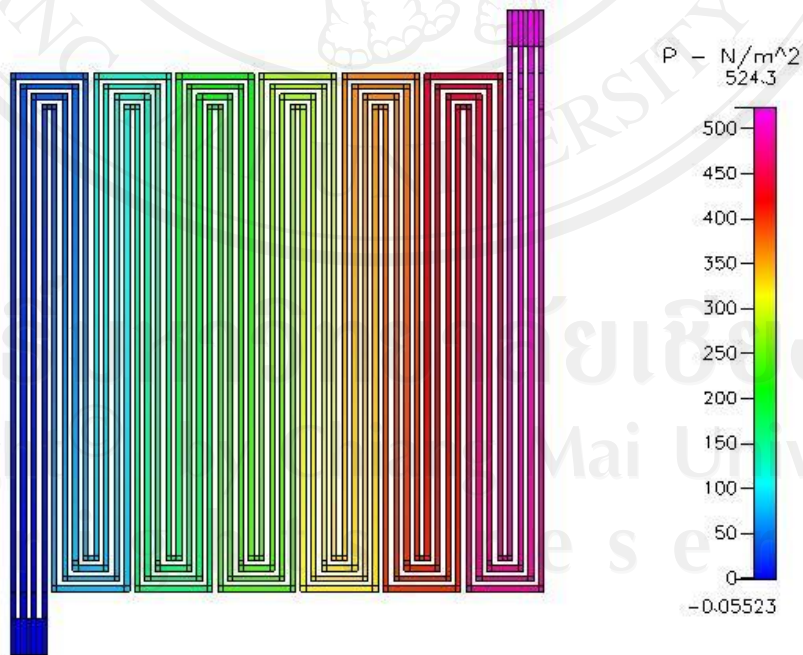
Figure B.92 Pressure distribution at 200 cm^3/min of 4 channels manifold
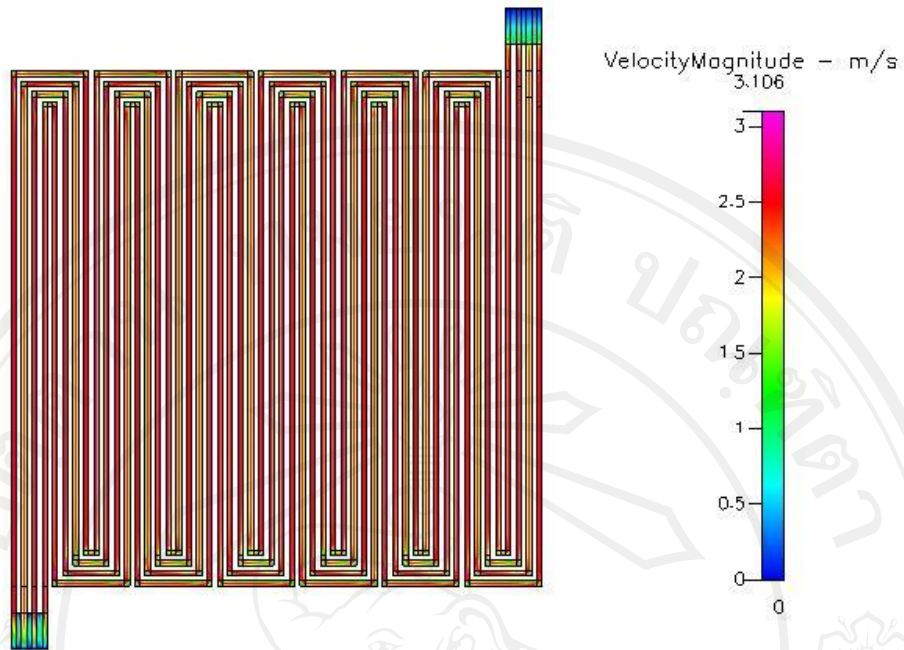
Figure B.93 Velocity distribution at 400 cm^3/min of 4 channels manifold
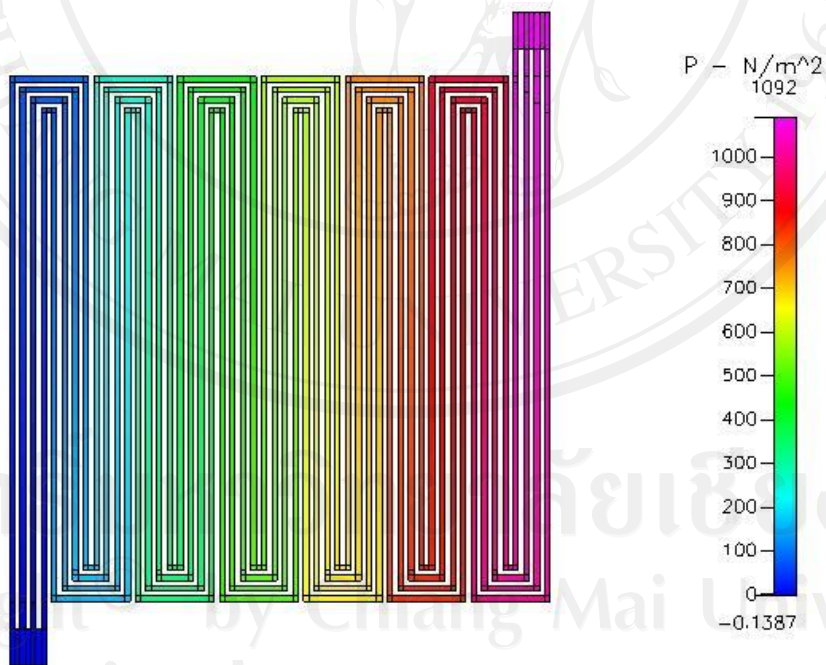
Figure B.94 Pressure distribution at 400 cm^3/min of 4 channels manifold
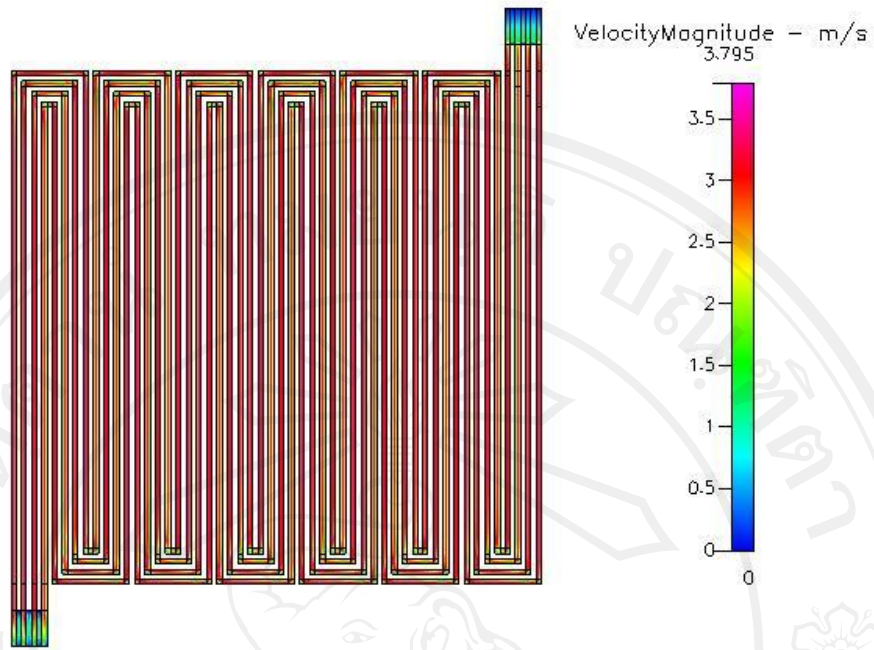
Figure B.95 Velocity distribution at 500 cm^3/min of 4 channels manifold
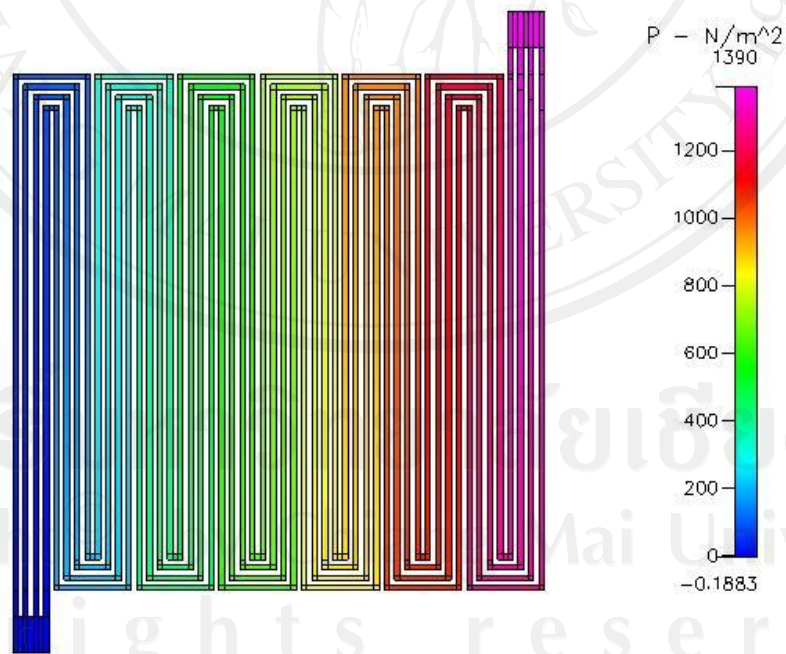
Figure B.96 Pressure distribution at 500 cm^3/min of 4 channels manifold

- **In 5 channels**
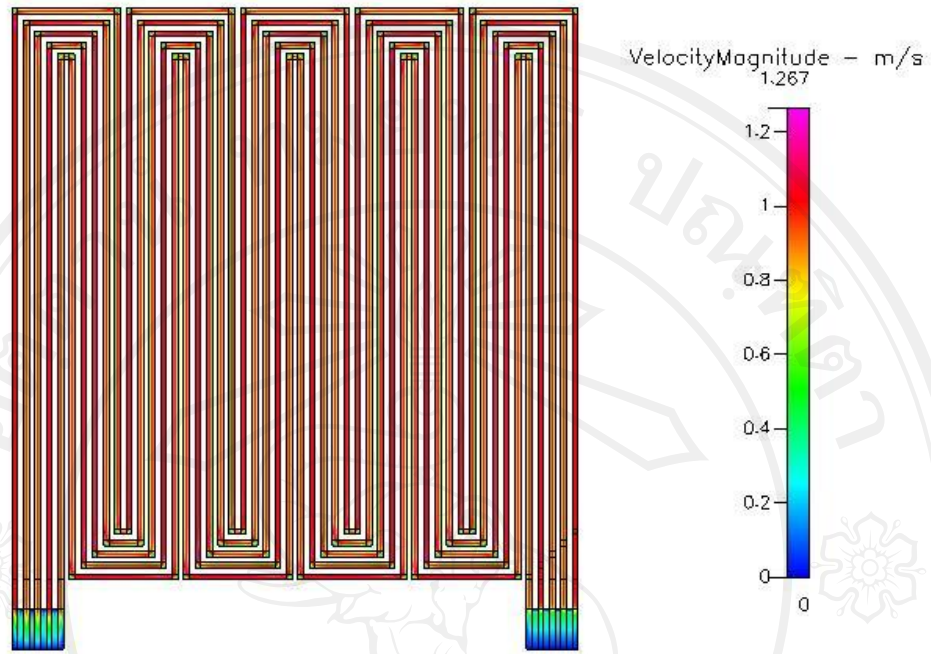
Figure B.97 Velocity distribution at 200 cm^3/min of 5 channels manifold
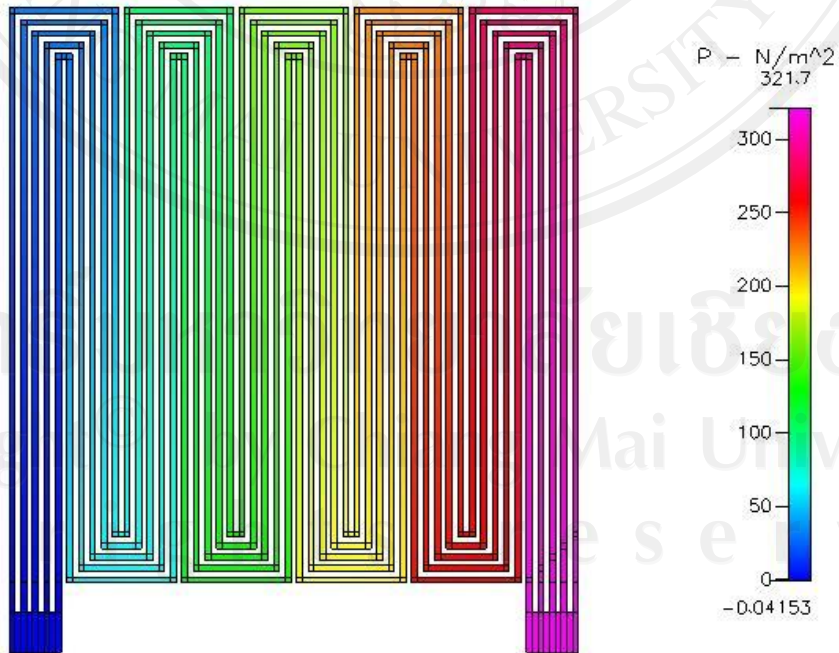
Figure B.98 Pressure distribution at 200 cm^3/min of 5 channels manifold
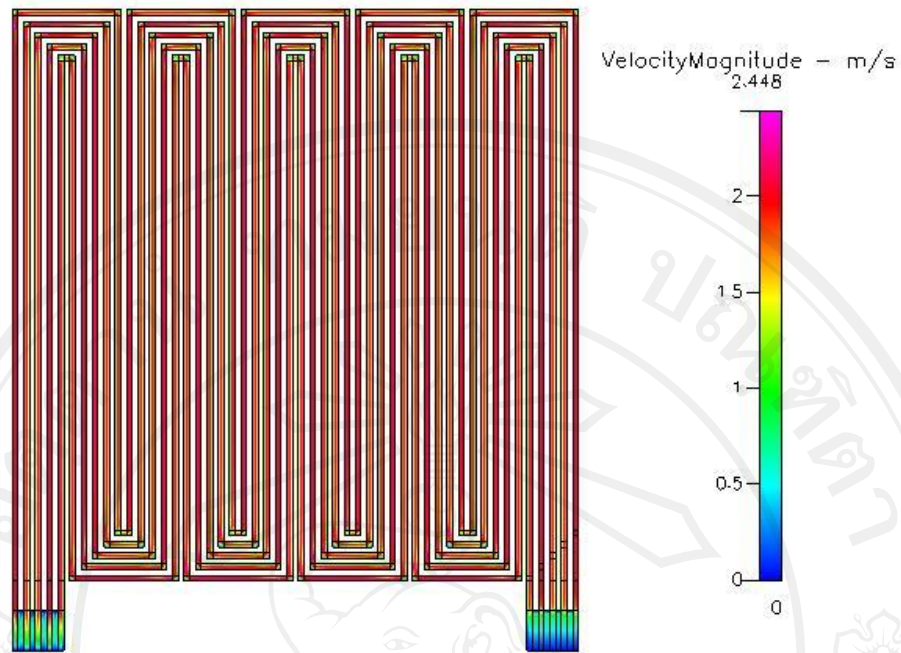
Figure B.99 Velocity distribution at 400 cm^3/min of 5 channels manifold
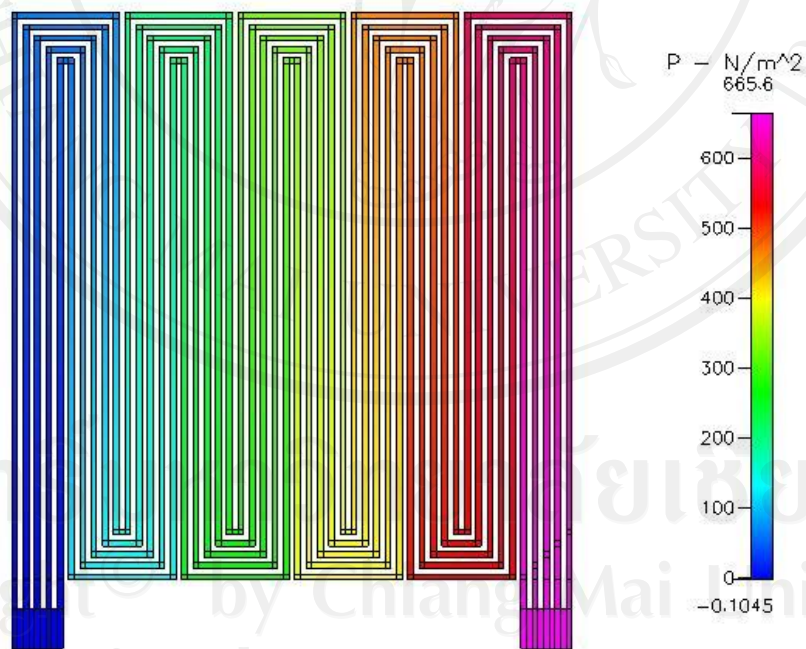
Figure B.100 Pressure distribution at 400 cm^3/min of 5 channels manifold
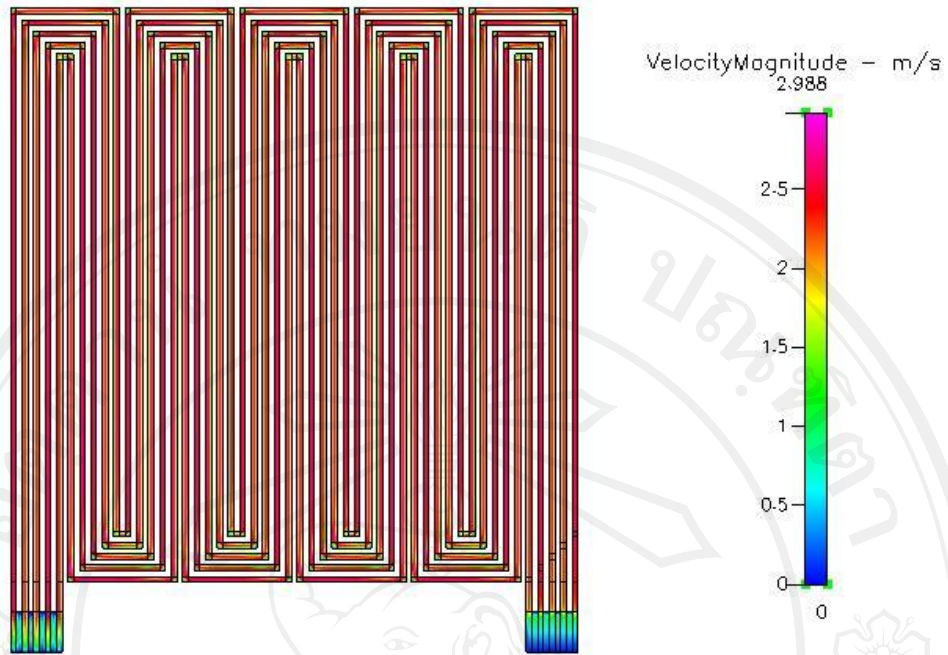
Figure B.101 Velocity distribution at 500 cm^3/min of 5 channels manifold
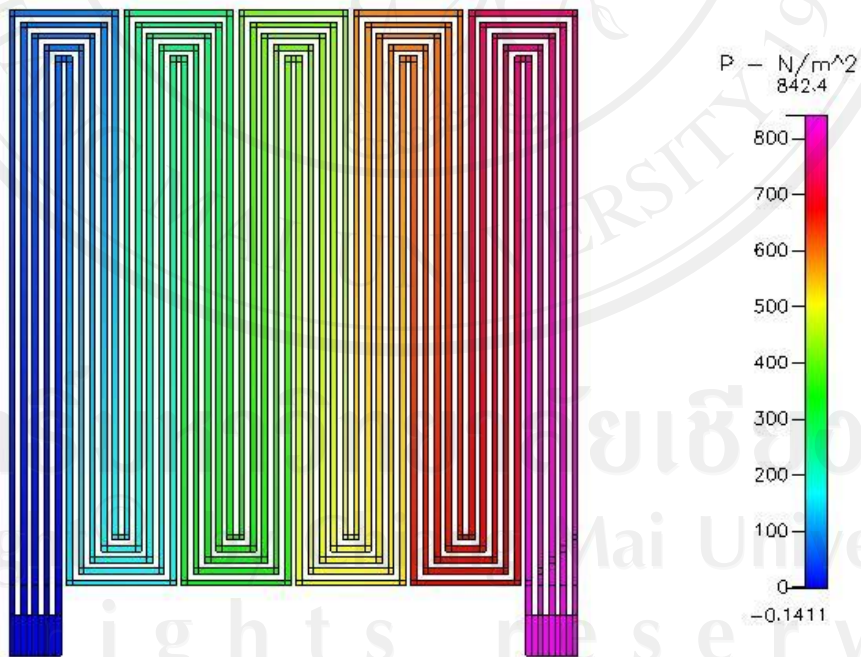
Figure B.102 Pressure distribution at 500 cm^3/min of 5 channels manifold

- **In 6 channels**

Figure B.103 Velocity distribution at 200 cm^3/min of 6 channels manifold
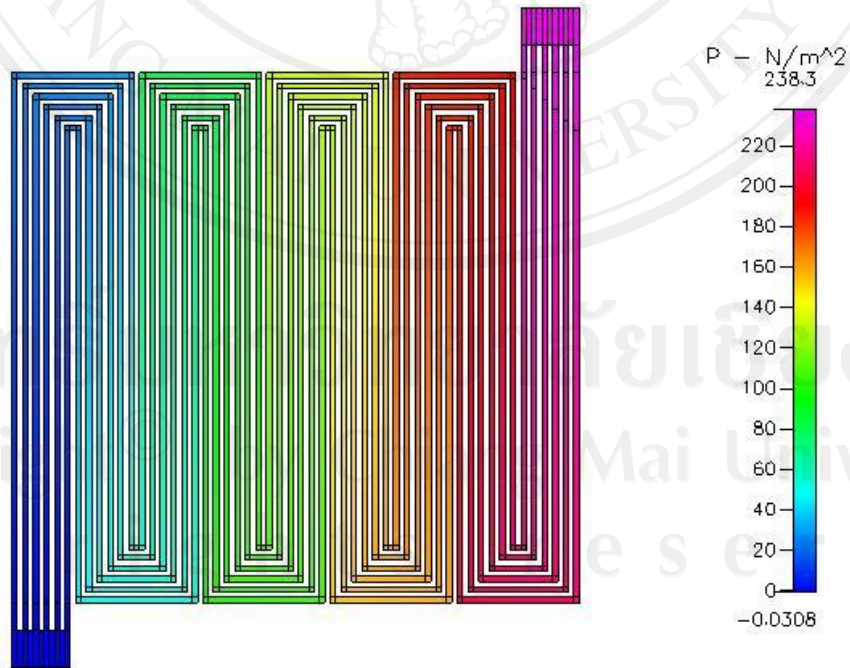
Figure B.104 Pressure distribution at 200 cm^3/min of 6 channels manifold

Figure B.105 Velocity distribution at 400 cm^3/min of 6 channels manifold
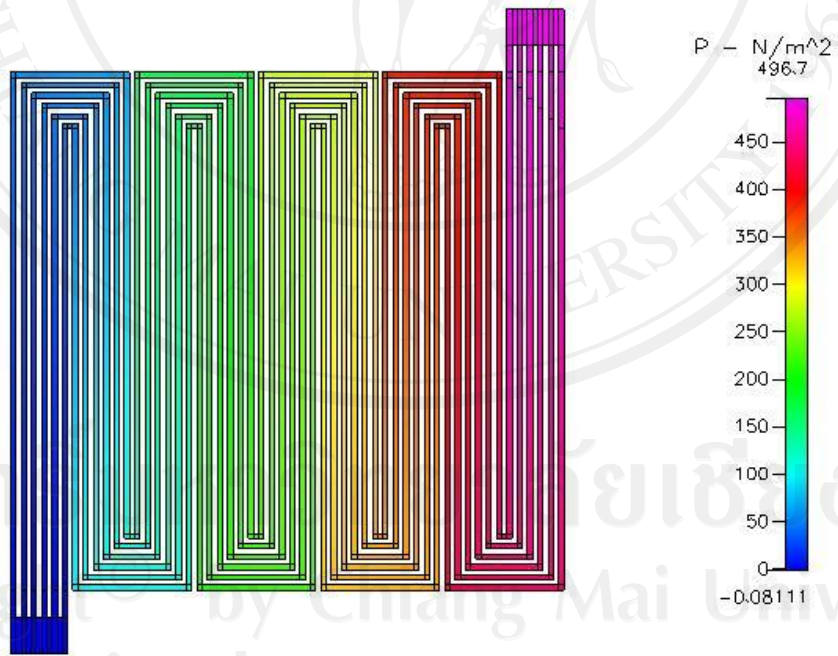
Figure B.106 Pressure distribution at 400 cm^3/min of 6 channels manifold
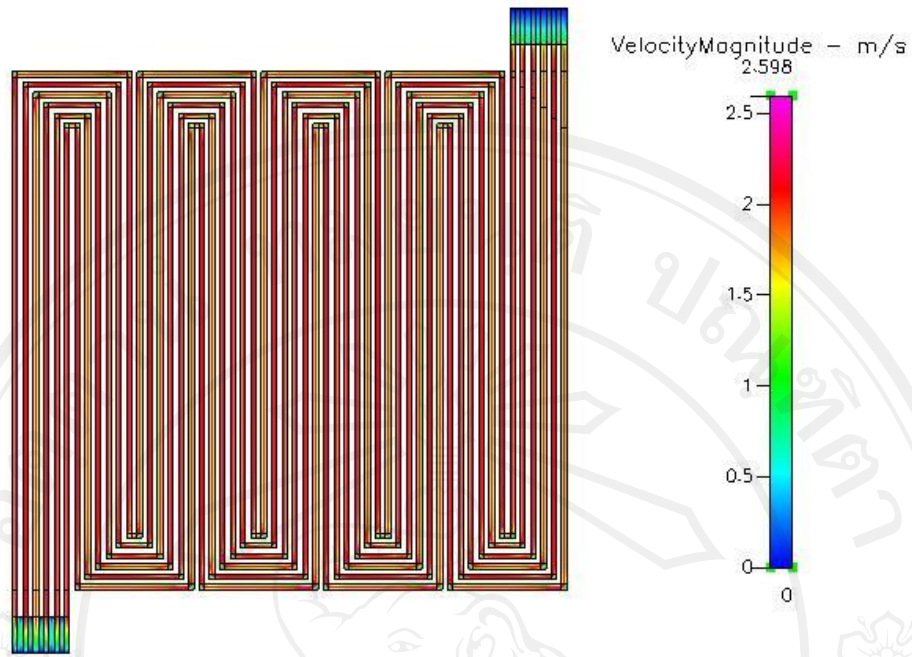
Figure B.107 Velocity distribution at 500 cm^3/min of 6 channels manifold
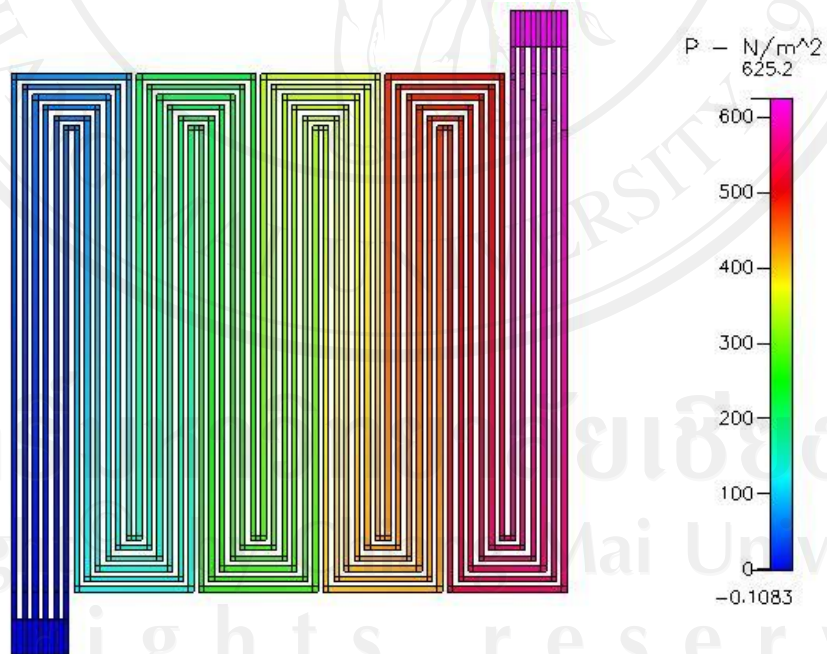
Figure B.108 Pressure distribution at 500 cm^3/min of 6 channels manifold

- **In 90 turn non-fillet manifold**

Figure B.109 Velocity distribution at 200 cm^3/min of 90 turn non-fillet manifold
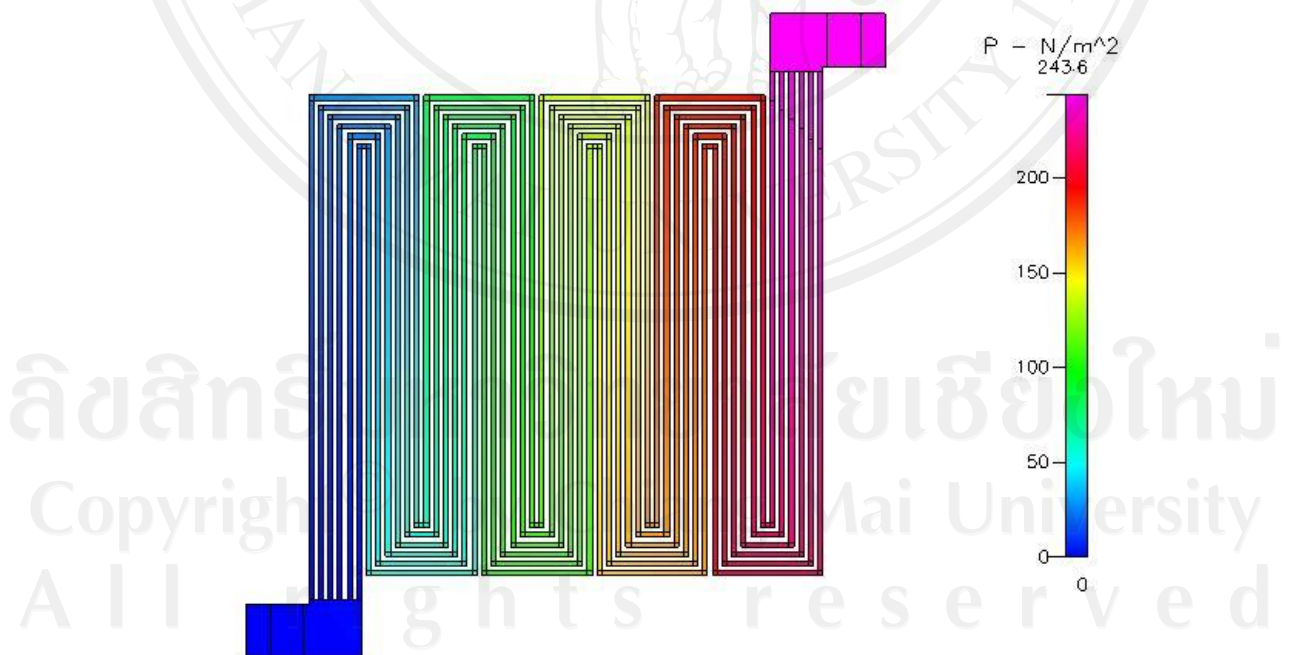
Figure B.110 Pressure distribution at 200 cm^3/min of 90 turn non-fillet manifold
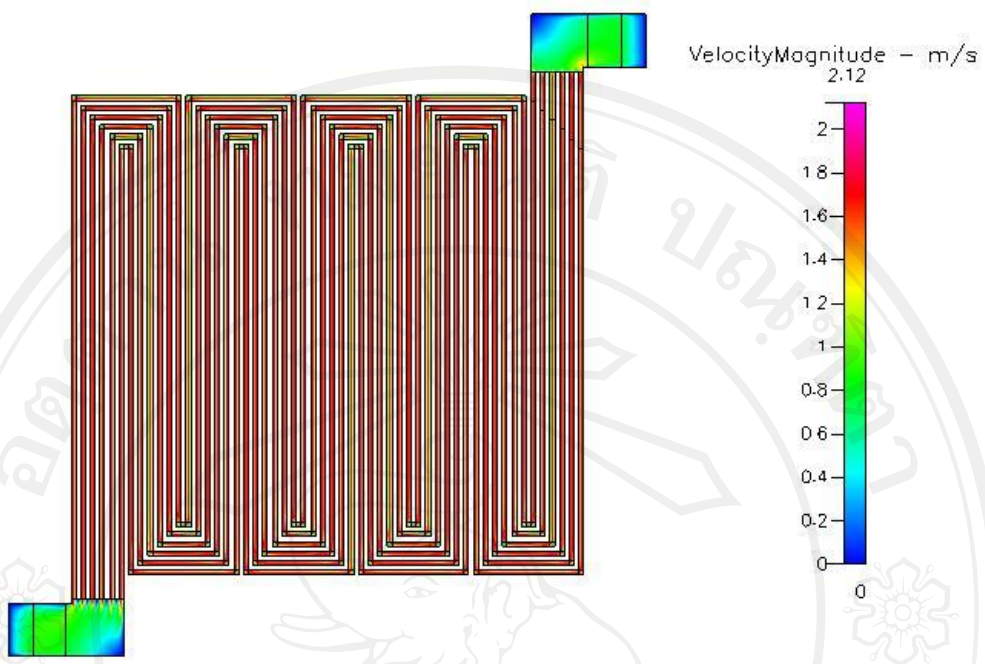
Figure B.111 Velocity distribution at 400 cm^3/min of 90 turn non-fillet manifold
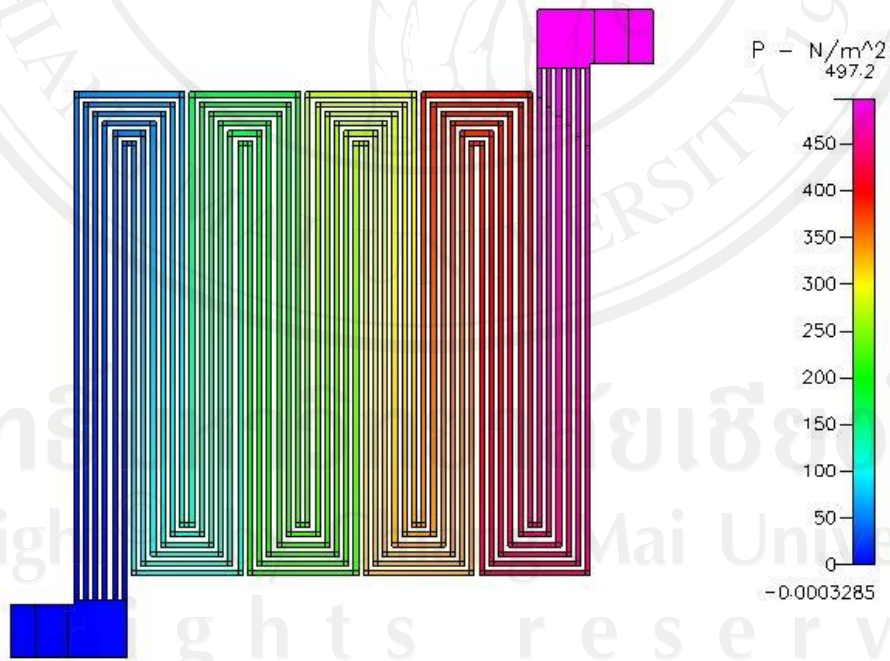
Figure B.112 Pressure distribution at 400 cm^3/min of 90 turn non-fillet manifold
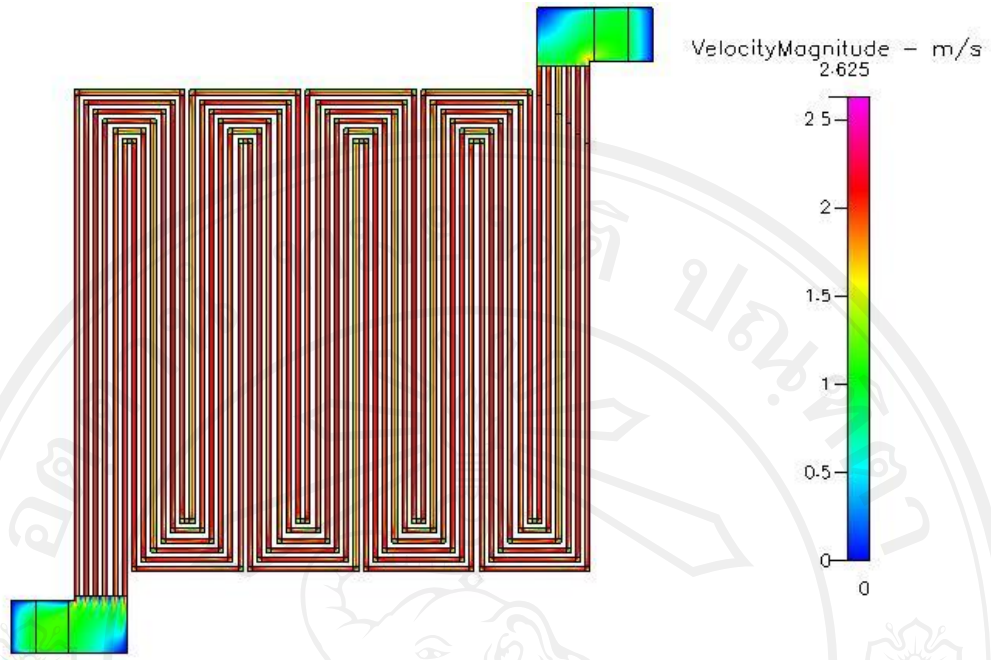
Figure B.113 Velocity distribution at 500 cm^3/min of 90 turn non-fillet manifold
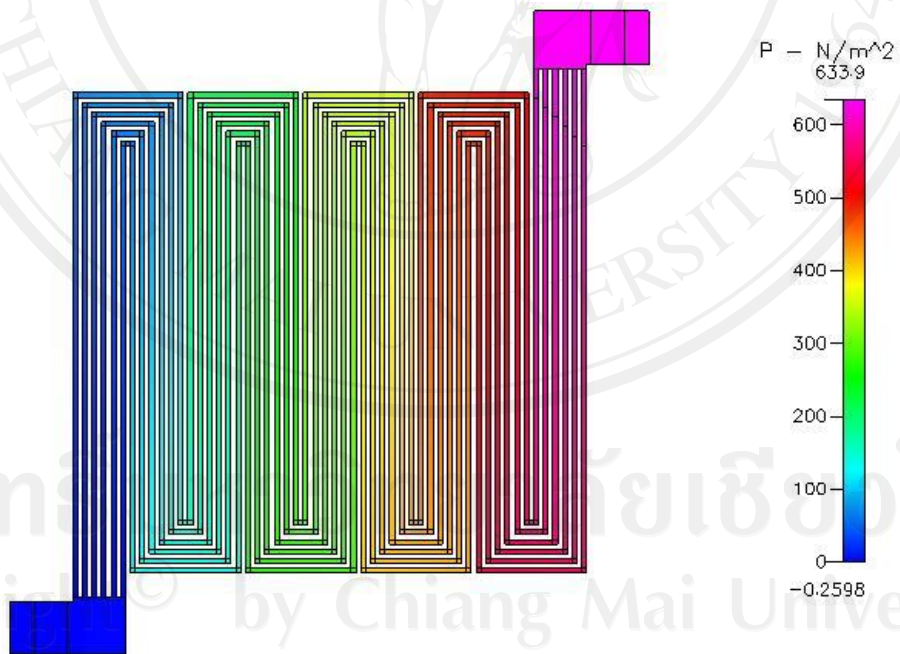
Figure B.114 Pressure distribution at 500 cm^3/min of 90 turn non-fillet manifold

- **In 90 turn outside fillet manifold**
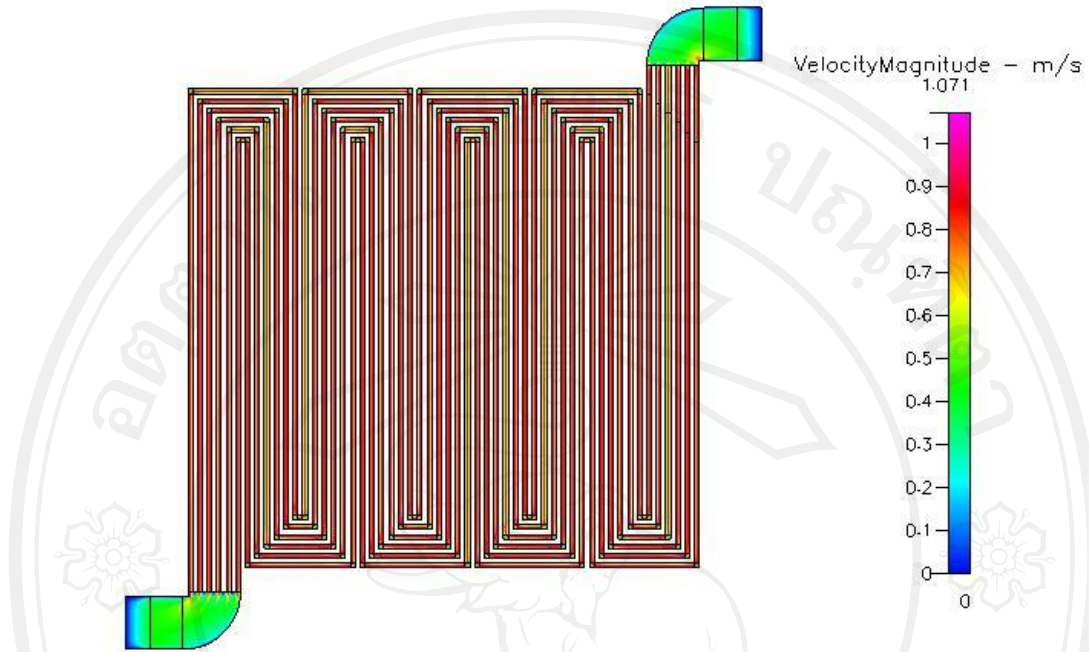
Figure B.115 Velocity distribution at 200 cm^3/min of 90 turn outside fillet manifold
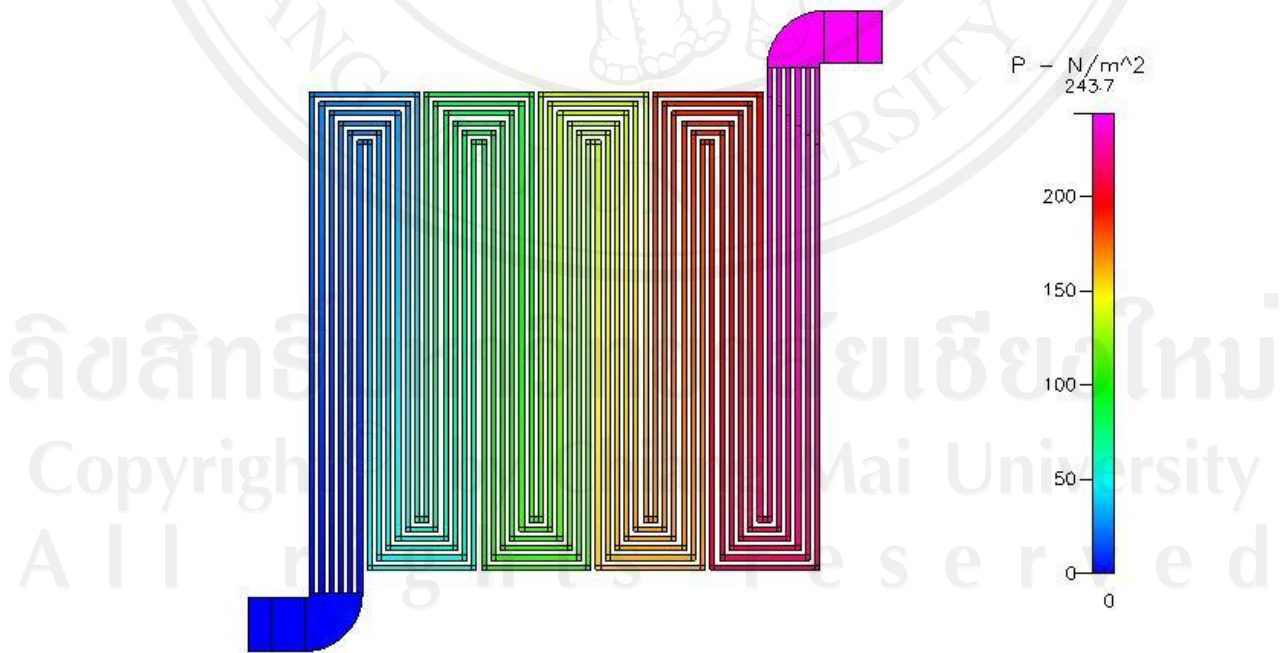
Figure B.116 Pressure distribution at 200 cm^3/min of 90 turn outside fillet manifold
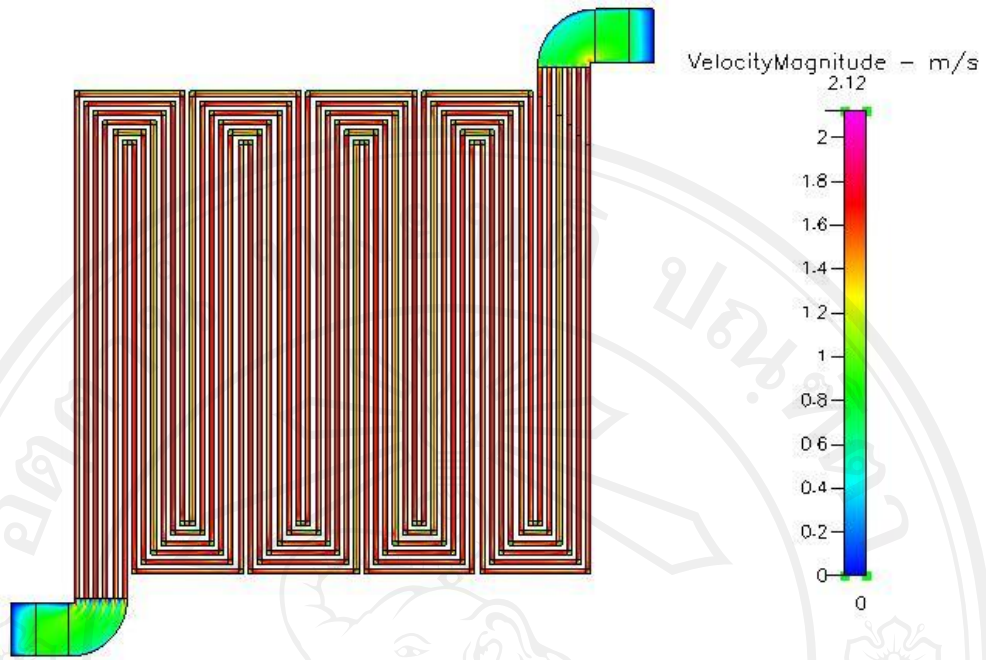
Figure B.117 Velocity distribution at 400 cm^3/min of 90 turn outside fillet manifold
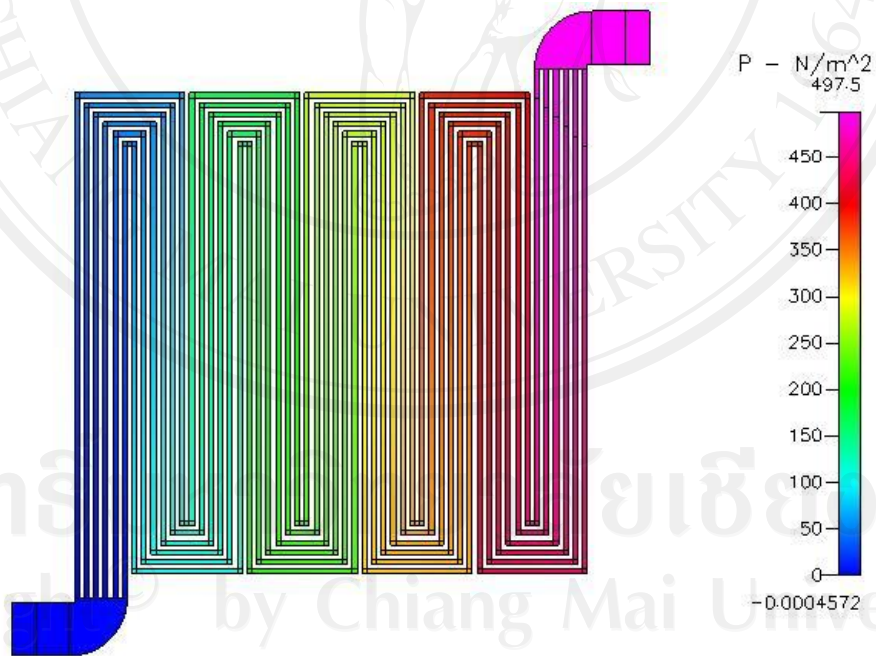
Figure B.118 Pressure distribution at 400 cm^3/min of 90 turn outside fillet manifold

Figure B.119 Velocity distribution at 500 cm^3/min of 90 turn outside fillet manifold
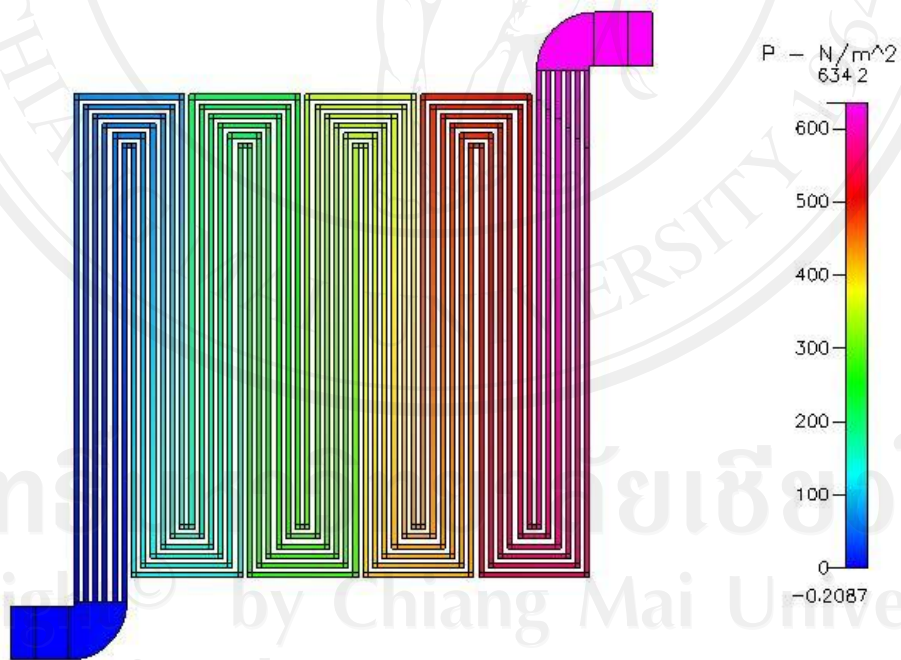
Figure B.120 Pressure distribution at 500 cm^3/min of 90 turn outside fillet manifold

- **In 90 turn fillet manifold**
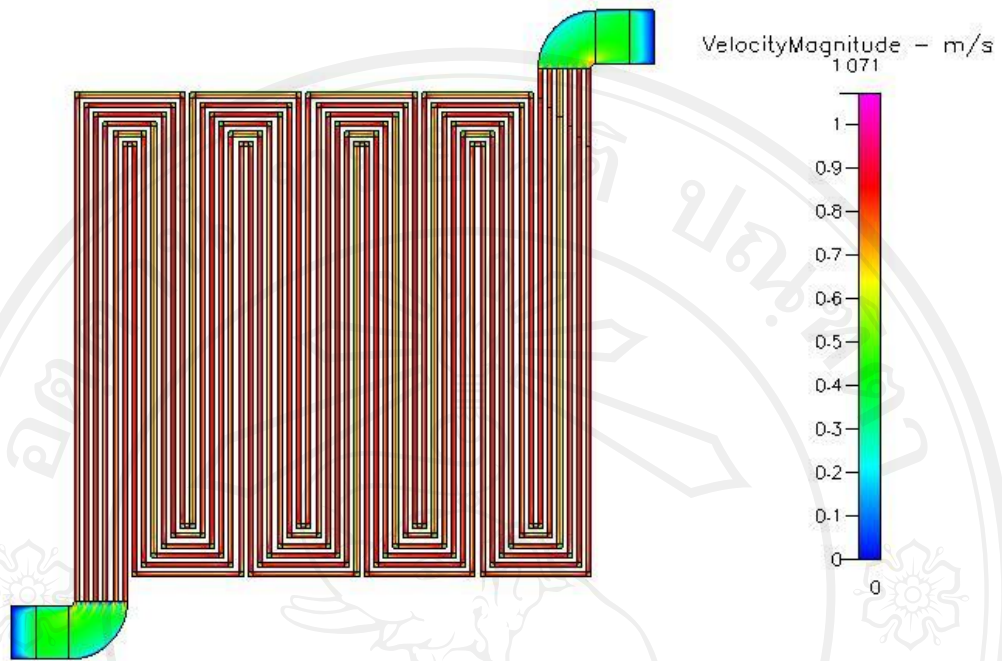
Figure B.121 Velocity distribution at 200 cm^3/min of 90 turn fillet manifold
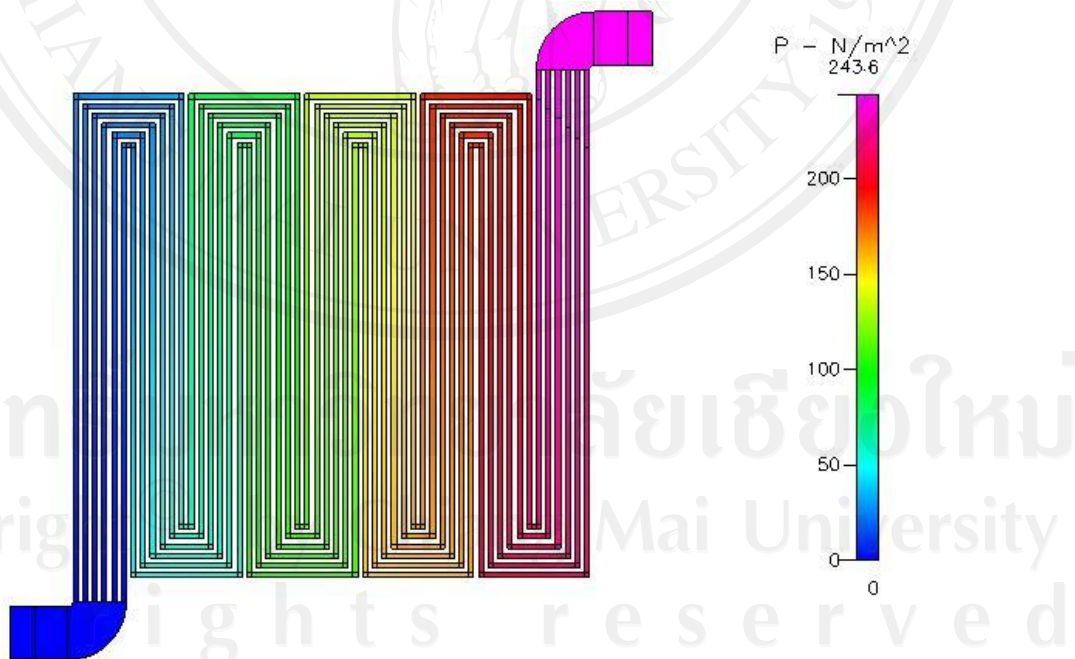
Figure B.122 Pressure distribution at 200 cm^3/min of 90 turn fillet manifold
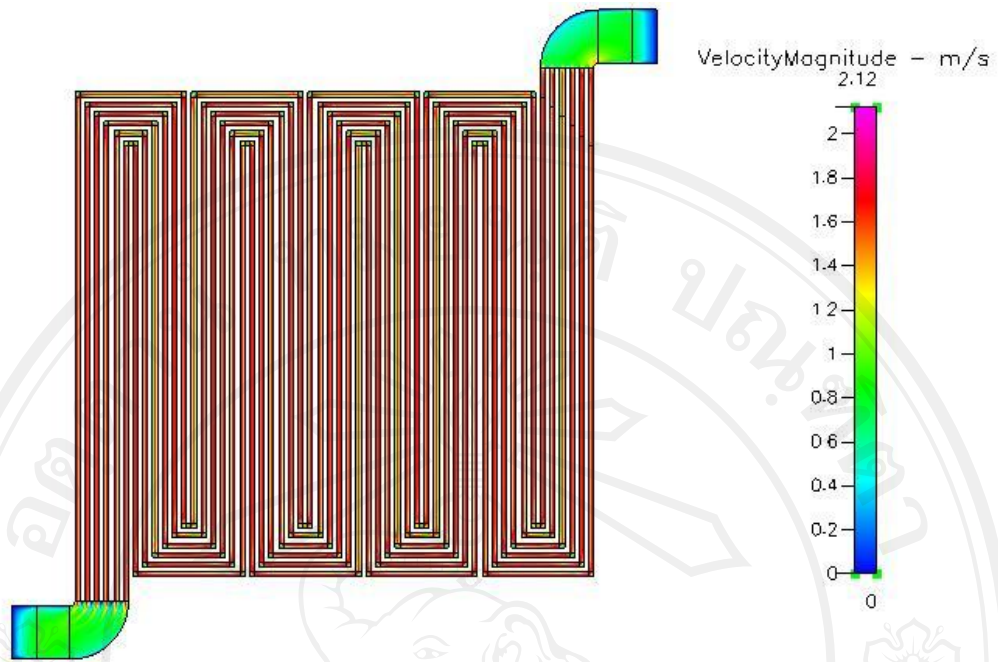
Figure B.123 Velocity distribution at 400 cm^3/min of 90 turn fillet manifold
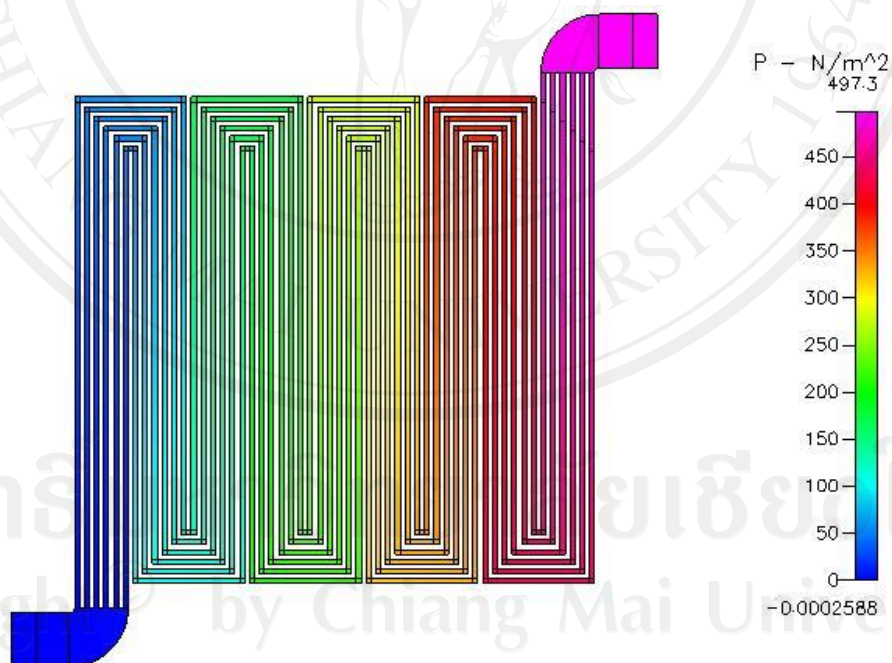
Figure B.124 Pressure distribution at 400 cm^3/min of 90 turn fillet manifold

Figure B.125 Velocity distribution at 500 cm^3/min of 90 turn fillet manifold
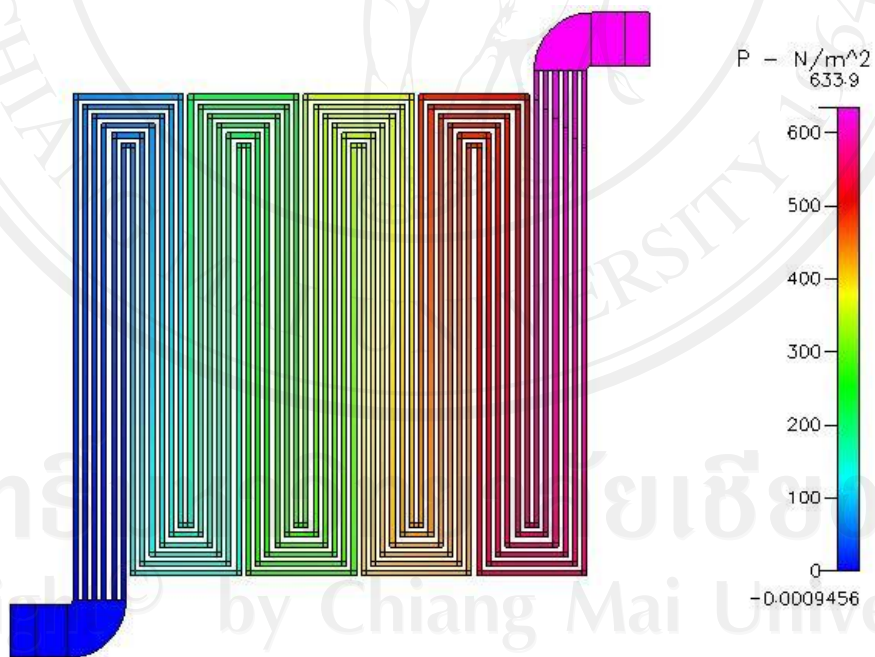
Figure B.126 Pressure distribution at 500 cm^3/min of 90 turn fillet manifold

- **In 45 turn manifold**
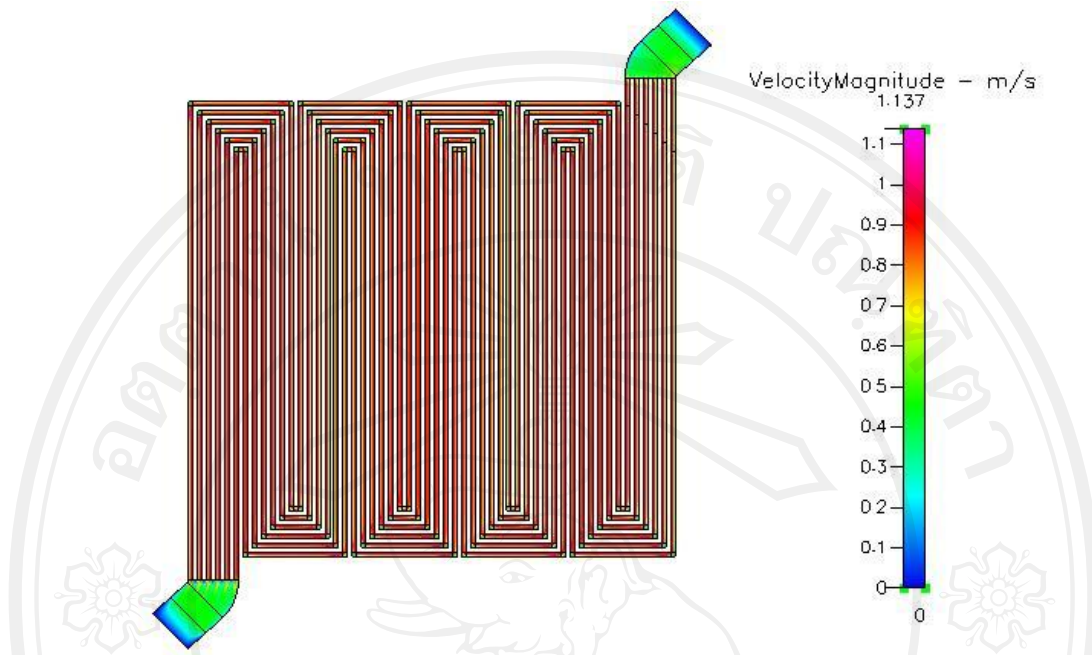
Figure B.127 Velocity distribution at 200 cm^3/min of 45 turn manifold
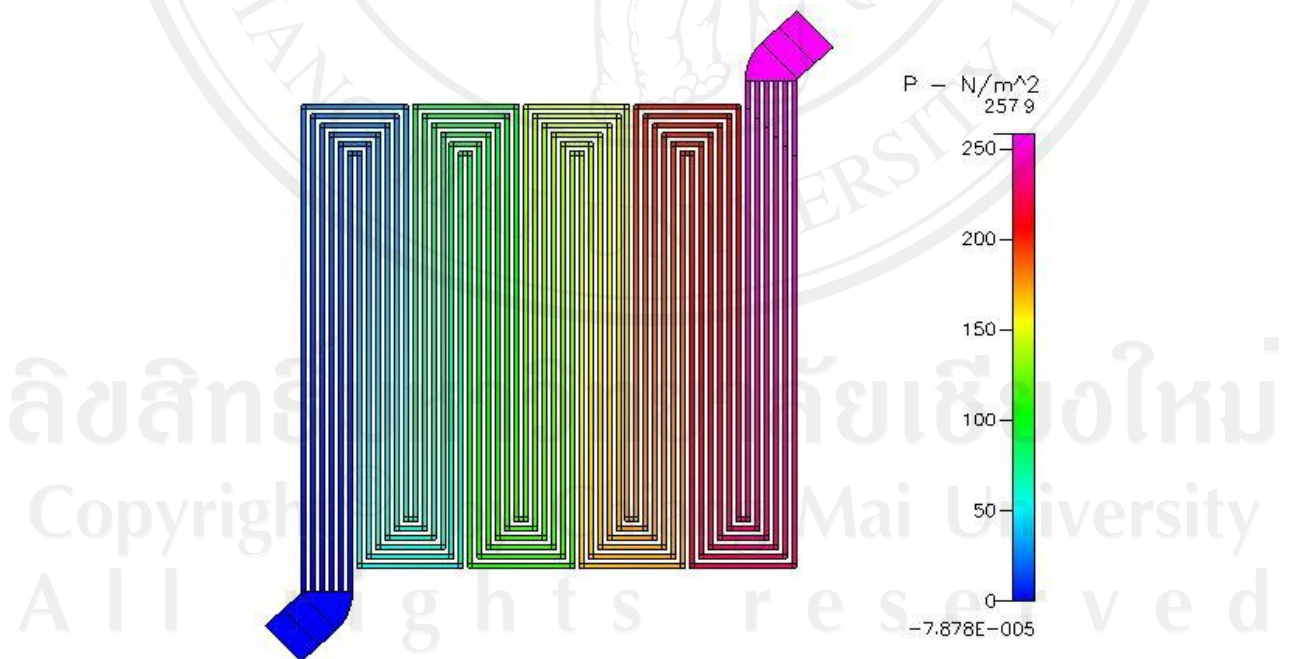
Figure B.128 Pressure distribution at 200 cm^3/min of 45 turn manifold
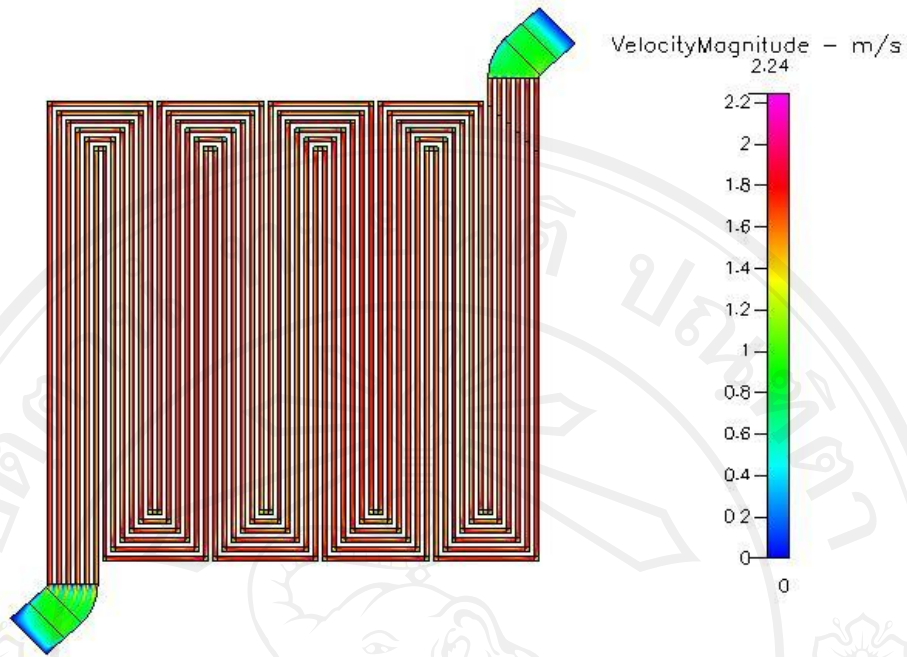
Figure B.129 Velocity distribution at 400 cm^3/min of 45 turn manifold
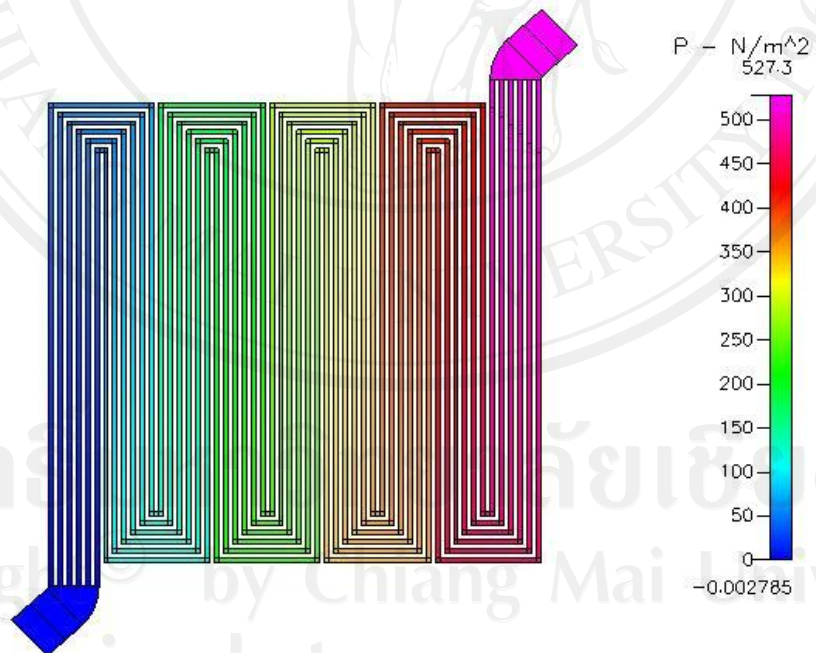
Figure B.130 Pressure distribution at 400 cm^3/min of 45 turn manifold
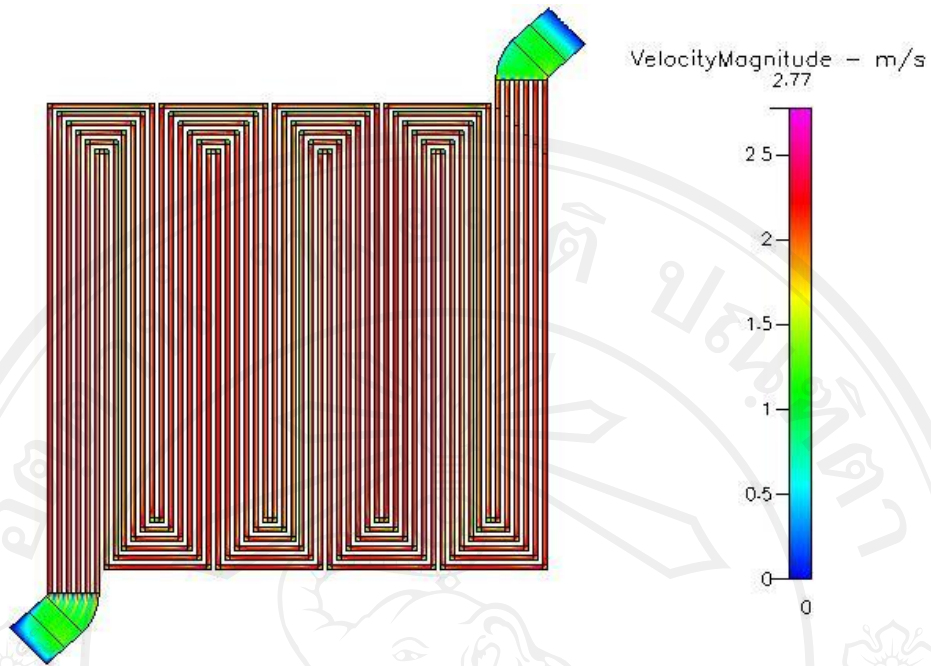
Figure B.131 Velocity distribution at 500 cm^3/min of 45 turn manifold
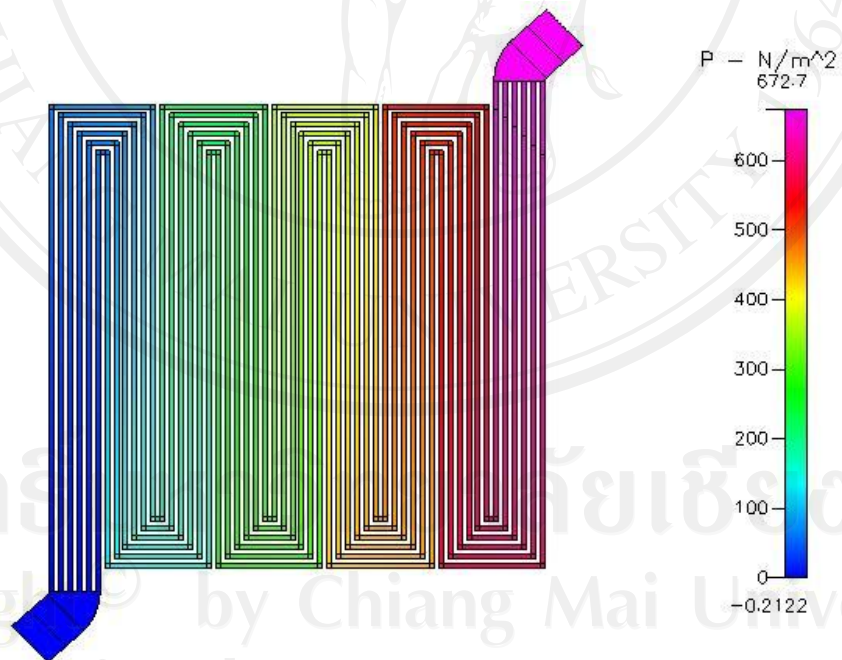
Figure B.132 Pressure distribution at 500 cm^3/min of 45 turn manifold

- **In 2 ways multi-serpentine with header**
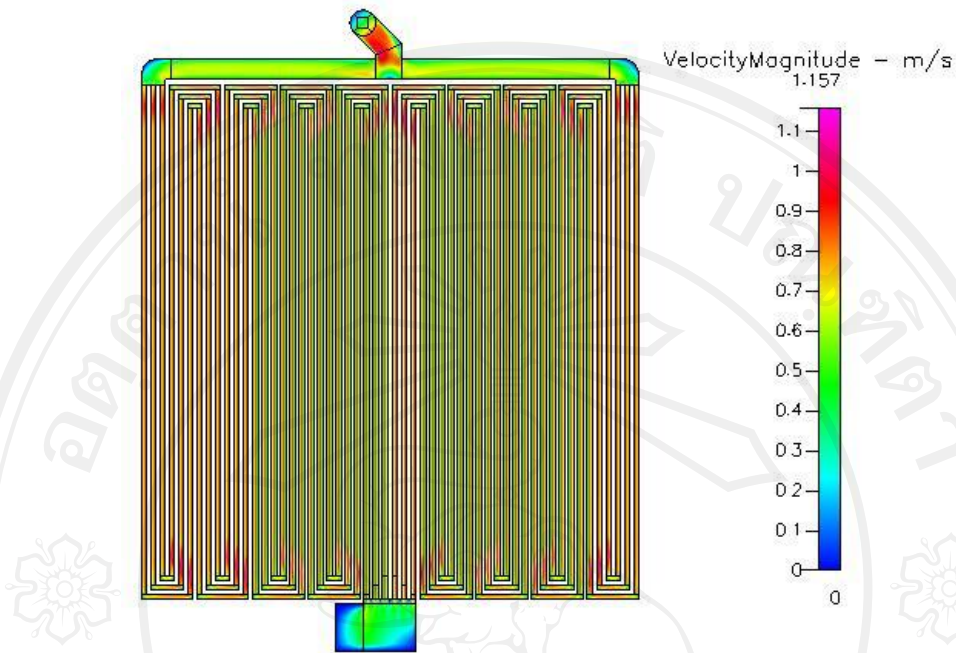
Figure B.133 Velocity distribution at 200 cm^3/min of 2 ways multi-serpentine with header
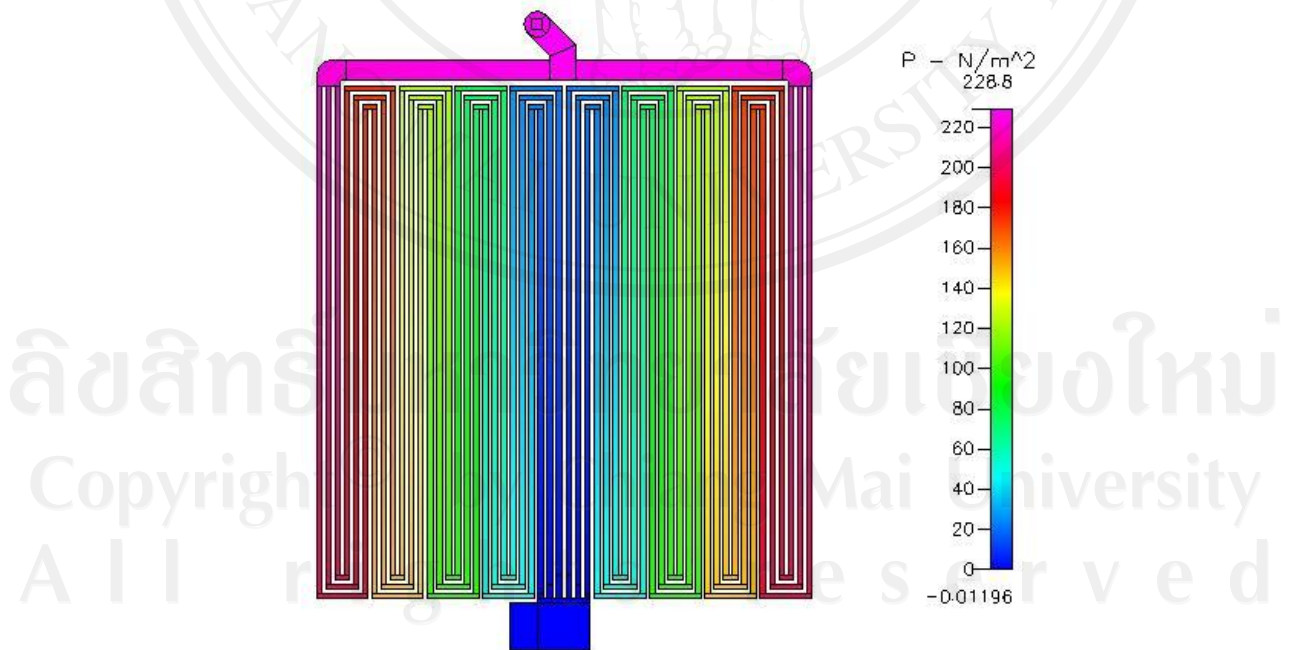
Figure B.134 Pressure distribution at 200 cm^3/min of 2 ways multi-serpentine with header
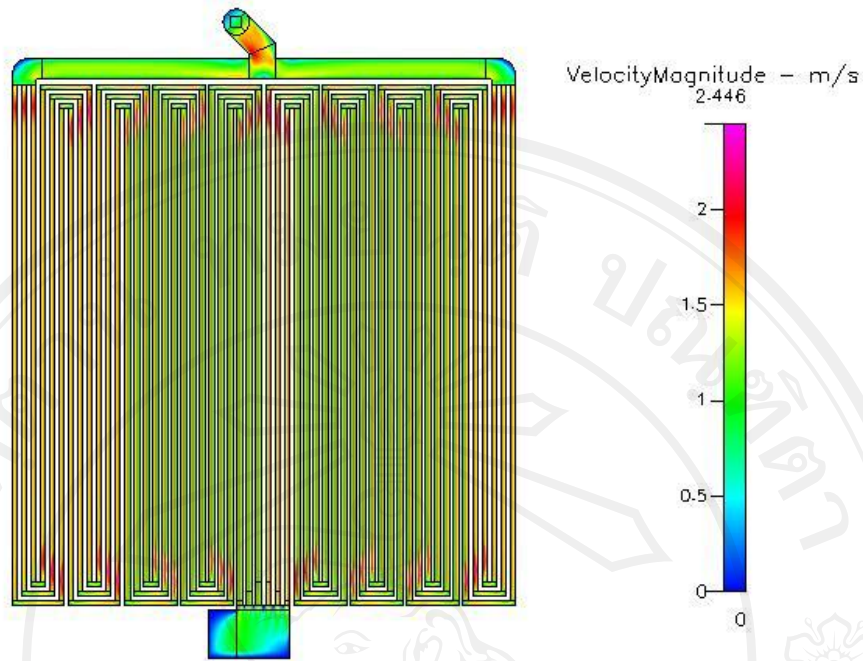
Figure B.135 Velocity distribution at 400 cm^3/min of 2 ways multi-serpentine with
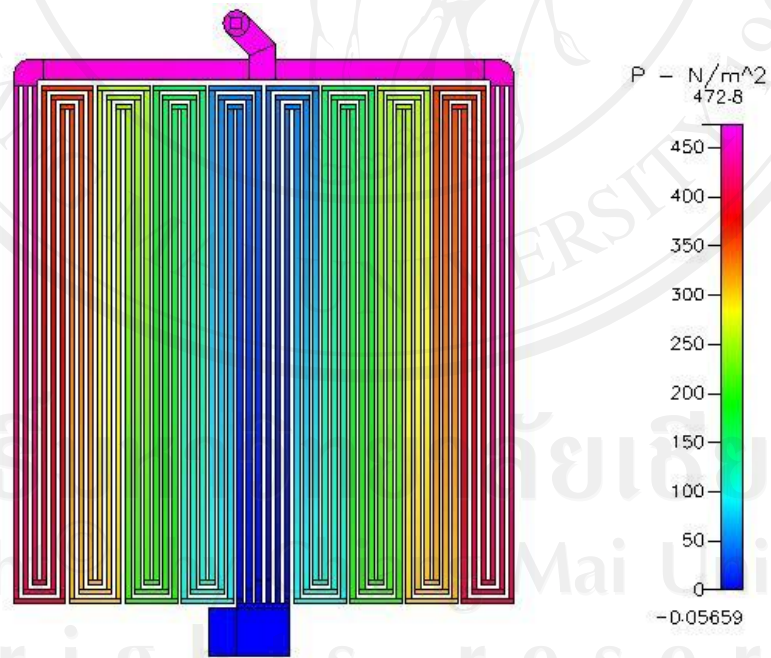
header

Figure B.136 Pressure distribution at 400 cm^3/min of 2 ways multi-serpentine with
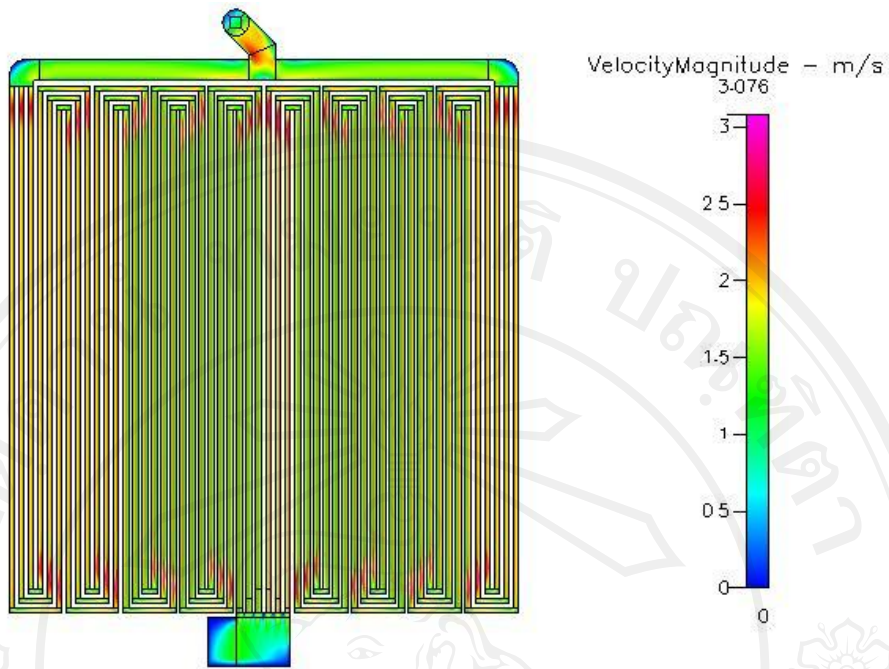
header

Figure B.137 Velocity distribution at 500 cm^3/min of 2 ways multi-serpentine with header
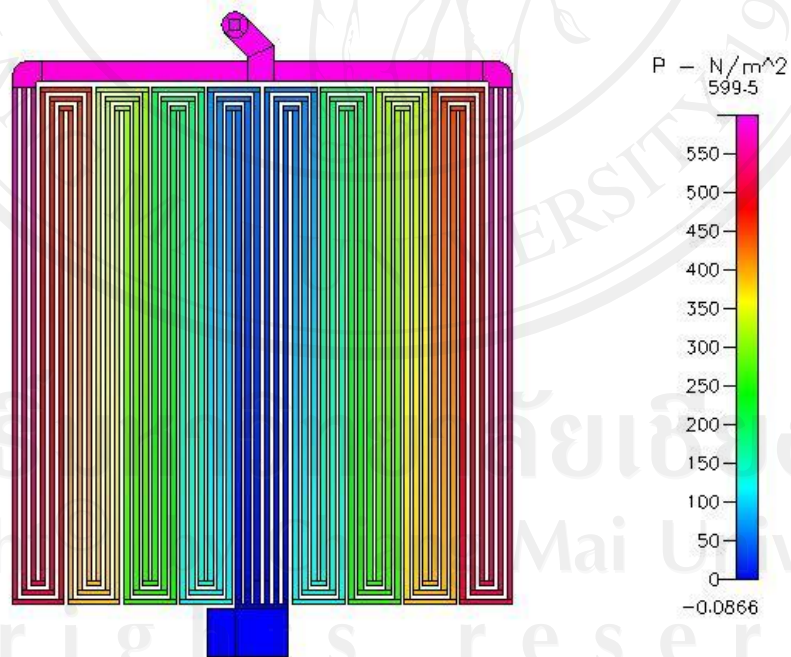
Figure B.138 Pressure distribution at 500 cm^3/min of 2 ways multi-serpentine with header

252
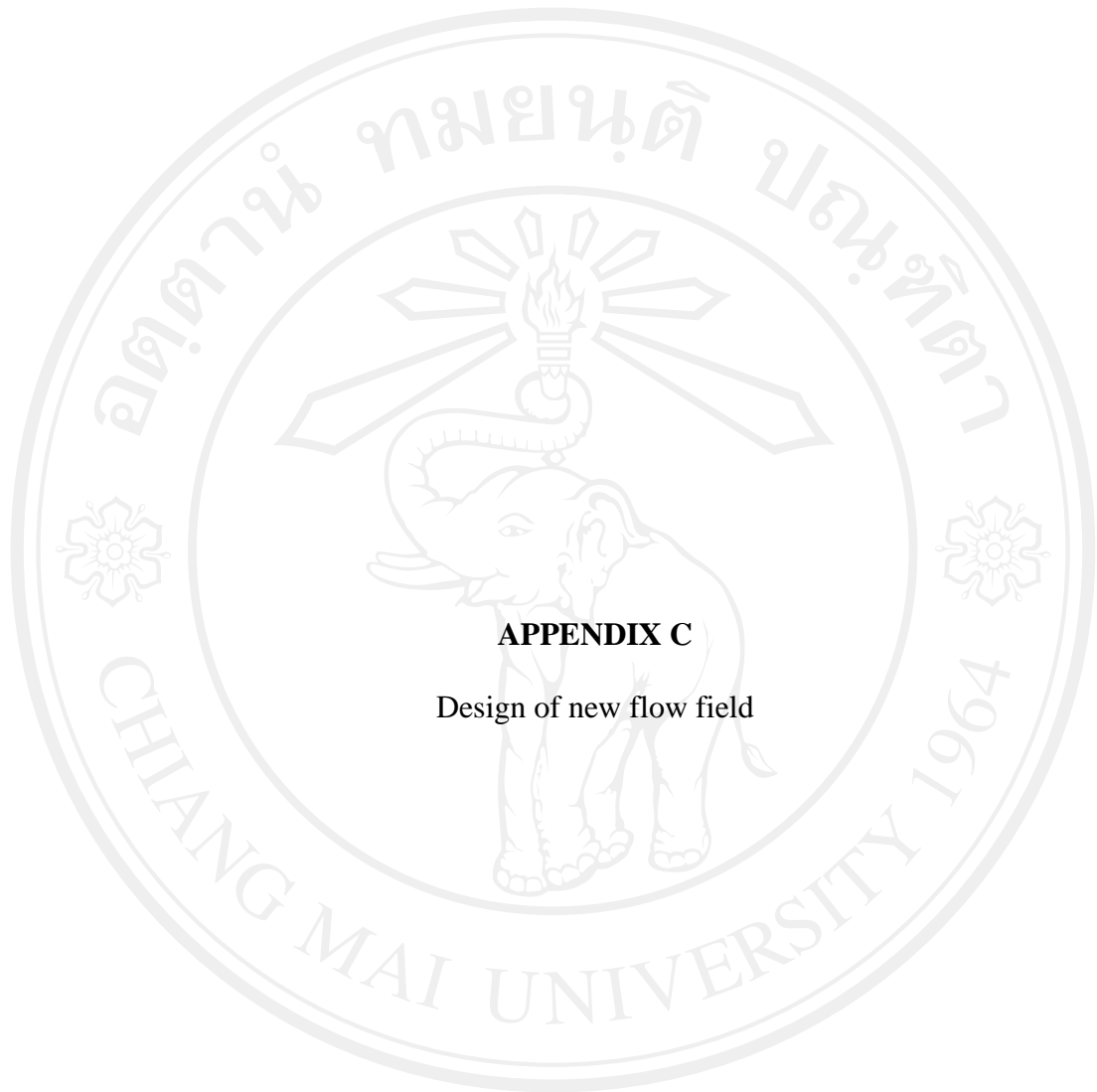
APPENDIX C

Design of new flow field
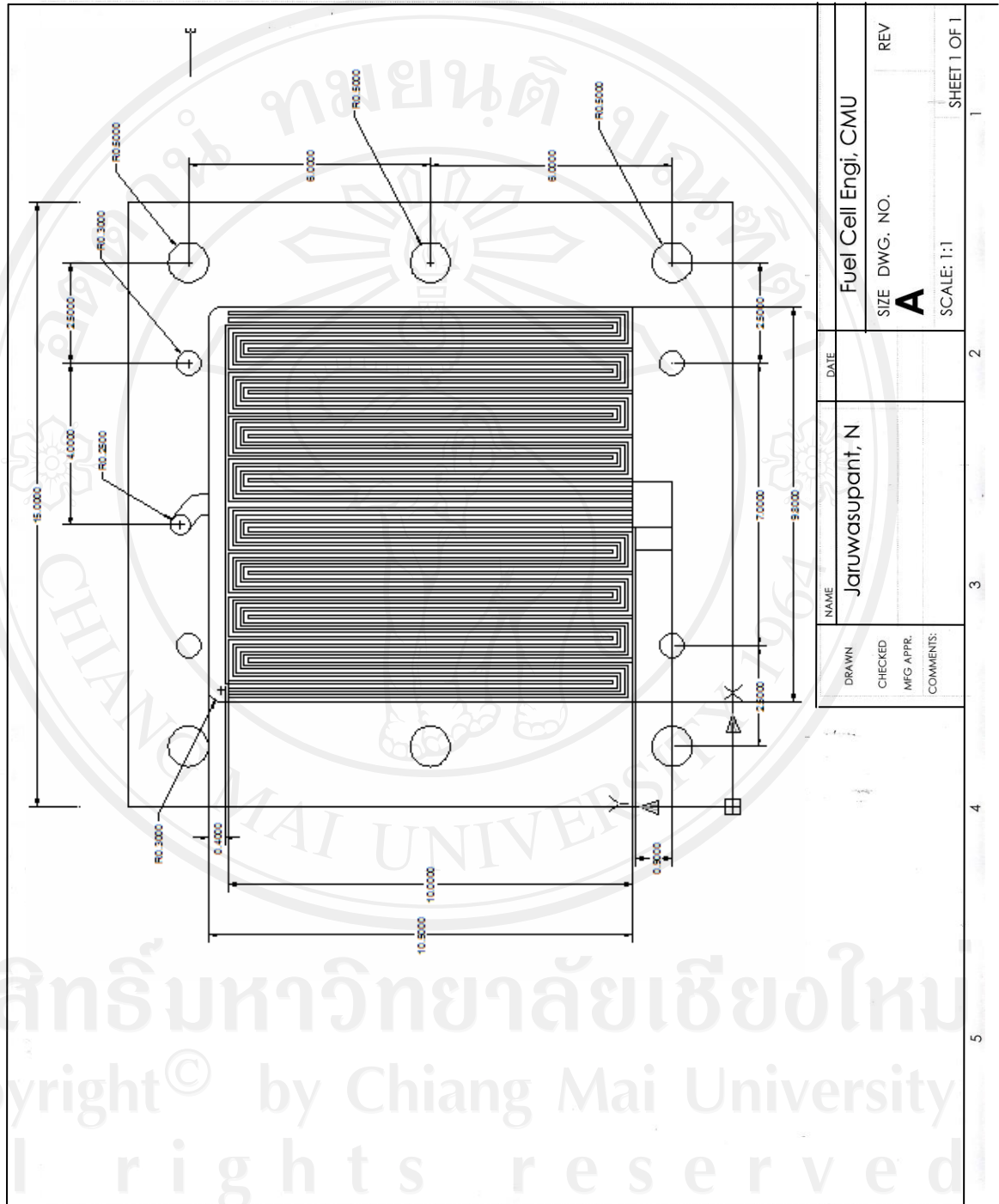
APPENDIX D

Experimental data from testing PEMFC

Table D.1 Experimental data of 4 channels sepentine fuel cell
At temperature 50 ^{o}C flow rate 500 sccm

I	I	V (Volt)				P(mWatt/cm^2)
(Amp)	(mAmp/cm^2)	1	2	3	Total	
0	0	0.929	0.931	0.927	0.929	0.000
0.5	50	0.825	0.827	0.827	0.826	41.317
1	100	0.786	0.786	0.796	0.789	78.933
1.5	150	0.757	0.769	0.779	0.768	115.250
2	200	0.734	0.738	0.744	0.739	147.733
2.5	250	0.736	0.739	0.747	0.741	185.167
3	300	0.699	0.705	0.702	0.702	210.600
3.5	350	0.688	0.691	0.709	0.696	243.600
4	400	0.679	0.685	0.697	0.687	274.800
4.5	450	0.660	0.676	0.696	0.677	304.800
5	500	0.663	0.664	0.685	0.671	335.333
5.5	550	0.643	0.653	0.674	0.657	361.167
6	600	0.645	0.648	0.664	0.652	391.400
6.5	650	0.626	0.633	0.653	0.637	414.267
7	700	0.627	0.624	0.633	0.628	439.600
7.5	750	0.614	0.614	0.623	0.617	462.750
8	800	0.603	0.605	0.623	0.610	488.267
8.5	850	0.594	0.595	0.604	0.598	508.017
9	900	0.583	0.586	0.584	0.584	525.900

Table D.2 Experimental data of 4 channels sepentine fuel cell
At temperature 60 ^{o}C flow rate 500 sccm

I (Amp)	I (mAmp/cm^2)	V (Volt)				P(mWatt/cm^2)
		1	2	3	Total	
0	0	0.931	0.927	0.930	0.929	0.000
0.5	50	0.842	0.837	0.836	0.838	41.917
1	100	0.804	0.805	0.804	0.804	80.433
1.5	150	0.774	0.777	0.781	0.777	116.600
2	200	0.752	0.759	0.764	0.758	151.667
2.5	250	0.737	0.747	0.746	0.743	185.833
3	300	0.722	0.727	0.730	0.726	217.900
3.5	350	0.709	0.719	0.717	0.715	250.250
4	400	0.695	0.701	0.699	0.698	279.333
4.5	450	0.696	0.696	0.688	0.693	312.000
5	500	0.672	0.680	0.677	0.676	338.167
5.5	550	0.661	0.670	0.661	0.664	365.200
6	600	0.654	0.661	0.655	0.657	394.000
6.5	650	0.642	0.651	0.648	0.647	420.550
7	700	0.634	0.640	0.636	0.637	445.667
7.5	750	0.625	0.627	0.625	0.626	469.250
8	800	0.621	0.621	0.618	0.620	496.000
8.5	850	0.610	0.611	0.608	0.610	518.217
9	900	0.601	0.600	0.599	0.600	540.000

Table D.3 Experimental data of 4 channels sepentine fuel cell
At temperature 70 °C flow rate 500 sccm

I (Amp)	I (mAmp/cm^2)	V (Volt)				P(mWatt/cm^2)
		1	2	3	Total	
0	0	0.944	0.935	0.931	0.937	0.000
0.5	50	0.851	0.840	0.839	0.843	42.167
1	100	0.810	0.801	0.806	0.806	80.567
1.5	150	0.788	0.778	0.781	0.782	117.350
2	200	0.767	0.765	0.765	0.766	153.133
2.5	250	0.751	0.747	0.747	0.748	187.083
3	300	0.736	0.722	0.730	0.729	218.800
3.5	350	0.722	0.718	0.714	0.718	251.300
4	400	0.713	0.699	0.699	0.704	281.467
4.5	450	0.700	0.691	0.695	0.695	312.900
5	500	0.691	0.682	0.678	0.684	341.833
5.5	550	0.685	0.668	0.661	0.671	369.233
6	600	0.678	0.667	0.666	0.670	402.200
6.5	650	0.662	0.647	0.646	0.652	423.583
7	700	0.644	0.636	0.637	0.639	447.300
7.5	750	0.635	0.628	0.627	0.630	472.500
8	800	0.626	0.632	0.626	0.628	502.400
8.5	850	0.617	0.612	0.605	0.611	519.633
9	900	0.606	0.600	0.598	0.601	541.200

Table D.4 Experimental data of 6 channels sepentine fuel cell
At temperature 50 ^{o}C flow rate 500 sccm

I	I	V (Volt)				P(mWatt/cm^2)
(Amp)	(mAmp/cm^2)	1	2	3	Total	
0	0	0.949	0.951	0.946	0.949	0.000
0.5	50	0.842	0.847	0.848	0.846	42.283
1	100	0.806	0.806	0.820	0.811	81.067
1.5	150	0.777	0.779	0.799	0.785	117.750
2	200	0.754	0.758	0.784	0.765	153.067
2.5	250	0.736	0.739	0.767	0.747	186.833
3	300	0.719	0.725	0.752	0.732	219.600
3.5	350	0.706	0.711	0.739	0.719	251.533
4	400	0.693	0.704	0.727	0.708	283.200
4.5	450	0.682	0.696	0.716	0.698	314.100
5	500	0.673	0.684	0.705	0.687	343.667
5.5	550	0.663	0.673	0.694	0.677	372.167
6	600	0.655	0.664	0.684	0.668	400.600
6.5	650	0.646	0.653	0.673	0.657	427.267
7	700	0.641	0.644	0.663	0.649	454.533
7.5	750	0.634	0.634	0.653	0.640	480.250
8	800	0.623	0.625	0.643	0.630	504.267
8.5	850	0.613	0.615	0.634	0.621	527.567
9	900	0.603	0.605	0.624	0.611	549.600

Table D.5 Experimental data of 6 channels sepentine fuel cell
At temperature 60 $^{\circ}$C flow rate 500 sccm

I (Amp)	I (mAmp/cm^2)	V (Volt)				P(mWatt/cm^2)
		1	2	3	Total	
0	0	0.953	0.949	0.951	0.951	0.000
0.5	50	0.860	0.855	0.856	0.857	42.850
1	100	0.823	0.823	0.826	0.824	82.400
1.5	150	0.796	0.799	0.803	0.799	119.900
2	200	0.775	0.781	0.785	0.780	156.067
2.5	250	0.757	0.764	0.767	0.763	190.667
3	300	0.742	0.749	0.750	0.747	224.100
3.5	350	0.728	0.736	0.734	0.733	256.433
4	400	0.719	0.723	0.719	0.720	288.133
4.5	450	0.711	0.712	0.705	0.709	319.200
5	500	0.699	0.700	0.692	0.697	348.500
5.5	550	0.688	0.690	0.681	0.686	377.483
6	600	0.677	0.680	0.674	0.677	406.200
6.5	650	0.667	0.673	0.666	0.669	434.633
7	700	0.656	0.662	0.656	0.658	460.600
7.5	750	0.649	0.651	0.645	0.648	486.250
8	800	0.640	0.641	0.636	0.639	511.200
8.5	850	0.630	0.631	0.625	0.629	534.367
9	900	0.620	0.622	0.616	0.619	557.400

Table D.6 Experimental data of 6 channels sepentine fuel cell
At temperature 70 $^{\circ}$C flow rate 500 sccm

I (Amp)	I (mAmp/cm^2)	V (Volt)				P(mWatt/cm^2)
		1	2	3	Total	
0	0	0.961	0.953	0.951	0.955	0.000
0.5	50	0.871	0.860	0.856	0.862	43.117
1	100	0.833	0.823	0.826	0.827	82.733
1.5	150	0.808	0.796	0.803	0.802	120.350
2	200	0.787	0.775	0.785	0.782	156.467
2.5	250	0.770	0.757	0.767	0.765	191.167
3	300	0.756	0.742	0.750	0.749	224.800
3.5	350	0.746	0.728	0.734	0.736	257.600
4	400	0.733	0.719	0.719	0.724	289.467
4.5	450	0.721	0.711	0.705	0.712	320.550
5	500	0.713	0.699	0.692	0.701	350.667
5.5	550	0.705	0.688	0.681	0.691	380.233
6	600	0.698	0.677	0.674	0.683	409.800
6.5	650	0.692	0.667	0.666	0.675	438.750
7	700	0.684	0.656	0.656	0.665	465.733
7.5	750	0.675	0.649	0.645	0.656	492.250
8	800	0.666	0.640	0.636	0.647	517.867
8.5	850	0.657	0.630	0.625	0.637	541.733
9	900	0.648	0.620	0.616	0.628	565.200

Table D.7 Experimental data of 2 ways multi-serpentine with header
At temperature 50 ^{o}C flow rate 500 sccm

I (Amp)	I (mAmp/cm^2)	V (Volt)				P(mWatt/cm^2)
		1	2	3	Total	
0	0	0.949	0.952	0.949	0.950	0.000
0.5	50	0.905	0.907	0.908	0.907	45.333
1	100	0.863	0.867	0.871	0.867	86.700
1.5	150	0.838	0.839	0.857	0.845	126.700
2	200	0.824	0.828	0.843	0.832	166.333
2.5	250	0.806	0.802	0.816	0.808	202.000
3	300	0.781	0.781	0.798	0.787	236.000
3.5	350	0.771	0.778	0.789	0.779	272.767
4	400	0.758	0.769	0.787	0.771	308.533
4.5	450	0.752	0.753	0.774	0.760	341.850
5	500	0.731	0.745	0.768	0.748	374.000
5.5	550	0.732	0.733	0.751	0.739	406.267
6	600	0.715	0.727	0.737	0.726	435.800
6.5	650	0.711	0.711	0.733	0.718	466.917
7	700	0.702	0.711	0.722	0.712	498.167
7.5	750	0.694	0.694	0.710	0.699	524.500
8	800	0.684	0.685	0.691	0.687	549.333
8.5	850	0.674	0.681	0.694	0.683	580.550
9	900	0.663	0.666	0.688	0.672	605.100

Table D.8 Experimental data of 2 ways multi-serpentine with header
At temperature 60 $^{\circ}$C flow rate 500 sccm

I (Amp)	I (mAmp/cm^2)	V (Volt)				P(mWatt/cm^2)
		1	2	3	Total	
0	0	0.953	0.950	0.953	0.952	0.000
0.5	50	0.920	0.915	0.916	0.917	45.850
1	100	0.884	0.885	0.886	0.885	88.500
1.5	150	0.858	0.855	0.862	0.858	128.750
2	200	0.835	0.831	0.841	0.836	167.133
2.5	250	0.818	0.825	0.827	0.823	205.833
3	300	0.807	0.809	0.812	0.809	242.800
3.5	350	0.789	0.799	0.793	0.794	277.783
4	400	0.779	0.780	0.779	0.779	311.733
4.5	450	0.767	0.773	0.776	0.772	347.400
5	500	0.759	0.761	0.768	0.763	381.333
5.5	550	0.745	0.748	0.745	0.746	410.300
6	600	0.732	0.747	0.735	0.738	442.800
6.5	650	0.727	0.733	0.726	0.729	473.633
7	700	0.715	0.720	0.710	0.715	500.500
7.5	750	0.709	0.710	0.704	0.708	530.750
8	800	0.700	0.701	0.696	0.699	559.200
8.5	850	0.695	0.688	0.685	0.689	585.933
9	900	0.681	0.685	0.672	0.679	611.400

Table D.9 Experimental data of 2 ways multi-serpentine with header
At temperature 70 ^{o}C flow rate 500 sccm

I (Amp)	I (mAmp/cm^2)	V (Volt)				P(mWatt/cm^2)
		1	2	3	Total	
0	0	0.957	0.959	0.955	0.957	0.000
0.5	50	0.951	0.925	0.918	0.931	46.567
1	100	0.910	0.888	0.887	0.895	89.500
1.5	150	0.888	0.856	0.868	0.871	130.600
2	200	0.866	0.845	0.845	0.852	170.400
2.5	250	0.837	0.817	0.817	0.824	205.917
3	300	0.836	0.805	0.810	0.817	245.100
3.5	350	0.825	0.796	0.797	0.806	282.100
4	400	0.813	0.779	0.789	0.794	317.467
4.5	450	0.800	0.773	0.777	0.783	352.500
5	500	0.793	0.759	0.752	0.768	384.000
5.5	550	0.781	0.748	0.748	0.759	417.450
6	600	0.767	0.737	0.739	0.748	448.600
6.5	650	0.768	0.727	0.726	0.740	481.217
7	700	0.738	0.716	0.717	0.724	506.567
7.5	750	0.747	0.705	0.705	0.719	539.250
8	800	0.736	0.702	0.701	0.713	570.400
8.5	850	0.724	0.687	0.685	0.699	593.867
9	900	0.716	0.680	0.678	0.691	622.200
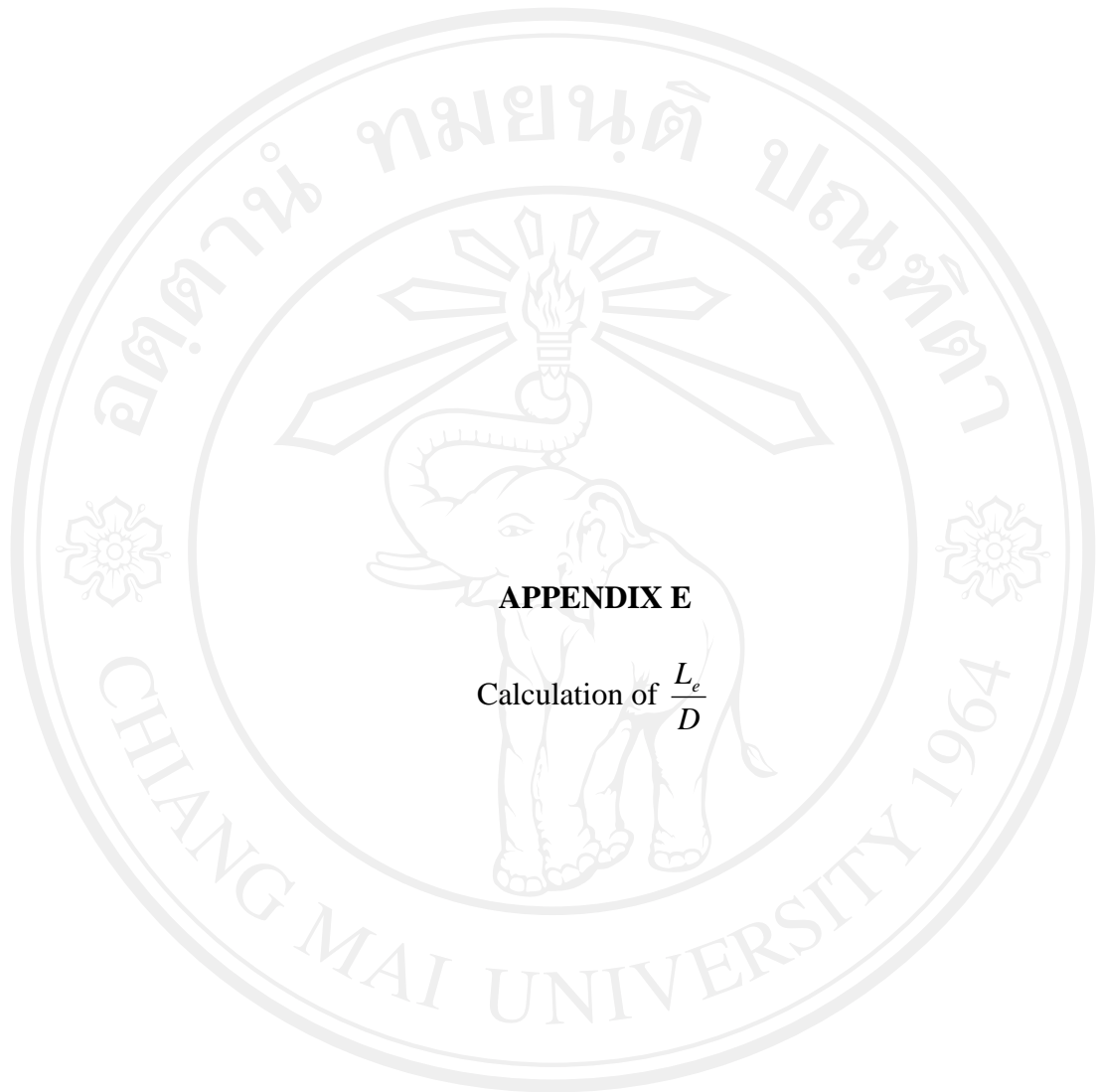
APPENDIX E

Calculation of $\dfrac{L_e}{D}$

Table E.1 Calculate of $\dfrac{L_e}{D}$ in 1 mm. channel width

Flow Rate (cm³/min)	Cross-Section Area (mm²) (W × D)	R/D$_H$	V (m/s)	P$_{DROP}$ (N/m²)	R_e	f_t	L_e/D_H
200	1 × 1	1.5	3.33	1593.92	32.93	1.94	1661.992
200	1 × 1	3.5	3.33	1595.76	32.93	1.94	1663.914
200	1 × 1	5.5	3.33	1597.22	32.93	1.94	1665.436
200	1 × 1	7.5	3.33	1599.48	32.93	1.94	1667.793
200	1 × 1	9.5	3.33	1600.81	32.93	1.94	1669.18
200	1 × 1	11.5	3.33	1602.62	32.93	1.94	1671.067
300	1 × 1	1.5	5.00	2551.85	49.44	1.29	1772.118
300	1 × 1	3.5	5.00	2553.34	49.44	1.29	1773.153
300	1 × 1	5.5	5.00	2555.11	49.44	1.29	1774.382
300	1 × 1	7.5	5.00	2557.72	49.44	1.29	1776.194
300	1 × 1	9.5	5.00	2559.66	49.44	1.29	1777.542
300	1 × 1	11.5	5.00	2561.67	49.44	1.29	1778.938
400	1 × 1	1.5	6.67	3607.70	65.96	0.97	1878.071
400	1 × 1	3.5	6.67	3609.15	65.96	0.97	1878.826
400	1 × 1	5.5	6.67	3611.20	65.96	0.97	1879.893
400	1 × 1	7.5	6.67	3613.32	65.96	0.97	1880.997
400	1 × 1	9.5	6.67	3615.46	65.96	0.97	1882.111
400	1 × 1	11.5	6.67	3617.80	65.96	0.97	1883.329
500	1 × 1	1.5	8.33	4743.88	82.37	0.78	1977.408
500	1 × 1	3.5	8.33	4745.06	82.37	0.78	1977.899
500	1 × 1	5.5	8.33	4747.59	82.37	0.78	1978.954
500	1 × 1	7.5	8.33	4749.76	82.37	0.78	1979.859
500	1 × 1	9.5	8.33	4751.71	82.37	0.78	1980.671
500	1 × 1	11.5	8.33	4753.59	82.37	0.78	1981.455

Table E.2 Calculate of $\dfrac{L_e}{D}$ in 0.8 channel width

Flow Rate (cm³/min)	Cross-Section Area (mm²) (W × D)	R/D_H	V (m/s)	P_DROP (N/m²)	R_e	f_t	L_e/D_H
200	0.8×1	1.69	4.17	2102.42	36.67	1.75	1559.29
200	0.8×1	3.93	4.17	2104.26	36.67	1.75	1560.66
200	0.8×1	6.18	4.17	2105.72	36.67	1.75	1561.74
200	0.8×1	8.43	4.17	2107.98	36.67	1.75	1563.42
200	0.8×1	10.67	4.17	2109.31	36.67	1.75	1564.40
200	0.8×1	12.92	4.17	2111.12	36.67	1.75	1565.75
300	0.8×1	1.69	6.25	3249.25	55.01	1.16	1606.57
300	0.8×1	3.93	6.25	3250.74	55.01	1.16	1607.31
300	0.8×1	6.18	6.25	3252.51	55.01	1.16	1608.19
300	0.8×1	8.43	6.25	3255.12	55.01	1.16	1609.48
300	0.8×1	10.67	6.25	3257.06	55.01	1.16	1610.44
300	0.8×1	12.92	6.25	3259.07	55.01	1.16	1611.43
400	0.8×1	1.69	8.33	4453.00	73.31	0.87	1651.98
400	0.8×1	3.93	8.33	4454.45	73.31	0.87	1652.52
400	0.8×1	6.18	8.33	4456.50	73.31	0.87	1653.28
400	0.8×1	8.43	8.33	4458.62	73.31	0.87	1654.07
400	0.8×1	10.67	8.33	4460.76	73.31	0.87	1654.86
400	0.8×1	12.92	8.33	4463.10	73.31	0.87	1655.73
500	0.8×1	1.69	10.42	5707.58	91.71	0.70	1692.71
500	0.8×1	3.93	10.42	5708.76	91.71	0.70	1693.06
500	0.8×1	6.18	10.42	5711.29	91.71	0.70	1693.81
500	0.8×1	8.43	10.42	5713.46	91.71	0.70	1694.45
500	0.8×1	10.67	10.42	5715.41	91.71	0.70	1695.03
500	0.8×1	12.92	10.42	5717.29	91.71	0.70	1695.59

Table E.3 Calculate of $\dfrac{L_e}{D}$ in 1.2 channel width

Flow Rate (cm³/min)	Cross-Section Area (mm²) (W × D)	R/D$_H$	V (m/s)	P$_{DROP}$ (N/m²)	R_e	f_t	L_e/D_H
200	1.2×1	1.38	2.78	1391.32	29.97	2.14	1894.15
200	1.2×1	3.21	2.78	1393.16	29.97	2.14	1896.66
200	1.2×1	5.05	2.78	1394.62	29.97	2.14	1898.65
200	1.2×1	6.88	2.78	1396.88	29.97	2.14	1901.73
200	1.2×1	8.72	2.78	1398.21	29.97	2.14	1903.54
200	1.2×1	10.55	2.78	1400.02	29.97	2.14	1906.00
300	1.2×1	1.38	4.17	2245.65	44.95	1.42	2038.17
300	1.2×1	3.21	4.17	2247.14	44.95	1.42	2039.52
300	1.2×1	5.05	4.17	2248.91	44.95	1.42	2041.13
300	1.2×1	6.88	4.17	2251.52	44.95	1.42	2043.50
300	1.2×1	8.72	4.17	2253.46	44.95	1.42	2045.26
300	1.2×1	10.55	4.17	2255.47	44.95	1.42	2047.08
400	1.2×1	1.38	5.55	3211.20	59.82	1.07	2189.82
400	1.2×1	3.21	5.55	3212.65	59.82	1.07	2190.81
400	1.2×1	5.05	5.55	3214.70	59.82	1.07	2192.21
400	1.2×1	6.88	5.55	3216.82	59.82	1.07	2193.65
400	1.2×1	8.72	5.55	3218.96	59.82	1.07	2195.11
400	1.2×1	10.55	5.55	3221.30	59.82	1.07	2196.71
500	1.2×1	1.38	6.94	4287.08	74.81	0.86	2337.95
500	1.2×1	3.21	6.94	4288.26	74.81	0.86	2338.60
500	1.2×1	5.05	6.94	4290.79	74.81	0.86	2339.98
500	1.2×1	6.88	6.94	4292.96	74.81	0.86	2341.16
500	1.2×1	8.72	6.94	4294.91	74.81	0.86	2342.22
500	1.2×1	10.55	6.94	4296.79	74.81	0.86	2343.25

Table E.4 Compare P_{drop} of $\frac{L_e}{D}$ in 1 mm. channel width, 300 cm^3/min.

Flow Rate	Channel Width (mm.)	R/D_H	P_{drop} from calculation (N/m^2)	P_{drop} from modeling (N/m^2)	Different of P_{drop} (N/m^2)
300	1	1.5	2070.58	2551.85	481.27
		3.5	2105.67	2553.34	447.67
		5.5	2160.24	2555.11	394.87
		7.5	2228.73	2557.72	328.99
		9.5	2314.21	2559.66	245.45
		11.5	2378.50	2561.67	183.17
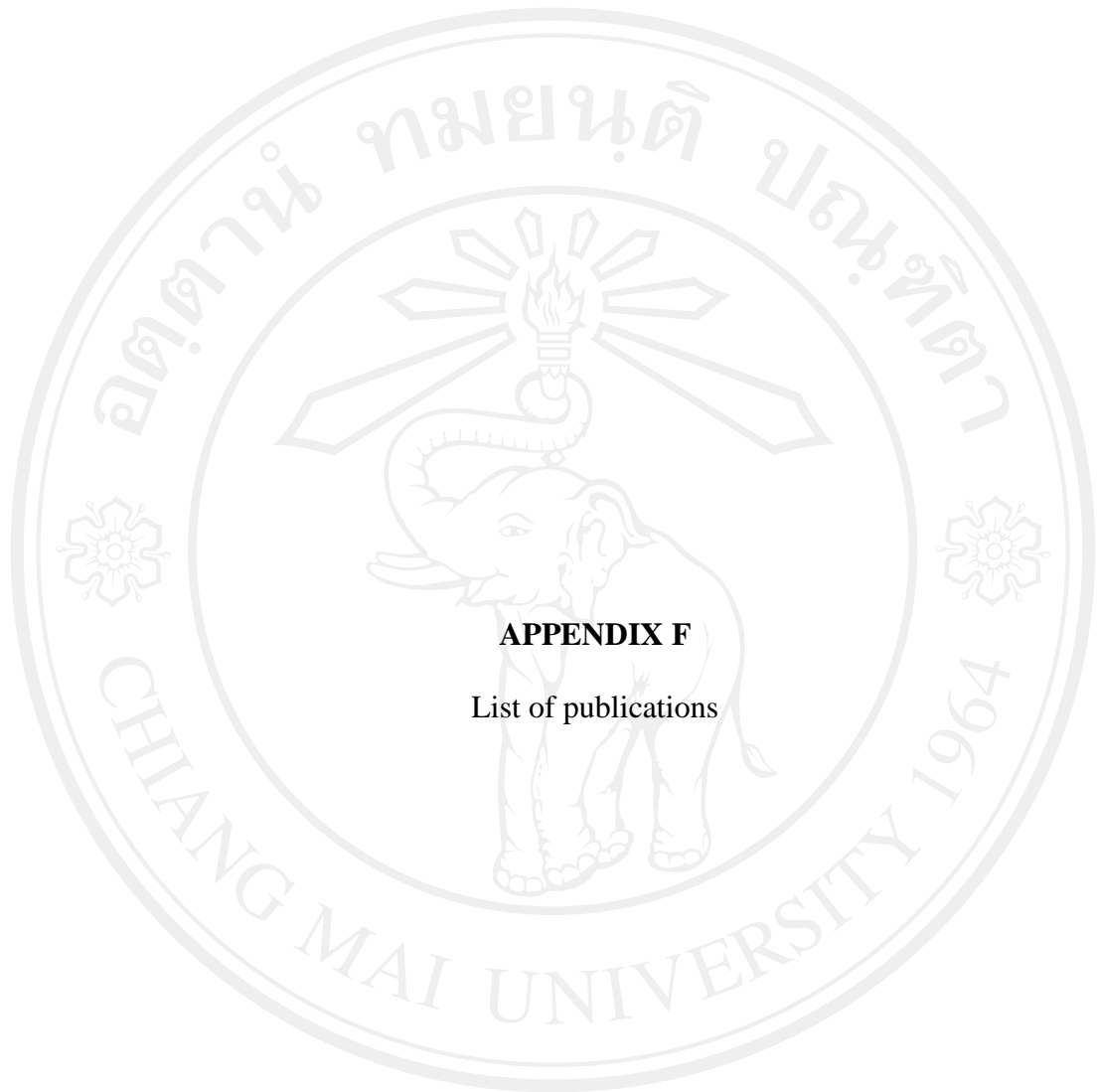
APPENDIX F

List of publications
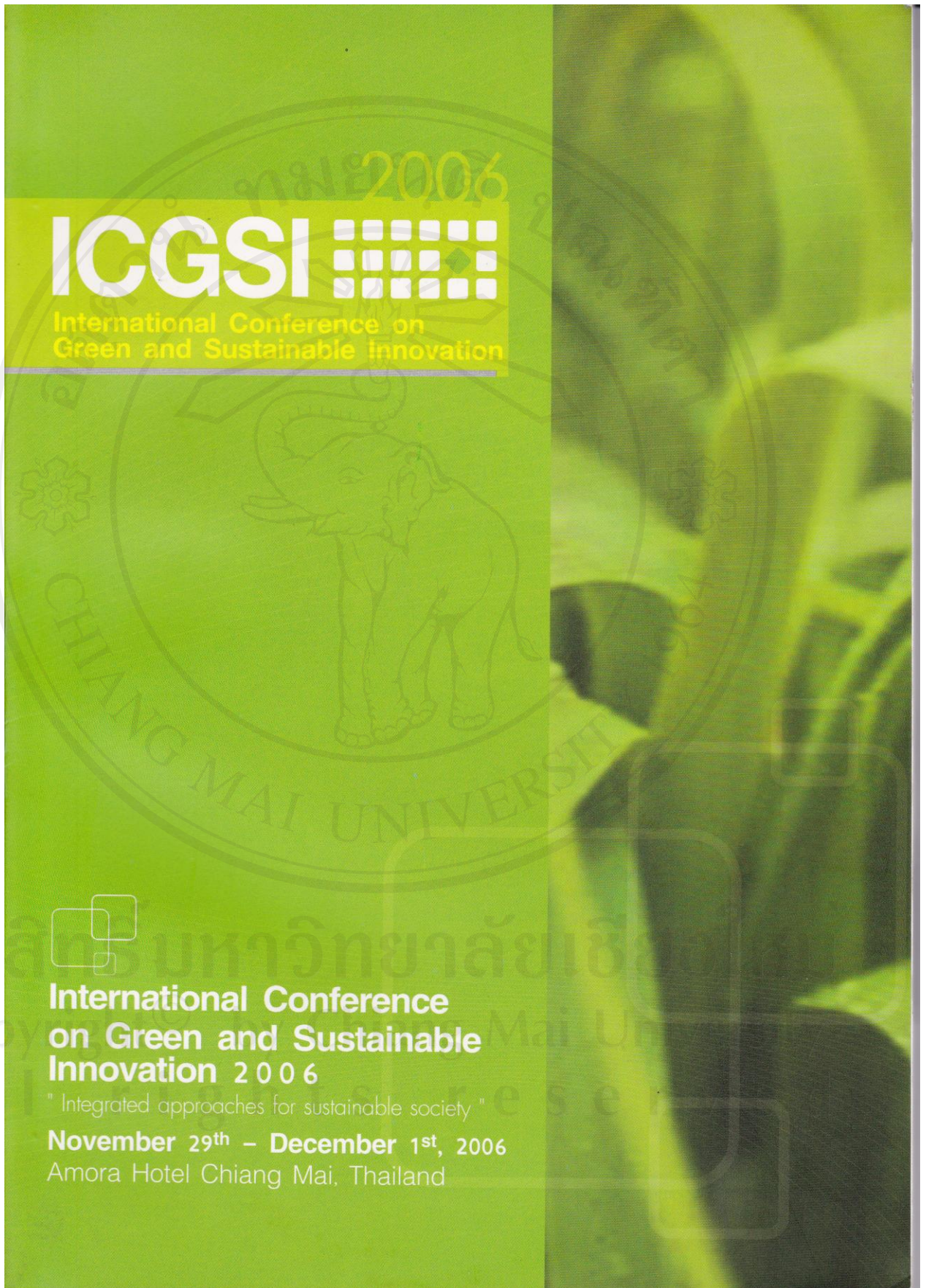
ICGSI

International Conference on Green and Sustainable Innovation

International Conference on Green and Sustainable Innovation 2006

" Integrated approaches for sustainable society "

November 29th – **December** 1st, 2006

Amora Hotel Chiang Mai, Thailand

Three-Dimensional Model and Experiment of New Flow Field for Proton Exchange Membrane Fuel Cell using CFDRC®

N. Jaruwasupant and Y. Khunatorn*

Department of Mechanical Engineering, Faculty of Engineering, Chiang Mai University,
Chiang Mai, Thailand 50200
E-mail* : piakman@dome.eng.cmu.ac.th

ABSTRACT

This research is to study the gas distribution within the Proton Exchange Membrane Fuel Cell (PEMFC) that using the homebuilt developed flow field. This flow field combines curve header together with parallel-serpentine in order to extend the reaction area. A 3D numerical modeling of PEMFC was set up and solved by using commercial computational fluid dynamics (CFD) software, the "CFDRC®". The affect of gas flow field on the gas distribution caused by the chemical reaction inside the fuel cell were numerically studied.

The result shows the developed flow field has the density of electric power about 81.25 mA/cm^2 and the conventional flow field fuel cell is about 69.22 mA/cm^2 which is better around 17.5%. From the test of developed fuel cell with the temperature and the flow rate, found that at the work in temperature; 50 ^{o}C and the flow rate at 150 sccm gave the best density of electric power.

Keywords : PEMFC, CFD, CFDRC, Numerical Modeling, Flow field, Fuel cell

1. INTRODUCTION

Proton exchange membrane fuel cells (PEMFCs) transforms the chemical energy into electricity. Hence, it is a environment friendly energy source. Its performance and efficiency still needed to be improved, and the issues of cost, reliability and safety are needed to be considered to realize the fuel cell commerciality. In order to enhance its performance and reliability, it is necessary to learn more about the mechanism that causes the performance loss, such as, non-uniform concentration, current density distributions, high ionic resistance due to dry membrane, or high diffusive resistance due to the flooding on the cathode. The flow field and water/thermal management of fuel cell need optimal design to achieve high performance and reliability. The numerical modeling and dedicated experimental technique development will be the effective tools to improve the optimal design of fuel cell system.

The major objectives of this work are to: first, building a 3-D new flow field (elbow middle P-S) for PEMFC model to predict the cell performance. Second, study the effect of this flow field patterns on distribution and concentration of gases. Last, Experiment of prototype PEMFC from this flow fields and compare with numerical modeling.

2. COMPONENT AND OPERATE OF FUEL CELL

2.1 Component of PEMFC

The single PEMFC components includes of flow field plates, gas diffusion, catalyst layer, membrane, shown in Figure. 1. Figure. 2 shown three conventional flow field commonly used in PEMFC. Those are Parallel straight, serpentine flow and parallel-serpentine flow patterns.

Nomenclature		Greek letters	
a_i	stoichiometric coefficients (') reactants (") products	α_c	cathode kinetic constant
D_i	effective mass diffusion coefficient of species I	ε	porosity
$D_{i,FS}$	free stream diffusion coefficient of ith species	κ	permeability (m^2)
F	Faraday constant	μ	dynamic viscosity (m^2/s)
H	Heat flux (J/cm^2)	ω_i	production rates of ith species in the
i_F	in porous media, the current flowing through the solid parts of the porous matrix (A)		gas phase
		ρ	density (kg/m^3)
i_S	in porous media, the current flowing through the pores (A)	Φ_S	solid potential (V)
		Φ_F	fluid potential (V)
j_0	reference current (A/m^3)	τ	shear force tension
J_i	diffusion flux		
u,v,w	velocity (m/s)		
M	mixture molecular weight		
p	pressure (N/m^2)		
T	Temperature (^{o}C)		
Y_i	mass-fractions of ith species		
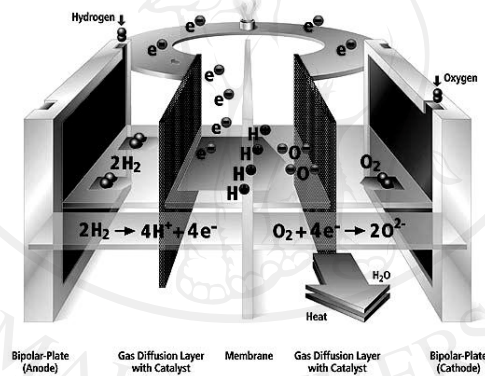
Figure.1 Schematic diagram of PEMFC
: http://www.princeton.edu/.../ Hydrogen/fuelcells.html

The components of PEMFC have the following functions:
   1. Membrane is a solid polymer which transport water and protons, and separates the reactants of H2 and O_2, but not transport of electron
   2. Electrodes are where the electrochemical reactions take place. The platinum has been used as a catalyst flow field for the chemical reaction..
   3. Gas Diffusion Layer (GDL) that transport reactant to and from the catalyst layers and conduct electrons from the catalyst layer to the collector plate
   4. Collector plates that acts as an electron conductor and that reactants
Characteristics of conventional flow fields show in Figure. 2 (Mennola, 2000)
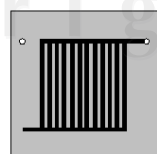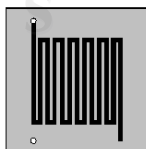
Parallel Channel   Serpentine Channels   Parallel-Serpentine Channel
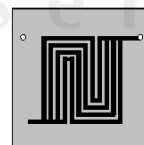
Figure.2 Characteristics of conventional flow field

2.2 Electrochemical Reaction Process in Fuel Cell

Fuel cells are energy source from electrochemical in cell. The reactions are from hydrogen gas flow pass the catalyst layer in Anode, it is Oxidation reaction and show in equation (1). Hydrogen ion from the reaction flow pass Electrolyte to Cathode and the reaction in the catalyst layer are Reduction, The Oxygen is reactance in the reaction and show in equation (2). The products from the reaction are water and electrons. The current in the Cathode and Anode from electron flow pass between two sides shown in Figure. 3

$$H_2 \cdots\!\!\blacktriangleright\ 2H^+ + 2e^- \qquad\qquad \text{Oxidation process} \qquad\qquad (1)$$
$$O_2 + 4e^- + 4H^+ \cdots\!\!\blacktriangleright 2H_2O \qquad \text{Reduction process} \qquad\qquad (2)$$
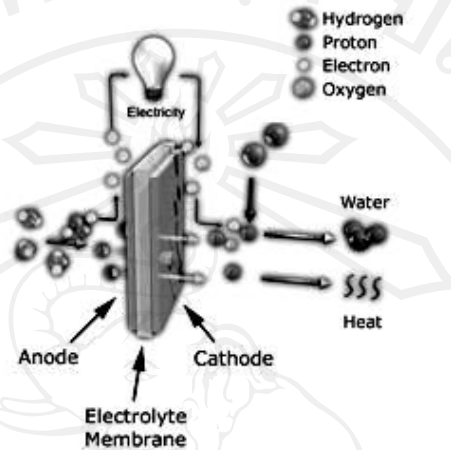
Figure.3 Diagram of Fuel Cell Operation
: www.rpi.edu/polymers/ research_fuel_cells.html

2.3 Efficiency of Fuel Cell

Electrical energy is obtained from a fuel cell only when a reasonable current is drawn, but the actual cell potential is decreased from its equilibrium potential because of irreversible losses as shown in Figureure.4. Several sources contribute to irreversible losses in a practical fuel cell. The losses, which are often called polarization, overpotential, or overvoltage, originate primarily from three sources: activation polarization, ohmic polarization, and concentration polarization. These losses result in a cell voltage for a fuel cell that is less than its ideal potential.
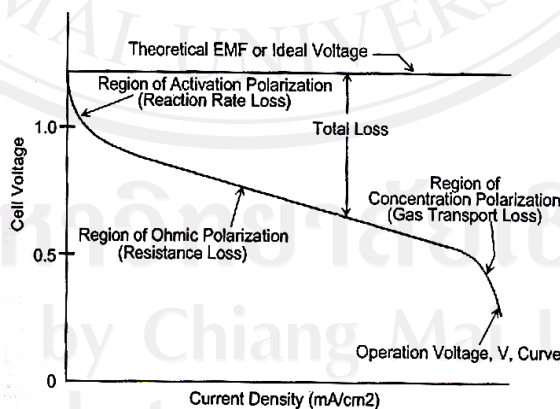
Figure. 4 Ideal and actual fuel cell voltage/current characteristic

The activation polarization loss is dominant at low current density. At this point, electronic barriers have to be overcome prior to current and ion flow. Activation losses show some increase as current increases. Ohmic polarization (loss) varies directly with current, increasing over the whole range of current because cell resistance remains essentially constant. Gas transport losses occur over the entire range of current density, but these losses become prominent at high limiting currents where it becomes difficult to provide enough reactant flow to the cell reaction sites.

3. Numerical modeling

In this study, present a 3-D numerical modeling, to prediction and analysis all components of proton exchange membrane fuel cells. The model is based on the solution of the conservation equations of mass, momentum, energy and species using the CFDRC®. Tables 1 and Tables 2 are the dimensions of PEMFC and the boundary conditions used in the numerical simulation from Su and etc (2005).

Table 1 Main Dimensions for the numerical model

Channel length (mm)	50
Channel width (mm)	1
Channel depth (mm)	1
Rib width (mm)	1
Diffusion layer thickness (mm)	0.26
Catalyst layer thickness (mm)	0.0287
Membrane thickness (mm)	0.023
Total reaction area (cm^2)	25

Table 2 Boundary Conditions

H_2 at fuel inlet (cm^3/min)	100
O_2 at fuel inlet (cm^3/min)	100
Operating pressure (atm)	1
Operating temperature (°C)	50

The main assumptions of the modeling are:
1. steady state
2. laminar flow
3. isothermal
4. reactants are treated as ideal gas
5. the Stefan–Maxwell equations for multi-species diffusion
6. Butler–Volmer equation is used to describe electrochemical reactions within the catalyst layers
7. Nerst–Planck equation is used for the transport of protons through the membrane

3.1 Channel flow field

These conservation equations in flow field are follows;

Mass conservation

$$\frac{\partial \rho}{\partial t} + \nabla(\rho U) = 0 \tag{3}$$

Momentum conservation

$$\frac{\partial \rho u}{\partial t} + \nabla \cdot (\rho U u) = -\frac{\partial P}{\partial x} + \nabla(\mu \nabla u) \tag{4}$$

$$\frac{\partial \rho v}{\partial t} + \nabla \cdot (\rho U v) = -\frac{\partial P}{\partial y} + \nabla(\mu \nabla v) \tag{5}$$

$$\frac{\partial \rho w}{\partial t} + \nabla \cdot (\rho U w) = -\frac{\partial P}{\partial z} + \nabla(\mu \nabla w) \tag{6}$$

Energy conservation

$$\nabla \cdot (\rho u H) - \nabla \cdot (k \nabla T) = 0 \tag{7}$$

Species conservation

$$\frac{\partial}{\partial t}(\varepsilon \rho Y_i) + \nabla \cdot (\varepsilon \rho U Y_i) = \nabla J_i \tag{8}$$

maybe written as;

$$J_i = \rho D_i \nabla Y_i + \frac{\rho Y_i}{M} D_i \nabla M - \rho Y_i \sum_j D_j \nabla Y_j$$

$$- \rho Y_i \frac{\Delta M}{M} \sum_j D_j \nabla Y_j \tag{9}$$

and

$$D_i = D_{i,FS} \varepsilon^{\tau} \tag{10}$$

3.2 Gas diffusion layer

GDLs are porous media, their are effects by porosity and permeability. These equations are follows;
Mass conservation

$$\frac{\partial}{\partial t}(\varepsilon \rho) + \nabla(\varepsilon \rho U) = 0 \tag{11}$$

Momentum conservation

$$\frac{\partial}{\partial t}(\varepsilon \rho) + \nabla \cdot (\varepsilon \rho U \cdot U) = -\varepsilon \nabla \rho + \nabla \cdot (\varepsilon \tau)$$

$$+ \varepsilon B + \frac{\varepsilon^2 \mu U}{k} \tag{12}$$

Species conservation in these layers in same flow field and continuity of current within any material under electro neutral conditions leads to

$$\nabla \cdot i = 0 \tag{13}$$

3.3 Catalyst layers

The mass and momentum conservation in these layers is same in GDLs
Species conservation

$$\frac{\partial}{\partial t}(\varepsilon \rho Y_i) + \nabla \cdot (\varepsilon \rho U Y_i) = \nabla J_i + \omega_i \tag{14}$$

When

$$\omega_i = \left(a_i^{"} - a_i^{'}\right) \frac{j_T}{F} \tag{15}$$

Where j_T is obtained from the Butler-Volmer conditions
The continuity of current within any material under electro neutral conditions leads to

$$\nabla \cdot i = 0 \tag{16}$$

If given i_F is ion phase and i_S is electron phase. It can be rewritten as

$$\nabla i_F + \nabla i_S = 0 \tag{17}$$

3.4 Membrane

In the membrane, equations of conservation are same as in the catalyst layers, but without chemical reaction.

4. 3-D model of new flow field (elbow middle P-S)

Elbow middle P-S flow field is developed from the result of tree conventional flow fields. It is applied by using parallel – serpentine flow field and the function of header for conveying the inlet gas channel. It is designed to curve into the inlet channel. This design makes the flow field applicable to stack cell. The inlet at the center of the flow field so that it will distribute the gas through the channel and the reaction area. Moreover, it will reduce the quantity of water which occurs in the channel so it will decrease the storing of water and provide a better heat distribution characteristic.. The last fold of the gas flow field before the exit will transform the channel; parallel-serpentine to be the serpentine in order to increase the flow rate to increase the pressure drop so it will help carry water out of the cell. Then the two channel will merge together at the lower center area of the flow field and let the water move along the gravity. From the first design of flow field, which is bending, it is smaller than the channel in the flow field because it will increase the speed and distribute the pressure highly so that it will release the water to be out of the cell.

5. Result and Discussion

The result of flow and distribution of hydrogen and oxygen at the anode and cathode are show in Figures 5-6.

| (a) velocity at anode | (b) velocity at cathode |
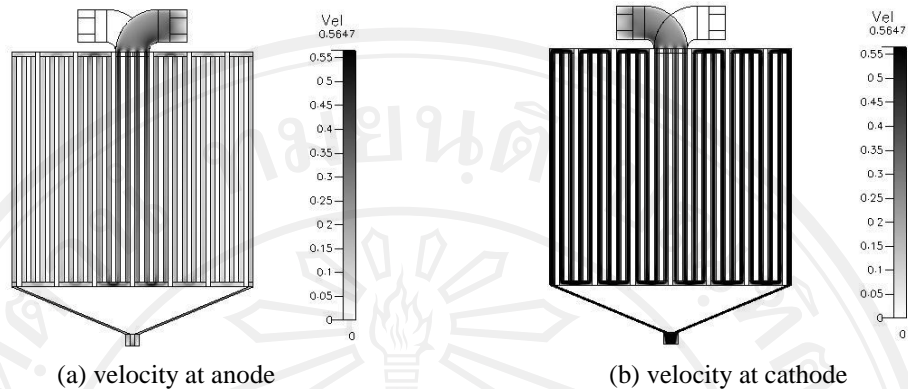
Figure. 5 Velocity of hydrogen and oxygen in elbow middle P – S flow field

| (a) Pressure distribute at anode | (b) Pressure distribute at cathode |
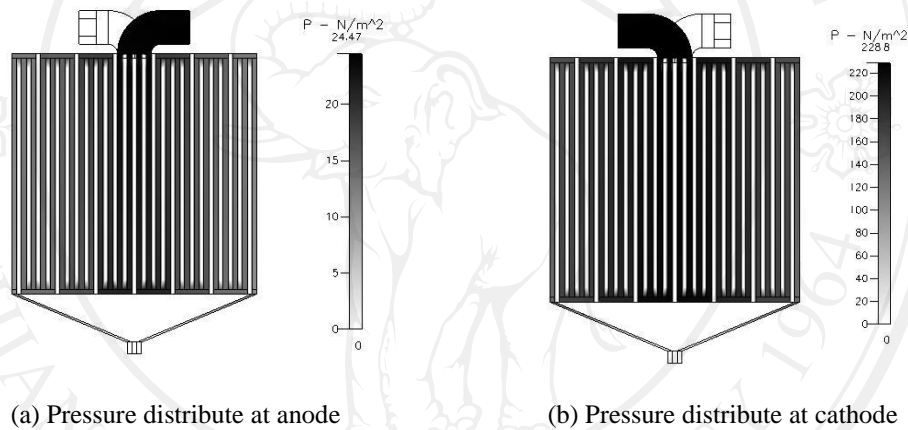
Figure. 6 Pressure distribute of hydrogen and oxygen in elbow middle P – S flow field

The result shows that the anode has the lower velocity than cathode. The anode has the highest velocity around 0.45 m/s and the cathode around 2 m/s but at the outlet, it has the highest velocity around 4.2 m/s. Furthermore, pressure drop at cathode is around 228 N/m but it is around 25 N/m at the anode which is much more lower than cathode. As a result, this makes the cathode has higher pressure drop, which can push the water out of the cell.

| (a) Concentration of hydrogen at anode | (b) Concentration of hydrogen at cathode |
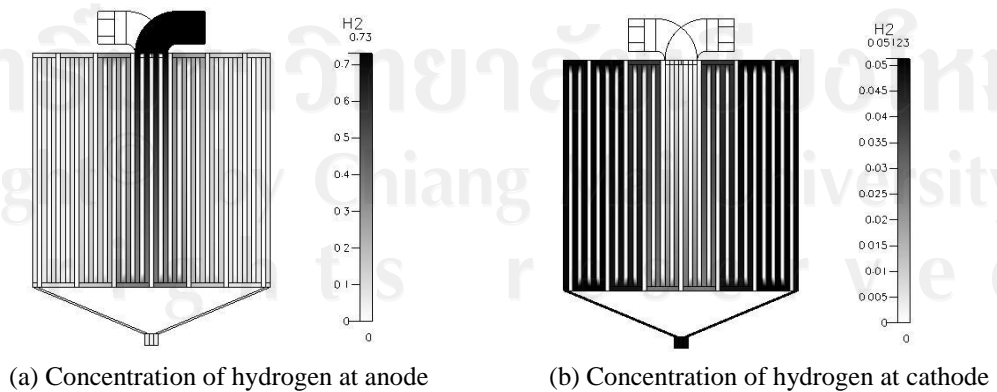
Figure. 7 Concentration of hydrogen in elbow middle P–S flow field
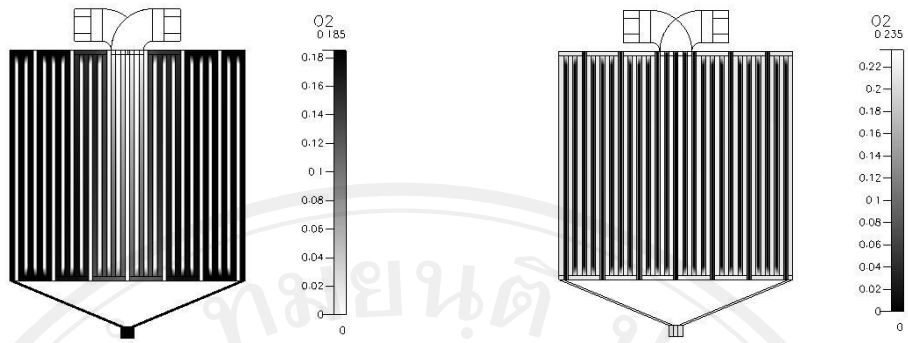
(a) Concentration of oxygen at anode   (b) Concentration of oxygen at cathode

Figure. 8 Concentration of oxygen in elbow middle P – S flow field
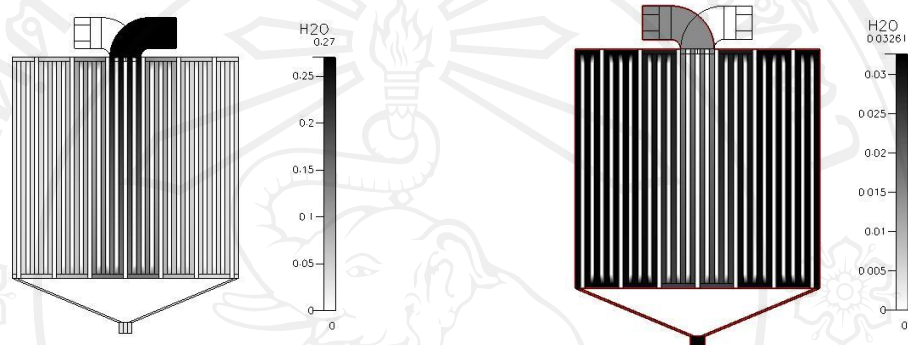
(a) Concentration of water at anode   (b) Concentration of water at cathode

Figure. 9 Concentration of water in elbow middle P–S flow field
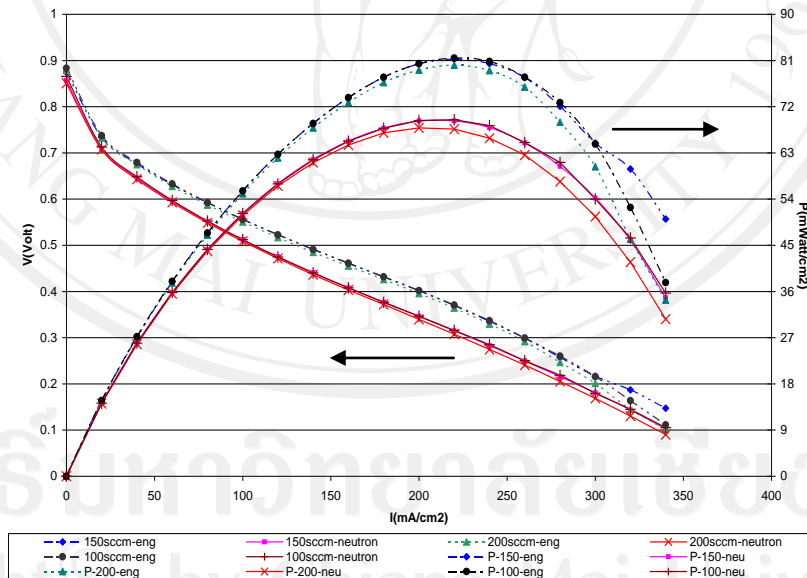
Figure. 10 Comparisons between the developed fuel cell and the old fuel cell on actual fuel cell voltage/current Characteristic

The consumption rate of hydrogen in anode is high at the center of the flow field. Then, it consumed along the channel gradually. The inlet gas concentration is 73% and the gas deplete before exit. Thus, the concentration of gas is reduce in high quantity. At cathode, hydrogen will increase gradually along the distance of channel. From the result, it has the highest quantity just 5% by mass as shown in Figure. 7. The concentration of oxygen at anode is increase gradually from the inlet to the outlet around 18.5% by mass. In contrast, the using rate of oxygen at cathode has a little using rate through flow field which is shown in Figure. 8. The concentration of water in cells will occur at cathode in the channel which will be distributed all

around the channel and the production rate of water will increase for 3.2% by mass. However, the quantity of water will decrease as shown in Figure. 9.

Velocity, pressure and the concentration of gas between the developed flow field comparison to the conventional flow field. It is found that the developed flow field and provides a better performance. Since the developed flow field has velocity and pressure drop which are quite high. However, each flow field has the similar pressure drop and at the outlet, it has the high pressure because there is the combination as the flowing in serpentine. Thus, it can release the water from the gas flow very well. Moreover, the concentration of gas in the developed flow field has the good attribution and it has the concentration of hydrogen that it is decreased highly which is like the parallel serpentine. Besides, the concentration of water is increased along the distance of channel. Thus, it is implied that there will be the good reaction the fuel cell.

6. Conclusion

Elbow Middle P-S flow field developed by the combination of curve header and parallel-serpentine has been on numerically studied. Another feature is the outlet, the flow field is changed from the parallel-serpentine to be serpentine which result in high pressure drop. From that result, the fuel cell with our flow field provides better performance. At the outlet, there is the distribution of gas regularly which release the water from fuel cell. Likewise, the study of the concentration of gas in the elbow middle P-S found that gas has good distribution, highly decrease of concentration of hydrogen which is along the distance of channel and the concentration of water is increased along the distance of flow field which is similar to parallel-serpentine. Thus, the elbow middle P-S is good to be the model of performing the single cell. So that the test of the efficiency of flow field will be developed.

From the study, we compared between the developed flow field and the conventional at the same working conditions. As the result, it found that the developed fuel cell has the density of electric power about 81.25 mA/cm^2 and the old fuel cell is about 69.22 mA/cm^2 which is better around 17.5%. From experiment study, fuel cell with the temperature and the flow rate, of 50 ^{o}C and 150 sccm gave the best electric power density as shown in Figure. 10. The study still yet to be continued in order to improve the fundamental knowledge and possibility to implement this technology in Thailand.

7. Reference

[1] Chu, D., Jiang, R., and Walker, C. (2000), Analysis of PEM fuel cell stacks using an empirical current-voltage equation, *Journal of Applied Electrochemistry*, Vol. 30, pp. 365-370.

[2] Jaruwasupant, N. and Khunatorn, Y. (2004), Numerical Modeling of Gas Flow in Proton Exchange Membrane Fuel Cell, paper presented in the *the first symposium on engineering and architecture for sustainable development in the greater Mekong sub-region*, January 13-14., Lao.

[3] Jaruwasupant, N., Khunatorn, Y., Vorayos, N. and Wongsuwan, V. (2005), Study of Gas Flow and Pressure Distribution in Proton Exchange Membrane Fuel Cell : Numerical Modeling, paper presented in the *Mechanical Engineering Network of Thailand the 19th Conference*, pp. 158, October 19-21.

[4] Mennola, T. (2000)., Design and Experimental Characterization of Polymer Electrolyte Membrane Fuel Cells, *Licentiate's thesis*, *Department of Engineering Physics and Mathematics*, Helsinki University of Technology, Finland.

[5] Sukkee, U and Wang,C.V. (2000), Three Dimensional Analysis of Transport and Reaction in Proton Exchange Membrane Fuel Cells, *Department of Mechanical and Nuclear Engineering*, Pennsylvania State University, USA.

[6] Wetton, B., Promislow, K., and Caglar, A., A simple thermal model of PEM fuel cell stacks. Available online: www.google.co.th.

[7] Kordesch,K. and Simader,G. (1996), *Fuel Cell and their applications*., Weinheim, Federal Replubic of Germany.

[8] Su, A., Chiu, Y.C. and Weng, F.B. (2005), The impact of flow field pattern on concentration and performance in PEMFC., *Department of Mechanical Engineering*, Yuan Ze University, Chung-Li, Taiwan. ; 29: 409-425.

Three-Dimensional Model and Experiment of Serpentine Flow Field for Proton Exchange Membrane Fuel Cell using CFD

Nattawoot Jaruwasupant* and Yottana Khunatorn1

[1]Faculty of Mechanical Engineering, Department of Engineering Chiang Mai University, 50200 Thailand
Tel. (66) 53-944100 fax. (66) 53-944145
* Corresponding Author. Email: eaw_eng@hotmail.com

Abstract: *The design flow field has important for development performance of PEMFC. It has many parameters for studied such as configuration channel, channel length, dimension channel and etc., but most studied focus only on couple parameters. However, there are more parameters that needed to be considered in order to design an appropriate gas flow field. That includes channel length and channel curvature. This research focuses on the gas dynamic in the gas channel with different channel curvature using CFD technique. The numerical results will provide understanding the effect of flow field pattern design on performance of the fuel cell. This will lead us to a better design of gas flow field, which improves the gas distribution and water management. This research will investigate the relationship between channel length and channel curvature with pressure drop, velocity distribution by using numerical model. The experiments will performed to verify the numerical predictions on polarization curve and power curve. The output from this research will enlight our on fundamental knowledge, which can be applied on design and operate the fuel cell.*

Keywords: *numerical models, flow field, PEMFC, CFD*

1. INTRODUCTION

Proton exchange membrane fuel cells (PEMFCs) transforms the chemical energy into electricity. Hence, it is an environment friendly energy source. Its performance and efficiency still needed to be improved, and the issues of cost, reliability and safety are needed to be considered to realize the fuel cell commerciality. In order to enhance its performance and reliability, it is necessary to learn more about the mechanism that causes the performance loss, such as, non-uniform concentration, current density distributions, high ionic resistance due to dry membrane, or high diffusive resistance due to the flooding on the cathode. The flow field and water/thermal management of fuel cell need optimal design to achieve high performance and reliability. The numerical modeling and dedicated experimental technique development are currently the effective tools to improve the optimal design of fuel cell system.

Many numerical model of PEMFC works have been accomplished during last 15 years. Most of these models compute the flow field along a single channel to study the reaction species and current density distributions. Mazumder and Cole (2003) and Su et al. (2005) presented three-dimensional models based on computational fluid dynamics approach. Beming et al. (2002) and Wang and Lu (2004) and Hu et al. (2004) have used self-developed PEMFC numerical base on of the SIMPLE algorithm. Their three-dimensional models account for the effect of the complex geometry, specifically interdigitated flow field. They allow a parametric study for a realistic flow field, concentration and current distributions. The simulation results are well compared with the experimental data of polarization curve. However, the influence of flow field design upon

concentration and current density distributions were less discussed. Mench et al. (2003) proved that the effects of cathode stoichiometry variation and transient flooding on local current density affect the current distribution on serpentine flow field. The efforts on fuel cell modeling and experimental measurement technique are valuable for fuel cell developers, which can optimize fuel cell designs and operations. Even though intensive studies have been carried on the affect of gas dynamics in flow field on fuel cell performance, the data of flow path configuration still needed to investigates. This research will focus on the gas dynamic within the channel length and channel curvature for design flow field. The numerical results will provide understanding the effect of these parameters. The results will investigate the relationship between channel length and channel curvature with pressure drop and velocity distribution by using numerical model. The experiments will be set up to compare the numerical predictions on polarization curve and power curve. These information will be implied as a guideline for design an appropriate flow field for PEMFC.

2. METHODOLOGY

2.1 Fundamental of PEMFC

Single PEMFC components includes of flow field plates, gas diffusion, catalyst layer, membrane, shown in Figure. 1.

Figure 1 Schematic diagram of PEMFC.
: http://www.princeton.edu/.../ Hydrogen/fuelcells.html

Fuel cells are energy source from electrochemical in cell. The reactions are from hydrogen gas flow pass the catalyst layer in Anode, it is Oxidation reaction and show in equation (1). Hydrogen ion from the reaction flow pass Electrolyte to Cathode and the reaction in the catalyst layer are Reduction, The Oxygen is reactance in the reaction and show in equation (2). The products from the reaction are water and electrons. The current in the Cathode and Anode from electron flow pass between two sides.

$$H_2 \quad \cdots\cdots\blacktriangleright \quad 2H^+ + 2e^- \qquad \text{Oxidation process} \qquad (1)$$
$$O_2 + 4e^- + 4H^+ \quad \cdots\cdots\blacktriangleright \quad 2H_2O \qquad \text{Reduction process} \qquad (2)$$

Electrical energy is obtained from a fuel cell only when a reasonable current is drawn, but the actual cell potential is decreased from its equilibrium potential because of irreversible losses as shown in Figure 2. Several sources contribute to irreversible losses in a practical fuel cell. The losses, which are often called polarization, overpotential, or overvoltage, originate primarily from

three sources: activation polarization, ohmic polarization, and concentration polarization. These losses result in a cell voltage for a fuel cell that is less than its ideal potential.

Figure 2 Ideal and actual fuel cell voltage/current characteristic.

2.2 Numerical modeling

In this study, present a 3-D numerical modeling, to analysis flow field of proton exchange membrane fuel cells. The model is based on the solution of the conservation equations of mass and momentum using the CFD. Tables 1 and Tables 2 are the dimensions of PEMFC and the boundary conditions used in the numerical simulation.

Table 1 Main Dimensions for the numerical model

Channel Area (cm^2)	10×10
Channel width (mm)	1
Channel depth (mm)	1
Rib width (mm)	1

Table 2 Boundary Conditions

gas fuel inlet (m/s)	2
Operating pressure (atm)	1

The main assumptions of the modeling are:
1. steady state
2. laminar flow
3. gas are treated as ideal gas

These conservation equations in flow field are follows;

Mass conservation

$$\frac{\partial \rho}{\partial t} + \nabla(\rho U) = 0 \tag{3}$$

Momentum conservation

$$\frac{\partial \rho u}{\partial t} + \nabla \cdot (\rho U u) = -\frac{\partial P}{\partial x} + \nabla(\mu \nabla u) \tag{4}$$

$$\frac{\partial \rho v}{\partial t} + \nabla \cdot (\rho U v) = -\frac{\partial P}{\partial y} + \nabla(\mu \nabla v) \tag{5}$$

282

$$\frac{\partial \rho w}{\partial t} + \nabla \cdot (\rho U w) = -\frac{\partial P}{\partial z} + \nabla(\mu \nabla w) \tag{6}$$

2.3 3-D model of channel length and channel curvature of flow field

We describe a detailed three-dimensional model of transport phenomena within the gas channel. The dimensions of the computational domains have 6 elements in the x-direction, 71 elements in the y-direction, 6 elements in the z-direction, for a total of about 2,556 elements.

Channel length and channel curvature of flow field is developed from the result of multi-serpentine flow fields. The channel curvature have 4 cases studied that show in figure 3 and channel length have 6 cases studied. The channel length has varied from 1 to 6 channels on multi serpentine flow field. Number of channel has independent of channel length, which increases number of channel has channel length is shorter.

Non Fillet

Inner Fillet

Outer Fillet

Smooth Fillet
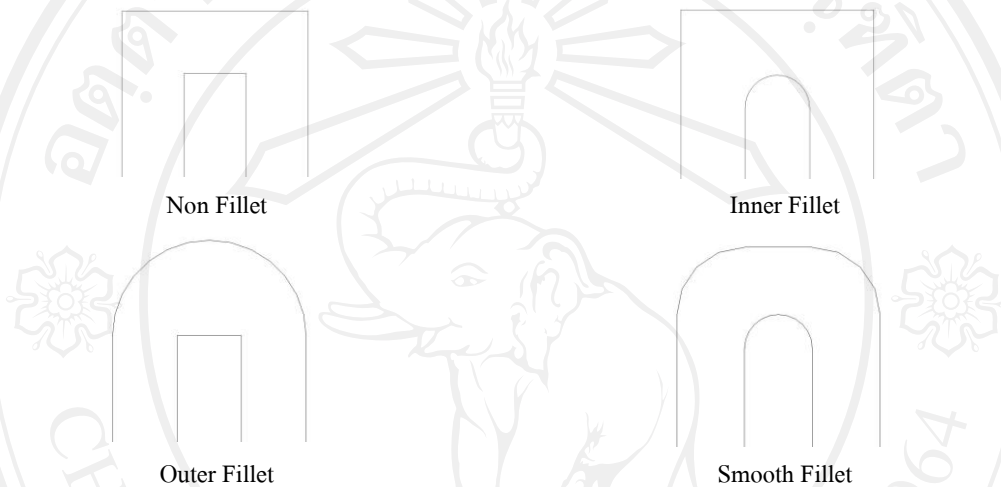
Figure 3 Channel curvatures.

2.4 Experimental details

An experimental system is setup to measure the current/ voltage polarization curves. Graphite plate is used as a current collector. Other materials used in the single cell are O-BASF 12E-W MEA, reaction area 100 cm² and brass current collector. The dimensions of components and operating conditions are consistent with the numerical model.

3. RESULTS AND DISCUSSION

(a) Non Fillet

(b) Inner Fillet
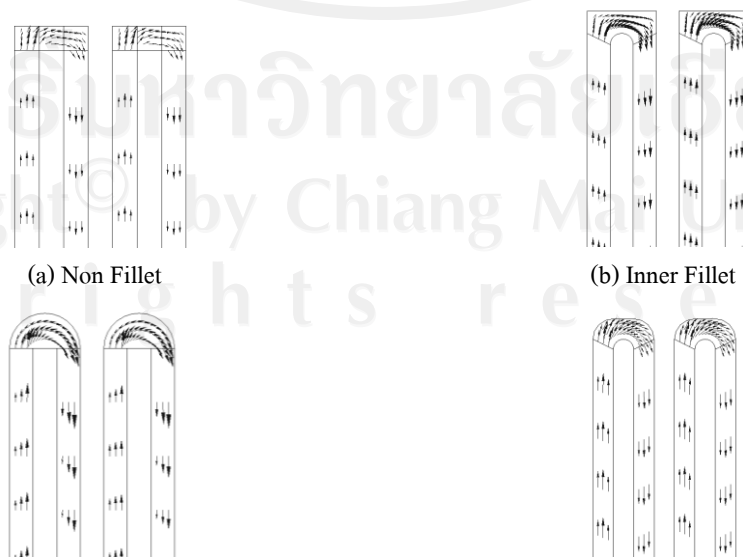
(c) Outer Fillet   (d) Smooth Fillet

Figure 4 Velocities distribution of channel curvatures.

The modeling results of gas flow with in each are channel curvature shows in figure 4. The result displays non-uniform velocity distribution on non fillet and inner fillet (4a and 4b). High gas distribution appears at upper curve and low gas distribution at bottom curve, its have avoid area at bottom center. Figure 4c shows uniform velocity distribution on outer filter. High gas distribution and smooth flow appears at upper curve and low gas distribution still occurs at bottom curve, its have avoid area at center bottom curve. Figure 4d provides uniform velocity distribution and gas distributes overall through the turn, which also confirm that it is the best configuration.

(a) Velocity of 1 channel   (b) Pressure of 1 channel

(c) Velocity of 3 channel   (d) Pressure of 3 channel

(e) Velocity of 6 channel   (f) Pressure of 6 channel
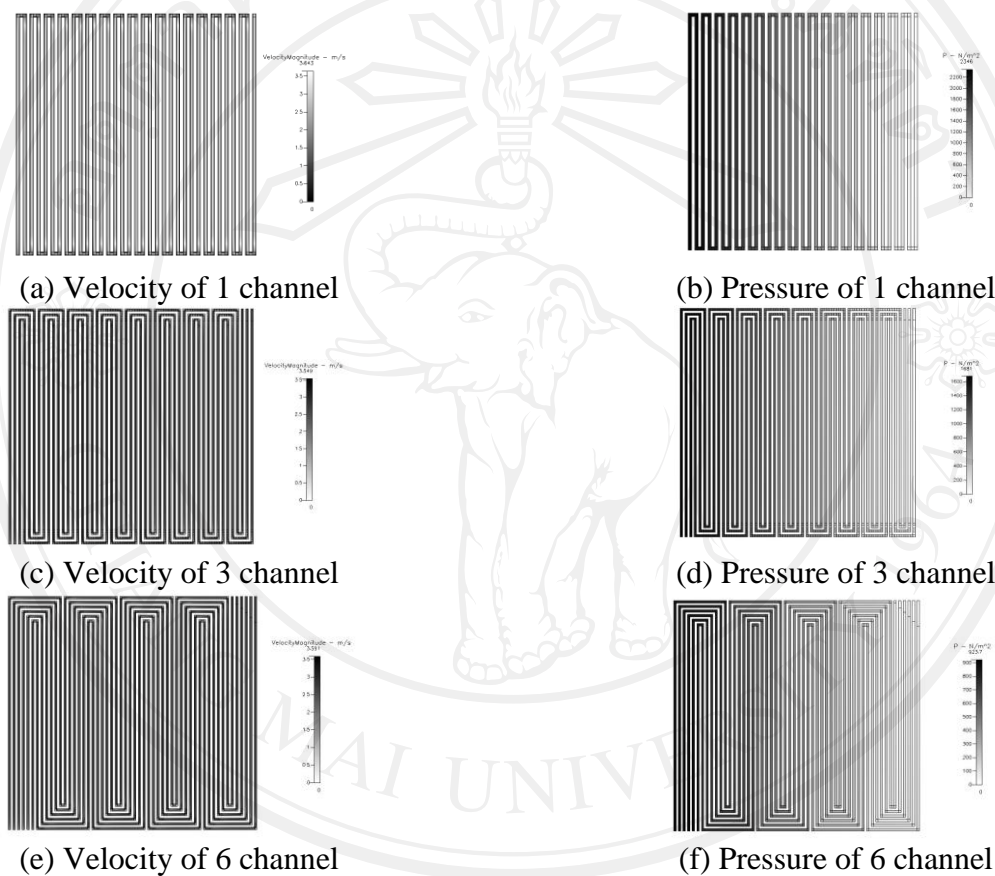
Figure 5 Velocity and Pressure distribution of channel length.

Figure 5 showed the velocities and pressure distribution in 1, 3 and 6 serpentine channel. Figure 5a and 5b, which are results form single channel has the average velocity around 3.10 m/s and pressure drop is around 2,346 N/m^2. Gas distribution has uniform for serpentine pattern. Lower velocities distribution appears at channel curvatures and high velocities distribution at downstream of channel. The pressure drop has decreases along length channel. Figure 5(c and d) 3 channels have the average velocity around 3.10 m/s and pressure drop is around 1,326 N/m^2. Lower velocities distribution appears at channel curvatures and it have avoid area than single channel and high velocities distribution at downstream of channel. The pressure drop has decreases along length channel as same as single channel. Figure 5e and 5f display the velocities and pressure distribution on 6 channels serpentine. It has the average velocity around 3.10 m/s and pressure drop is around 923.7 N/m^2. Lower velocities distribution appears at channel curvatures and it have avoid area less more than 1, 3 channels and high velocities distribution at downstream of channel. The pressure drop has decreases along length channel.
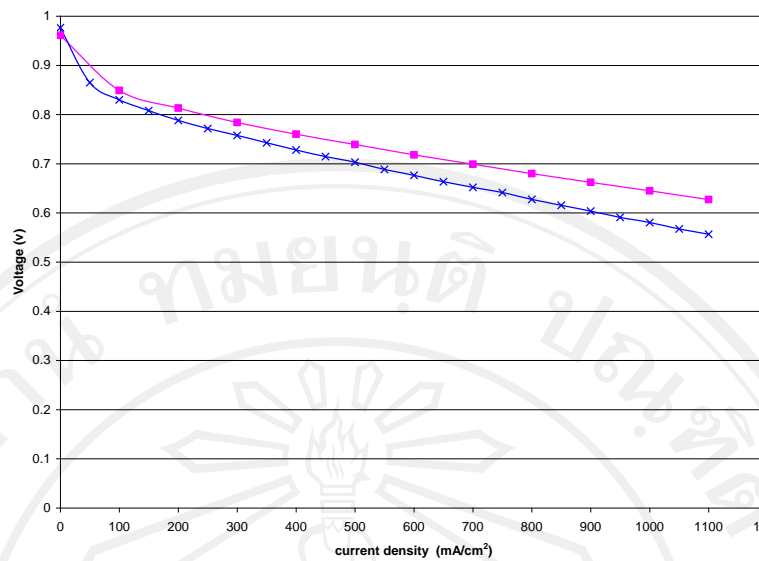
Figure 6 Polarization curve of fuel cell 3 channel (cross) and 6 channel (box) size 10 x 10 cm^2

4. CONCLUSION

A 3-D numerical modeling to predict velocities distribution and pressure drop is presented in this research. The influence of channel length and channel curvature is investigated. The best channel curvature from gas distribution is smooth curve and 6 channels serpentine because it has higher area of gas flow and high velocity and pressure drop when compare with channel length. From that result, the fuel cell with our flow field provides better performance. At the outlet, there is the distribution of gas regularly which releases the water from fuel cell.

From the experiment results on smooth fillet and 3 channels and 6 channels, it is found that the fuel cell has the density of electric power about 900 and 1200 mA/cm^2 at 0.6 V, respectively. Flow field has 6 channel is 25% better than 3 channels. The study still yet to be continued in order to improve the fundamental knowledge on other geometric parameters. These information will be implied as a guideline for design an appropriate flow field for PEMFC.

5. ACKNOWLEDGMENTS

6. REFERENCES

[1] Chu, D., Jiang, R., and Walker, C. (2000), Analysis of PEM fuel cell stacks using an empirical current-voltage equation, *Journal of Applied Electrochemistry*, 30, pp. 365-370.

[2] Fang-Bor Weng, Ay Su, Guo-Bin Jung, Yen-Chiao Chiu and Shih-Hung Chan. (2005), Numerical prediction of concentration and current distributions in PEMFC, *Journal of Power Sources*, 145, pp. 546–554

[3] Jaruwasupant, N. and Khunatorn, Y. (2004), Numerical Modeling of Gas Flow in Proton Exchange Membrane Fuel Cell, paper presented in the *the first symposium on engineering and architecture for sustainable development in the greater Mekong sub-region*, January 13-14., Lao.

[4] Jaruwasupant, N., Khunatorn, Y., Vorayos, N. and Wongsuwan, V. (2005), Study of Gas Flow and Pressure Distribution in Proton Exchange Membrane Fuel Cell : Numerical Modeling, paper presented in the *Mechanical Engineering Network of Thailand the 19th Conference*, pp. 158, October 19-21.

[5] Mennola, T. (2000)., Design and Experimental Characterization of Polymer Electrolyte Membrane Fuel Cells, *Licentiate's thesis*, *Department of Engineering Physics and Mathematics*, Helsinki University of Technology, Finland.

[6] Sukkee, U and Wang,C.V. (2000), Three Dimensional Analysis of Transport and Reaction in Proton Exchange Membrane Fuel Cells, *Department of Mechanical and Nuclear Engineering*, Pennsylvania State University, USA.

[7] Wetton, B., Promislow, K., and Caglar, A., A simple thermal model of PEM fuel cell stacks. Available online: www.google.co.th.

[8] Kordesch,K. and Simader,G. (1996), *Fuel Cell and their applications*., Weinheim, Federal Replubic of Germany.

[9] Su, A., Chiu, Y.C. and Weng, F.B. (2005), The impact of flow field pattern on concentration and performance in PEMFC., *Department of Mechanical Engineering*, Yuan Ze University, Chung-Li, Taiwan, 29, pp. 409-425.
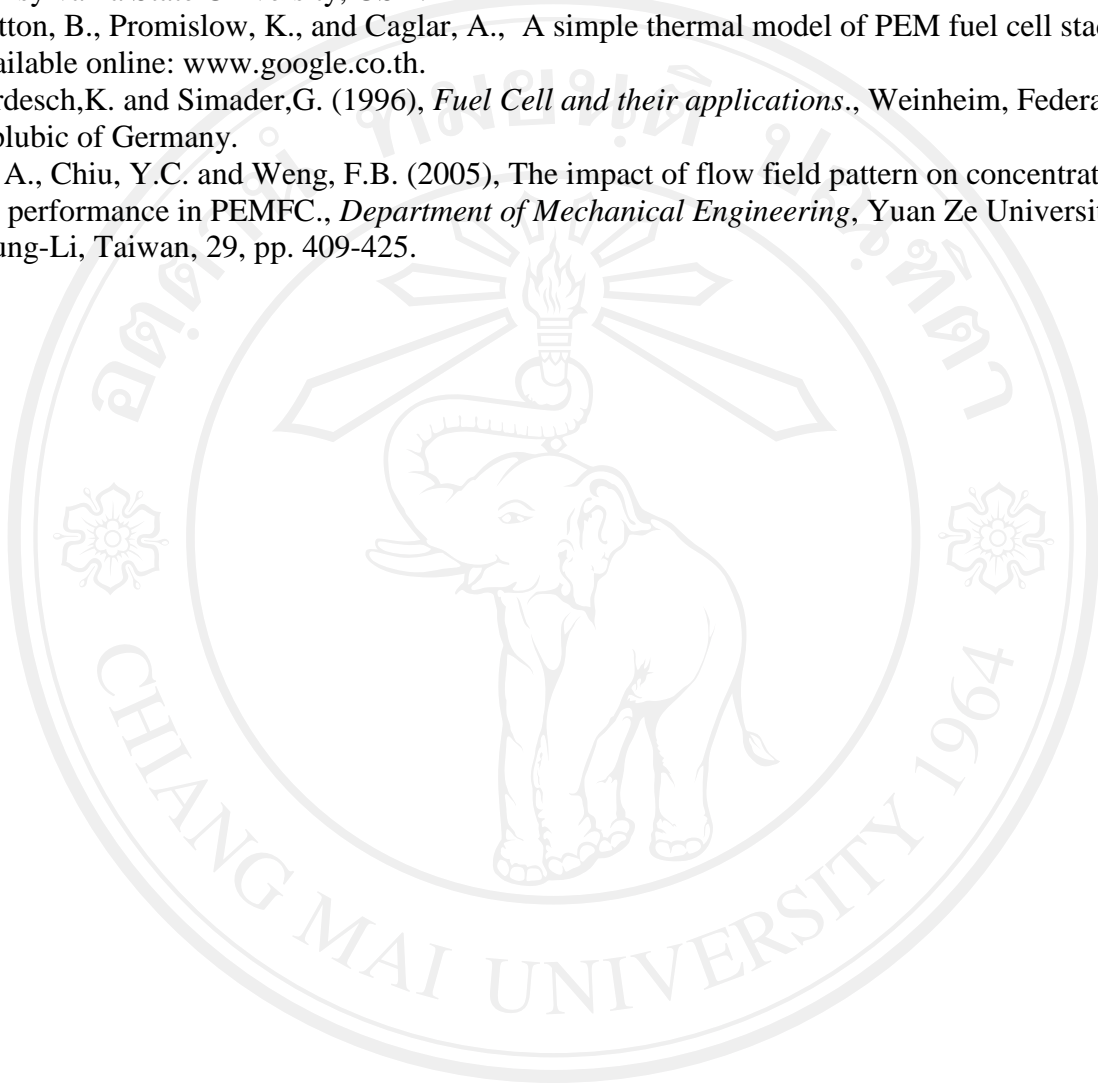
Abstract Book

9th Eco-Energy and Materials Science and Engineering Symposium

Energy technology, Environmental and Social Impact, Nanotechnology and Material Technology, Energy Economic and Management, Nuclear Technology, New Technology and Other topics related to energy field.

**On May 25-28, 2011
Wiang Inn, Chiang Rai
Thailand**

Organized by

Sponsored by

TAT

Effects of difference flow channel designs on Proton Exchange Membrane Fuel Cell using 3-D Model

Nattawut Jaruwasupant* and Yottana Khunatorn[1]

Abstract— This research is study to design of flow field on PEMFC for distributions in reaction gas. The distribution of the reaction causes gradients in concentration and water production over the area of the cell. Secondary effects can feedback to change the reaction rate and can also lead to ternary effects such as local flooding when the local partial pressure of water exceed. Many researchers have studied the problem of water management inside PEMFC for both steady state and transient operation. However, the effect of flow-field design on PEMFC performance has received less attention. The Design of flow field was studied the effects of channel configurations of flow field plates on the performance of a PEMFC. Effects of widths, length and curve channel of a flow field plate were studied in an effort to optimize the dimensions of channel. It was assumed that the development of these design techniques with CFD will require verification (of a subset of model predictions) but that proper design of experiments will expedite the development. That is, CFD experiments will be less costly than build-and-test experiments and they can be correlated to yield design for the next generation of PEMFC. This study used three-dimensional computational fluid dynamics (CFD) model was investigate the effects of serpentine flow channel designs on the performance of proton exchange membrane fuel cells. This model is validated by the experiments. The numerical results will provide understanding the effect of flow field pattern design on performance of the fuel cell. This will lead us to a better design of gas flow field, which improves the gas distribution and water management. This research will investigate the relationship between channel length, channel curvature and characteristics of flow field with pressure drop, velocity distribution by using numerical model. The experiments will performed to verify the numerical predictions on polarization curve and power curve. The output from this research will enlight our on fundamental knowledge, which can be applied on design and operate the fuel cell.

*Keywords— **Numerical Models, Flow Field, PEMFC, CFD***

1. INTRODUCTION

Proton exchange membrane fuel cells (PEMFCs) transforms the chemical energy into electricity. Hence, it is an environment friendly energy source. Its performance and efficiency still needed to be improved, and the issues of cost, reliability and safety are needed to be considered to realize the fuel cell commerciality. In order to enhance its performance and reliability, it is necessary to learn more about the mechanism that causes the performance loss, such as, non-uniform concentration, current density distributions, high ionic resistance due to dry membrane, or high diffusive resistance due to the flooding on the cathode. The flow field and water/thermal management of fuel cell need optimal design to achieve high performance and reliability. The numerical modeling and dedicated experimental technique development are currently the effective tools to improve the optimal design of fuel cell system.

Many numerical model of PEMFC works have been accomplished during last 15 years. Most of these models compute the flow field along a single channel to study the reaction species and current density distributions. Mazumder and Cole (2003) and Su et al. (2005) presented three-dimensional models based on computational fluid dynamics approach. Beming et al. (2002) and Wang and Lu (2004) and Hu et al. (2004) have used self-developed PEMFC numerical base on of the SIMPLE algorithm. Their three-dimensional models account for the effect of the complex geometry, specifically interdigitated flow field. They allow a parametric study for a realistic flow field, concentration and current distributions. The simulation results are well compared with the experimental data of polarization curve. However, the influence of flow field design upon concentration and current density distributions were less discussed. Mench et al. (2003) proved that the effects of cathode stoichiometry variation and transient flooding on local current density affect the current distribution on serpentine flow field. The efforts on fuel cell modeling and experimental measurement technique are valuable for fuel cell developers, which can optimize fuel cell designs and operations. Even though intensive studies have been carried on the affect of gas dynamics in flow field on fuel cell performance, the data of flow path configuration still needed to investigates. This research will focus on the gas dynamic within the channel length and channel curvature for design flow field. The numerical results will provide understanding the effect of these parameters. The results will investigate the relationship between channel length and channel curvature with pressure drop and velocity distribution by using numerical model. The experiments will be set up to compare the numerical predictions on polarization curve and power curve. These information will be implied as a guideline for design an appropriate flow field for PEMFC.

2. METHODOLOGY

2.1 Fundamental of PEMFC

Single PEMFC components includes of flow field plates, gas diffusion, catalyst layer, membrane, shown in Figure. 1.
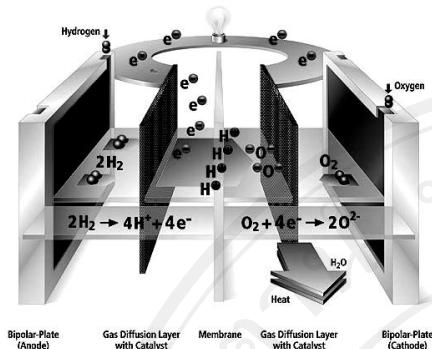

Fig.1. Schematic diagram of PEMFC
: http://www.princeton.edu/.../ Hydrogen/fuelcells.html

Fuel cells are energy source from electrochemical in cell. The reactions are from hydrogen gas flow pass the catalyst layer in Anode, it is Oxidation reaction and show in equation (1). Hydrogen ion from the reaction flow pass Electrolyte to Cathode and the reaction in the catalyst layer are Reduction, The Oxygen is reactance in the reaction and show in equation (2). The products from the reaction are water and electrons. The current in the Cathode and Anode from electron flow pass between two sides.

$$H2 \longrightarrow 2H+ + 2e- \qquad \text{Oxidation process} \quad (1)$$
$$O2 + 4e- + 4H+ \longrightarrow 2H2O \quad \text{Reduction process} \quad (2)$$

Electrical energy is obtained from a fuel cell only when a reasonable current is drawn, but the actual cell potential is decreased from its equilibrium potential because of irreversible losses as shown in Figure 2. Several sources contribute to irreversible losses in a practical fuel cell. The losses, which are often called polarization, overpotential, or overvoltage, originate primarily from three sources: activation polarization, ohmic polarization, and concentration polarization. These losses result in a cell voltage for a fuel cell that is less than its ideal potential.
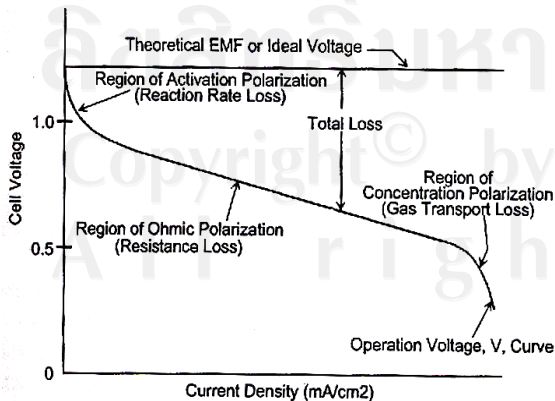

Fig.2. Ideal and actual fuel cell voltage and current

2.2 Numerical modeling

In this study, present a 3-D numerical modeling, to analysis flow field of proton exchange membrane fuel cells.

The model is based on the solution of the conservation equations of mass and momentum using the CFD. Tables 1. and Tables 2. are the dimensions of PEMFC and the boundary conditions used in the numerical simulation.

Table 1. Main Dimensions for the numerical model

Channel Area (cm²)	10×10
Channel width (mm)	1
Channel depth (mm)	1
Rib width (mm)	1

Table 2. Boundary Conditions

gas fuel inlet (cm³/min)	200-500
Operating pressure (atm)	1
Temperature (K)	
323	

The main assumptions of the modeling are:
1. steady state
2. laminar flow
3. gases are treated as ideal gas

These conservation equations used in flow field model are follows;

Mass conservation

$$\nabla(\rho U) = 0 \qquad (3)$$

Momentum conservation

$$\nabla \cdot (\rho U u) = -\frac{\partial P}{\partial x} + \nabla(\mu \nabla u)$$

$$\nabla \cdot (\rho U v) = -\frac{\partial P}{\partial y} + \nabla(\mu \nabla v) \qquad (4)$$

$$\nabla \cdot (\rho U w) = -\frac{\partial P}{\partial z} + \nabla(\mu \nabla w)$$

2.3 3-D model of channel length, channel curvature and characteristics of flow field

We describe a detailed three-dimensional model of transport phenomena within the gas channel. The dimensions of the computational domains have 6 elements in the x-direction, 71 elements in the y-direction, 6 elements in the z-direction, for a total of about 2,556 elements. The full domain flow field show in figure 3.

Channel length and channel curvature of flow field is developed from the result of multi-serpentine flow fields. The channel curvature have 4 cases studied that show in figure 4 and channel length have 6 cases studied. The channel length has varied from 1 to 6 channels on multi serpentine flow field. Number of channel has independent of channel length, which increases number of channel has channel length is shorter. Characteristics of channel are change the depth channels have 0.8, 1 and 1.2 mm.
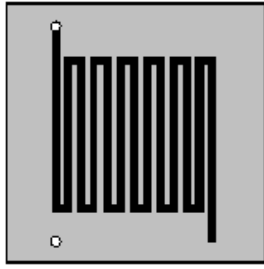
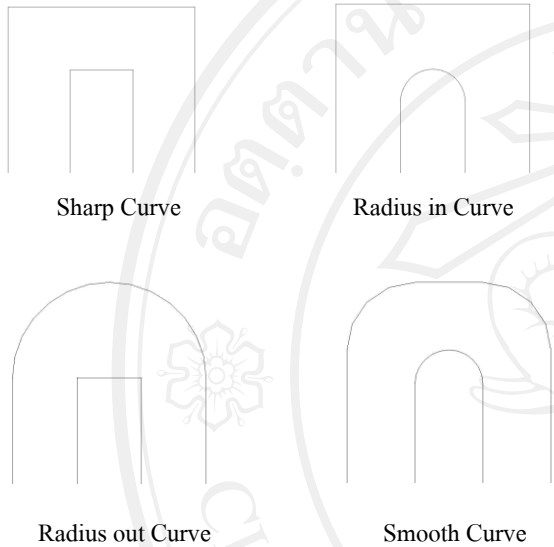**Fig.3. One Channel of Serpentine Flow Field**

Sharp Curve

Radius in Curve

Radius out Curve

Smooth Curve

Fig.4. Channel curvatures

2.4 Experimental details

An experimental system is setup to measure the current/ voltage polarization curves. Graphite plate is used as a current collector. Other materials used in the single cell are O-BASF 12E-W MEA, reaction area 100 cm^2 and brass current collector. The dimensions of components and operating conditions are consistent with the numerical model.

3. RESULT AND DISSCUSSION

3.1 The effect of channel curvature on flow field

The results of flow and pressure drop are effect of curvature show in figure 5-11
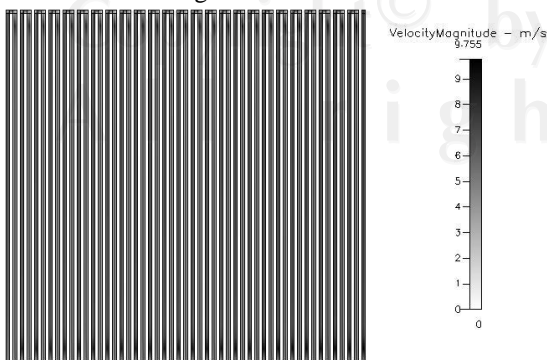

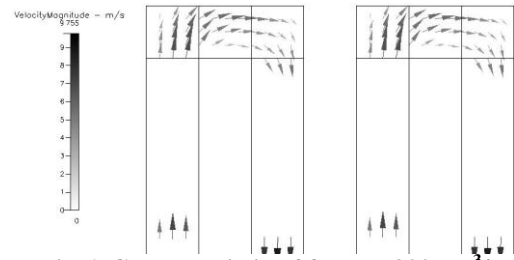**Fig.5. Velocity of flow field at 300 cm^3/min of Sharp Curve**

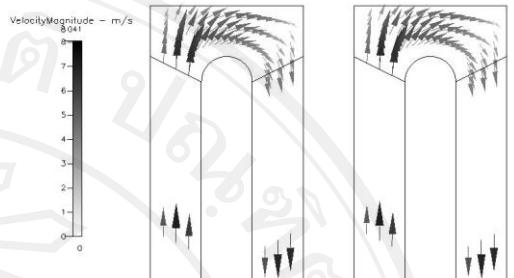**Fig.6. Characteristic of flow at 300 cm^3/min of Sharp Curve**

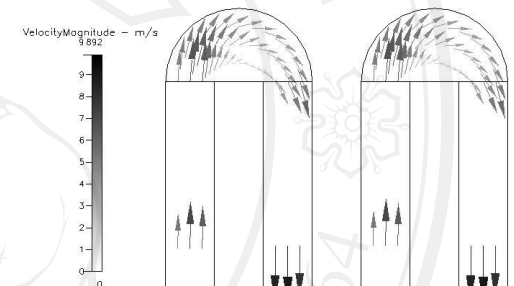**Fig.7. Characteristic of flow at 300 cm^3/min of Radius in Curve**

Fig.8. Characteristic of flow at 300 cm^3/min of Radius out Curve
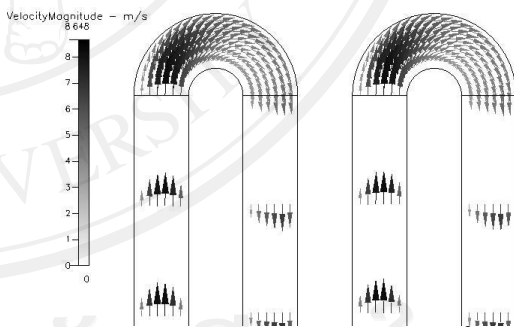

Fig.9. Characteristic of flow at 300 cm^3/min of Smooth Curve
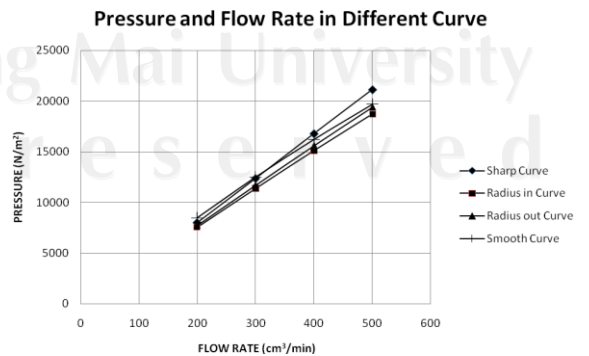

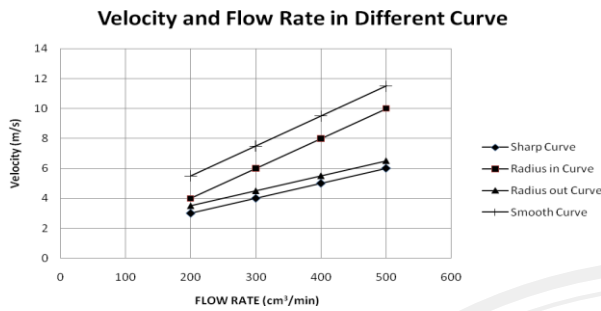**Fig.10. Pressure in different curve**

Fig.11. Velocity in different curve

In figure 6 and 7 are displays non-uniform velocity distribution on sharp curve and Radius in curve. High gas distribution appears at upper curve and low gas distribution at bottom curve, its have avoid area at bottom center. Figure 8 shows uniform velocity distribution on outer filter. High gas distribution and smooth flow appears at upper curve and low gas distribution still occurs at bottom curve, its have avoid area at center bottom curve. Figure 9 provides uniform velocity distribution and gas distributes overall through the turn. which also confirm that it is the best configuration. The result of different curve that the sharp curve is also confirm that it is the best configuration because it was non-uniform flow distribution and high pressure drop for the high electro chemical reaction in MEAs and water management. The pressure and velocity in different curve at all flow rate show in figure 10 and 11.

3.2 The effect of channel length on flow field

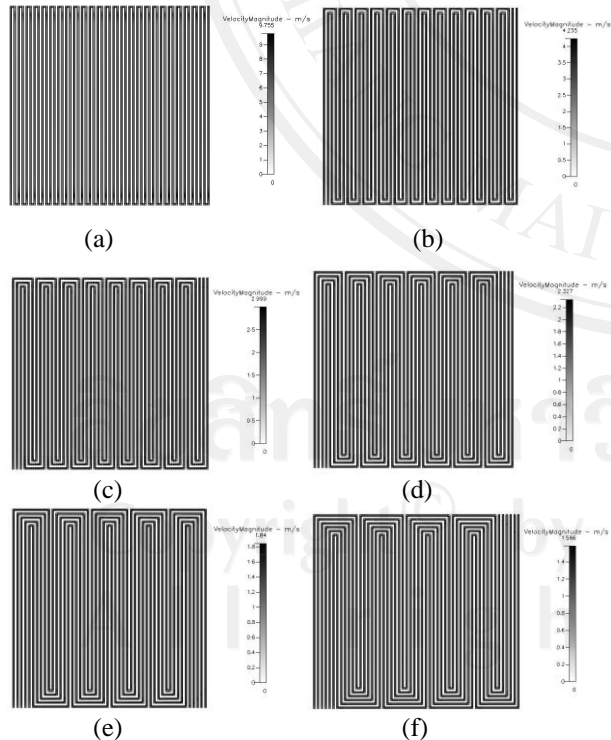The results of flow and pressure drop are effect of length show in figure 12-14

(a) (b)

(c) (d)

(e) (f)

Fig.12. Velocity of flow field at 300 cm^3/min
(a) 1 channel (b) 2 channels (c) 3 channels
(d) 4 channels (e) 5 channels (f) 6 channels

The velocities and pressure distribution in 1, 2, 3, 4, 5 and 6 serpentine channel at 300 cm^3/min. Figure 12 which

are results form 1 channel has the average velocity around 4 m/s and pressure drop is around 12,380 N/m^2. Gas distribution has uniform for serpentine pattern. Lower velocities distribution appears at channel curvatures and high velocities distribution at downstream of channel. The pressure drop has decreases along length channel. In 2 , 3, 4, 5 and 6 channels have a velocity around 3.5, 2.25, 2, 1.5 and 1.2 m/s, and pressure drop around 3,138, 1,385, 798.5, 489.4 and 359.5 N/m^2, respectively. The pressure and velocity in different length at all flow rate show in figure 13 and 14.
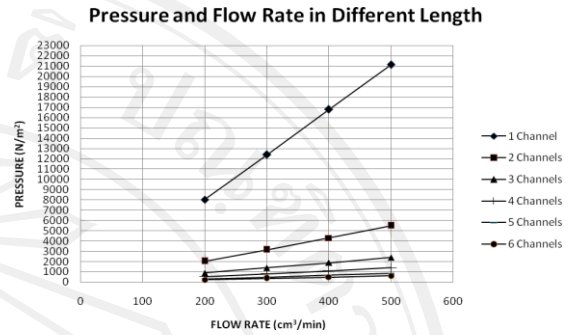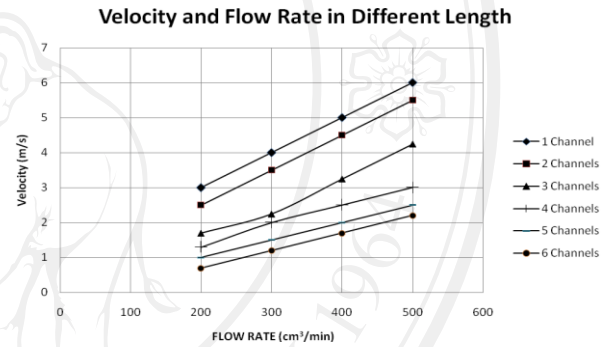

Fig.13. Pressure in different length

Fig.14. Velocity in different length

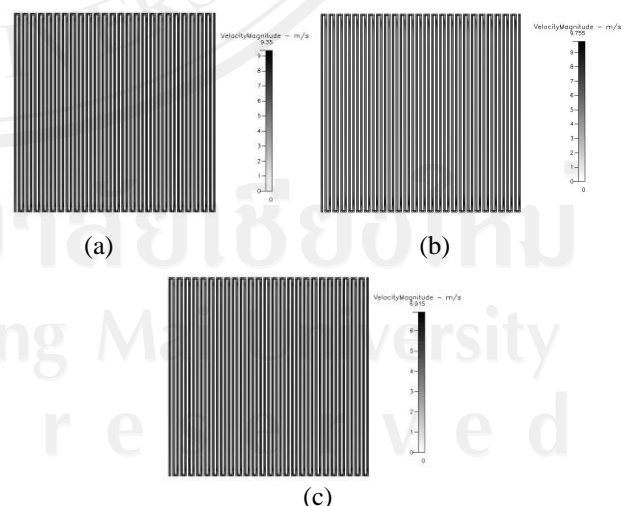### 3.3 The effect of channel depth on flow field

(a) (b)

(c)

Fig.15. Velocity of flow field at 300 cm^3/min
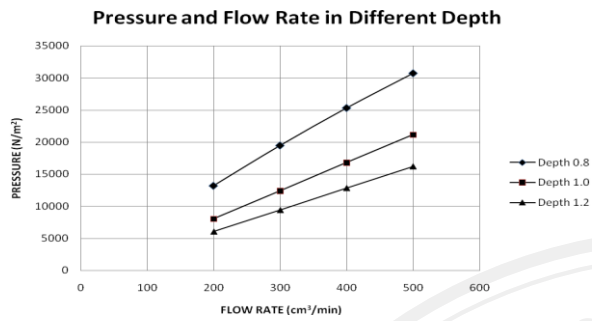**(a) 0.8 mm. (b) 1.0 mm. (c) 1.2 mm.**
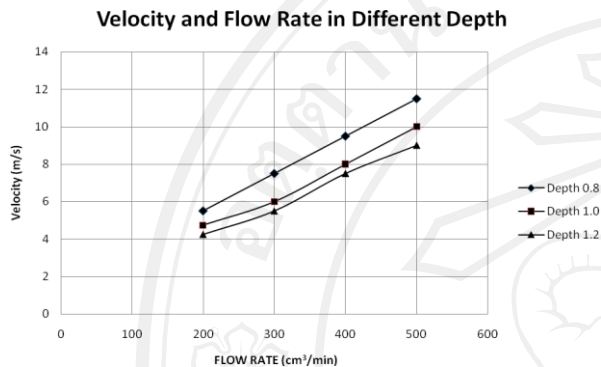
Fig.16. Pressure in different depth

Fig.17. Velocity in different depth

Figure 15 displays velocity of 3 depths channel at 300 cm³/min. In 0.8 depth channel has velocity about 7.5 m/s and pressure drop is 19,470 N/m². 1.0 and 1.2 depth channel have velocities about 6 and 5.5 m/s and pressure drop is 12,380 and 9,410 N/m², respectively. The pressure and velocity in different depth channels at all flow rate show in figure 16 and 17.
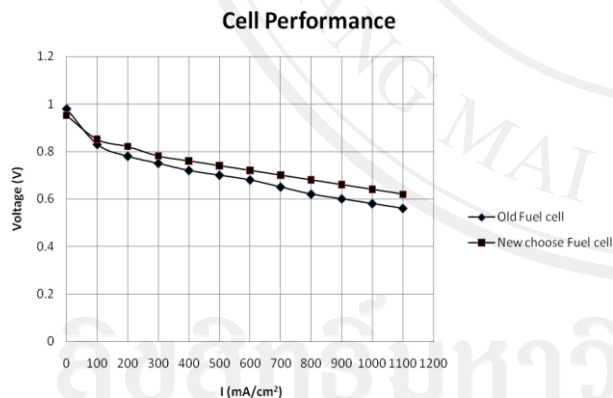

Fig.18. Comparisons between the old fuel cell and the new choose fuel cell

The performance of fuel cell predict from I-V curve. In figure 18 show the experiment test between old fuel test and new choose fuel cell, the old fuel cell is 4 channels, smooth curve and depth 1 mm.. The new choose is 6 channels, sharp curve and depth 1 mm.. The new fuel cell has better performance than old fuel cell.

4. CONCLUSION

A 3-D numerical modeling to predict velocities distribution and pressure drop is presented in this research.

The influence of channel length, channel curvature and channel depth is investigated. The best channel curvature from gas distribution is sharp curve and 6 channels serpentine because it has secondary flow and higher area of gas flow, high velocity and pressure drop when compare with channel length. From that result, the fuel cell with our flow field provides better performance. At the outlet, there is the distribution of gas regularly which releases the water from fuel cell. From the experiment results on 4 channels smooth curve and 6 channels sharp curve, there are found that the fuel cell has the density of electric power about 900 and 1200 mA/cm² at 0.6 V, respectively. Flow field has 6 channel is 25% better than 4 channels. The study still yet to be continued in order to improve the fundamental knowledge on other geometric parameters. These information will be implied as a guideline for design an appropriate flow field for PEMFC.

ACKNOWLEDGMENT

REFERENCES

[1] Fang-Bor Weng, Ay Su, Guo-Bin Jung, Yen-Chiao Chiu and Shih-Hung Chan. 2005. Numerical prediction of concentration and current distributions in PEMFC, *Journal of Power Sources*, 145 : 546–554.

[2] Jaruwasupant, N. and Khunatorn, Y. 2004. Numerical Modeling of Gas Flow in Proton Exchange Membrane Fuel Cell, paper presented in the *the first symposium on engineering and architecture for sustainable development in the greater Mekong sub-region*, 13-14 January. Lao.

[3] Jaruwasupant, N., Khunatorn, Y., Vorayos, N. and Wongsuwan, V. 2005. Study of Gas Flow and Pressure Distribution in Proton Exchange Membrane Fuel Cell : Numerical Modeling, paper presented in the *Mechanical Engineering Network of Thailand the 19th Conference*, pp. 158, 19-21 October. Thailand.

[4] Mennola, T. 2000. Design and Experimental Characterization of Polymer Electrolyte Membrane Fuel Cells, *Licentiate's thesis*, *Department of Engineering Physics and Mathematics*, Helsinki University of Technology, Finland.

[5] Sukkee, U and Wang,C.V. 2000. Three Dimensional Analysis of Transport and Reaction in Proton Exchange Membrane Fuel Cells, *Department of Mechanical and Nuclear Engineering*, Pennsylvania State University, USA.

[6] Kordesch,K. and Simader,G. (1996), *Fuel Cell and their applications.*, Weinheim, Federal Replubic of Germany.

[7] Su, A., Chiu, Y.C. and Weng, F.B. (2005), The impact of flow field pattern on concentration and performance in PEMFC., *Department of Mechanical Engineering*, Yuan Ze University, Chung-Li, Taiwan, 29, pp. 409-425.

9th Eco-Energy and Materials Science and Engineering Symposium

Effects of difference flow channel designs on Proton Exchange Membrane Fuel Cell using 3-D Model

Nattawut Jaruwasupant[a]*, Yottana Khunatorn[a]

[a]Department of Mechanical Engineering, Faculty of Engineering, Chiang Mai University,

239 Huay Kaew Road, Muang District, Chiang Mai 50200, Thailand

Abstract

This research was studied to design of flow field on Proton Exchange Membrane Fuel Cell for distributions in reaction gas. The design of flow field was studied the effects of channel configurations of flow field plates on the performance of a PEMFC. Effects of widths, length and curve channel of a flow field plate were studied in an effort to optimize the dimensions of channel. It was assumed that the development of these design techniques with CFD will require. This study used three-dimensional computational fluid dynamics (CFD) model was investigated the effects of serpentine flow channel designs on the performance of proton exchange membrane fuel cells. This model was validated by the experiments. The numerical results were provided understanding the effect of flow field pattern design on performance of the fuel cell. This led us to a better design of gas flow field, which improves the gas distribution and water management. This research will investigate the relationship between channel length, channel curvature and characteristics of flow field with pressure drop, velocity distribution by using numerical model. The experiments will performed to verify the numerical predictions on polarization curve and power curve. The output from this research will enlight our on fundamental knowledge, which can be applied on design and operate the fuel cell.

Keyword : *Numerical Models, Flow Field, PEMFC, CFD*

1. Introduction

Proton exchange membrane fuel cells (PEMFCs) transform the chemical energy into electricity. Hence, it was an environment friendly energy source. Its performance and efficiency still needed to be improved, and the issues of cost, reliability and safety

---

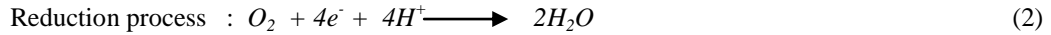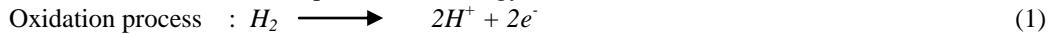* Corresponding author. Tel.: +66-53-944-146; fax: +66-53-944-145.
E-mail address: *lancelot_eaw@hotmail.com, ngairzai@hotmail.com,*

are needed to be considered to realize the fuel cell commerciality. In order to enhance its performance and reliability, it is necessary to learn more about the mechanism that causes the performance loss, such as, non-uniform concentration, current density distributions, high ionic resistance due to dry membrane, or high diffusive resistance due to the flooding on the cathode. The flow field and water/thermal management of fuel cell need optimal design to achieve high performance and reliability. The numerical modeling and dedicated experimental technique development are currently the effective tools to improve the optimal design of fuel cell system. Most of these models compute the flow field along a single channel to study the reaction species and current density distributions. Mazumder and Cole (2003) and Su et al. (2005) presented three-dimensional models based on computational fluid dynamics approach. Beming et al. (2002) and Wang and Lu (2004) and Hu et al. (2004) have used self-developed PEMFC numerical base on of the SIMPLE algorithm. Their three-dimensional models account for the effect of the complex geometry, specifically interdigitated flow field. They allow a parametric study for a realistic flow field, concentration and current distributions. The simulation results are well compared with the experimental data of polarization curve. However, the influence of flow field design upon concentration and current density distributions were less discussed. Mench et al. (2003) proved that the effects of cathode stoichiometry variation and transient flooding on local current density affect the current distribution on serpentine flow field. The efforts on fuel cell modeling and experimental measurement technique are valuable for fuel cell developers, which can optimize fuel cell designs and operations. Even though intensive studies have been carried on the affect of gas dynamics in flow field on fuel cell performance, the data of flow path configuration still needed to investigates. This research will focus on the gas dynamic within the channel length and channel curvature for design flow field. The numerical results will provide understanding the effect of these parameters. The results will investigate the relationship between channel length and channel curvature with pressure drop and velocity distribution by using numerical model. The experiments will be set up to compare the numerical predictions on polarization curve and power curve. This information will be implied as a guideline for design an appropriate flow field for PEMFC.

2. Methodology

2.1 Fundamental of PEMFC

Single PEMFC components includes of flow field plates, gas diffusion, catalyst layer, membrane, shown in Fig. 1. Fuel cells are energy source from electrochemical in cell. The reactions are from hydrogen gas flow pass the catalyst layer in Anode, it is Oxidation reaction and show in equation (1). Hydrogen ion from the reaction flow pass Electrolyte to Cathode and the reaction in the catalyst layer are Reduction, The Oxygen is reactance in the reaction and show in equation (2). The products from the reaction are water and electrons. The current in the Cathode and Anode from electron flow pass between two sides.

Oxidation process : $H_2 \longrightarrow 2H^+ + 2e^-$ (1)

Reduction process : $O_2 + 4e^- + 4H^+ \longrightarrow 2H_2O$ (2)

Electrical energy is obtained from a fuel cell only when a reasonable current is drawn, but the actual cell potential is decreased from its equilibrium potential because of irreversible losses as shown in Fig. 2. Several sources contribute to irreversible losses in a practical fuel cell. The losses, which are often called polarization, overpotential, or overvoltage, originate primarily from three sources: activation polarization, ohmic polarization, and concentration polarization. These losses result in a cell voltage for a fuel cell that is less than its ideal potential.
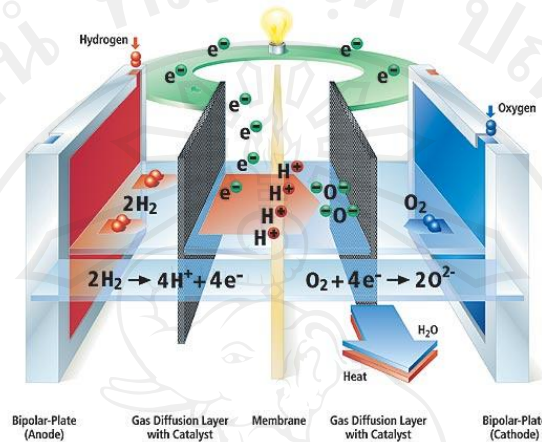

Fig.1. Schematic diagram of PEMFC
: http://www.princeton.edu/.../ Hydrogen/fuelcells.html

2.2 Numerical modeling

In this study, a 3-D numerical model is presented to analysis flow field of proton exchange membrane fuel cells. The model is based on the solution of the conservation equations of mass and momentum using the CFD. Tables 1. and 2. illustrate the dimensions of PEMFC and the boundary conditions used in the numerical simulation.
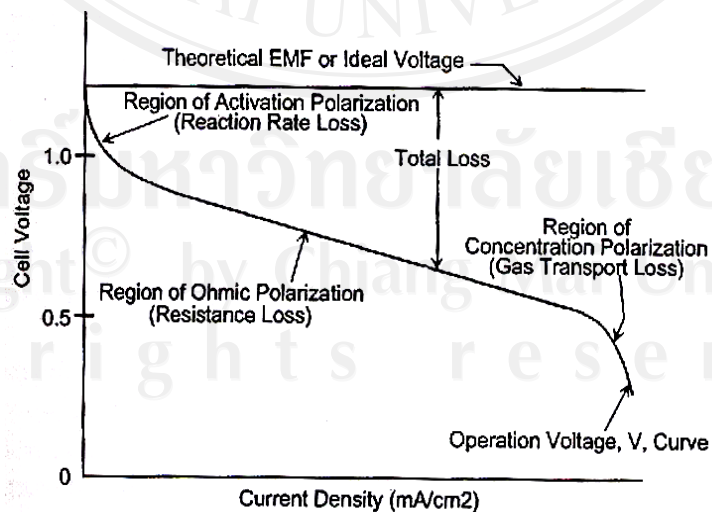
Fig.2. Ideal and actual fuel cell voltage and current

Table 1. Main Dimensions for the numerical model

Characteristics	Sizing
Channel Area (cm^2)	10×10
Channel width (mm)	1
Channel depth (mm)	1
Rib width (mm)	1

Table 2. Boundary Conditions

Boundary conditions	Value
Gas fuel inlet (cm^3/min)	200-500
Operating pressure (atm)	1
Temperature (K)	323

The main assumptions of the modeling are:
1. Steady state
2. Laminar flow
3. Gases are treated as ideal gas
4. Isothermal

These conservation equations used in flow field model are follows;
Mass conservation

$$\nabla(\rho U) = 0 \tag{3}$$

Momentum conservation

$$\nabla \cdot (\rho U u) = -\frac{\partial P}{\partial x} + \nabla(\mu \nabla u)$$

$$\nabla \cdot (\rho U v) = -\frac{\partial P}{\partial y} + \nabla(\mu \nabla v)$$

$$\tag{4}$$

$$\nabla \cdot (\rho U w) = -\frac{\partial P}{\partial z} + \nabla(\mu \nabla w)$$

2.3 3-D model of channel length, channel curvature and characteristics of flow field

The full domain flow field is shown in fig. 3., it describe a detailed three-dimensional model of transport phenomena within the gas channel. The dimensions of the computational domains have 6 elements in the x-direction, 71 elements in the y-direction, 6 elements in the z-direction, for a total of about 2,556 elements.

Channel length and channel curvature of flow field is developed from the result of multi-serpentine flow fields. The channel curvature has 4 cases which shown in fig. 4. and channel length has 6 cases studied. The channel length has varied 1 to 6 channels on multi serpentine flow field. Number of channel has independent of channel length, which increases number of channel get channel length is shorter. Characteristics of depth channel are change 0.8, 1 and 1.2 mm.
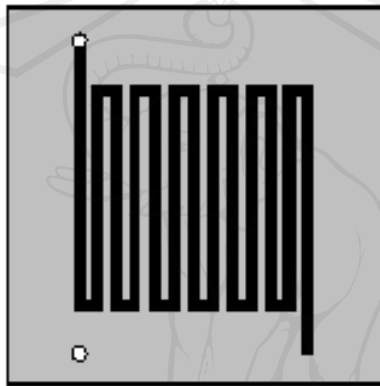
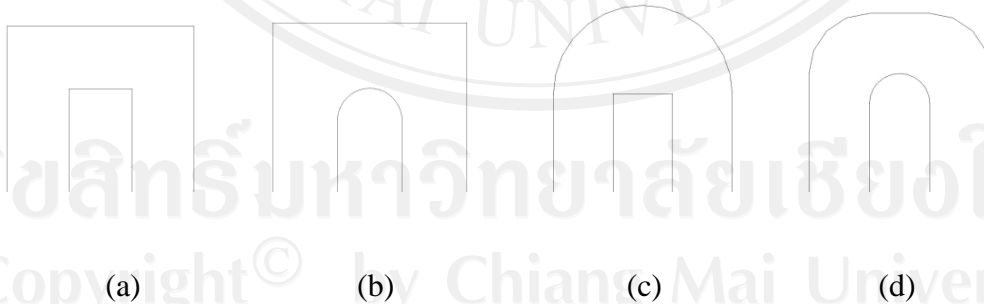Fig.3. One Channel of Serpentine Flow Field

(a)   (b)   (c)   (d)

Fig.4. Channel curvatures (a) sharp curve (b) Radius in Curve (c) Radius out Curve (d) Smooth Curve

2.4 Experimental details

An experimental system is setup to measure the current/ voltage polarization curves. Graphite plate is used as a current collector. Other materials used in the single cell are O-BASF 12E-W MEA, reaction area 100 cm^2 and brass current collector. The dimensions of components and operating conditions are consistent with the numerical model.
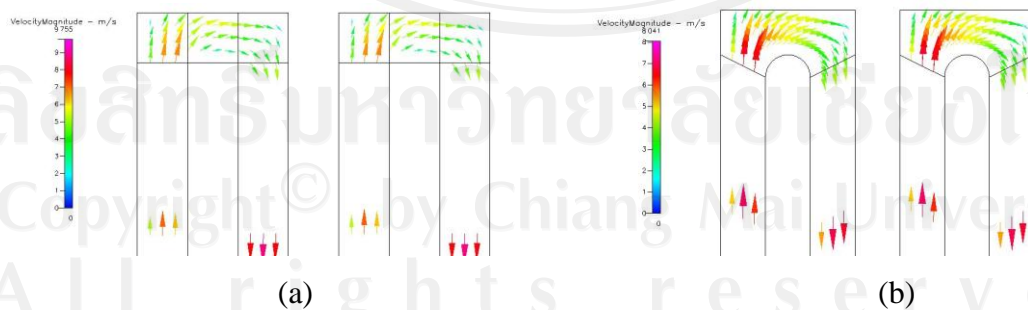
3. Result and discussion

3.1 The effect of channel curvature on flow field

The results of flow and pressure drop are effect of curvature are shown in figs. 5-8.

Fig.5. Velocity of flow field at 300 cm3/min of Sharp Curve

(a)   (b)
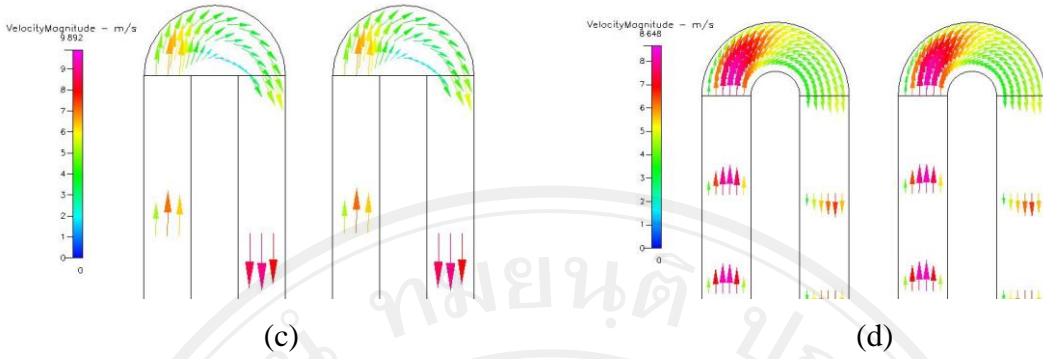
(c) (d)

Fig. 6. Characteristic of flow at 300 cm^3/min
(a) sharp curve (b) Radius in Curve (c) Radius out Curve (d) Smooth Curve

Fig.7. Pressure in different curve
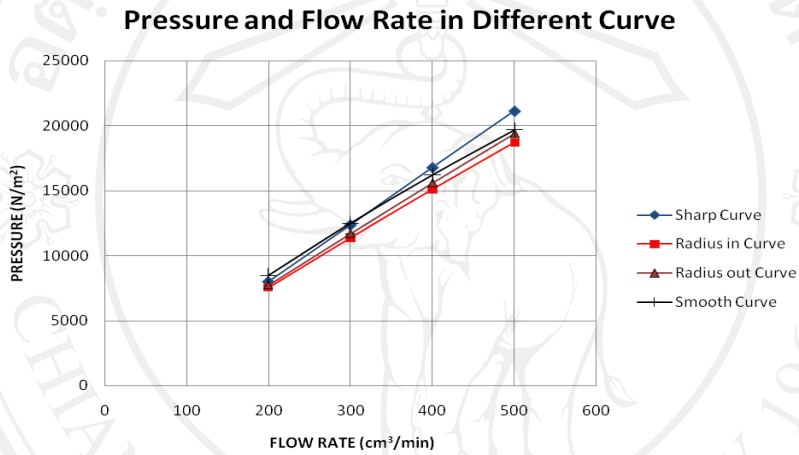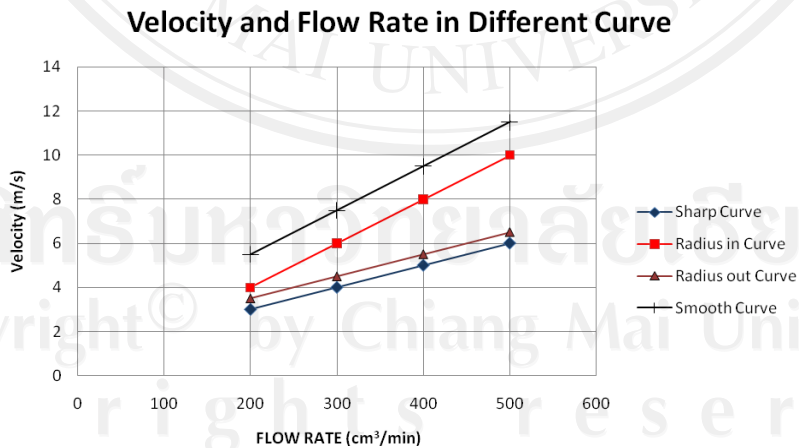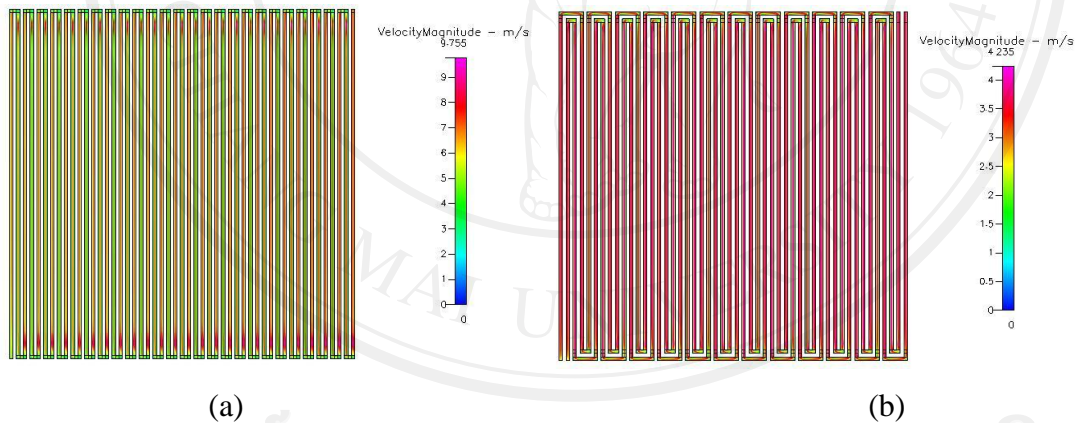
Fig.8. Velocity in different curve

Figure 6(a) and 6(b) are display non-uniform velocity distribution on sharp curve and radius in curve. High gas distribution appears at upper curve and low gas distribution at bottom curve, its have avoid area at bottom center. Figure 6(c) shows uniform velocity distribution on outer filter. High gas distribution and smooth flow appears at upper curve and low gas distribution still occurs at bottom curve, its have avoid area at center bottom curve. Figure 6(d) provides uniform velocity distribution and gas distributes overall through the turn. The result of different curve that the sharp curve is also confirm the best configuration because it has non-uniform flow distribution and high pressure drop for the high electro chemical reaction in MEAs and water management. The pressure drop and velocity in different curve at all flow rates are shown in figs. 7. and 8. The sharp curve is highest pressure drop but it has lowest velocity and smooth curve is high velocity.

3.2 The effect of channel length on flow field

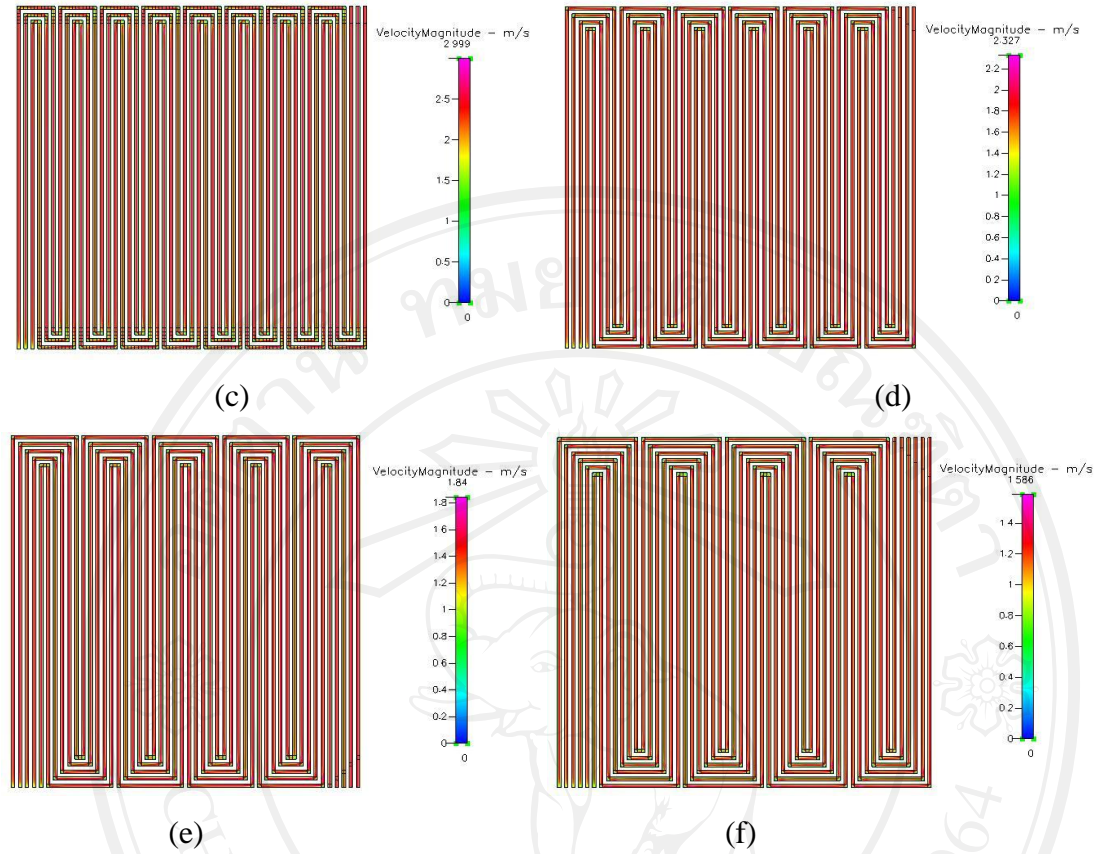The results of flow and pressure drop are effect of length show in figs. 9.-11.

(a)   (b)

Fig. 9. Velocity of flow field at 300 cm³/min
(a) 1 channel (b) 2 channels (c) 3 channels (d) 4 channels (e) 5 channels (f) 6 channels

Fig.10. Pressure in different length

Velocity and Flow Rate in Different Length
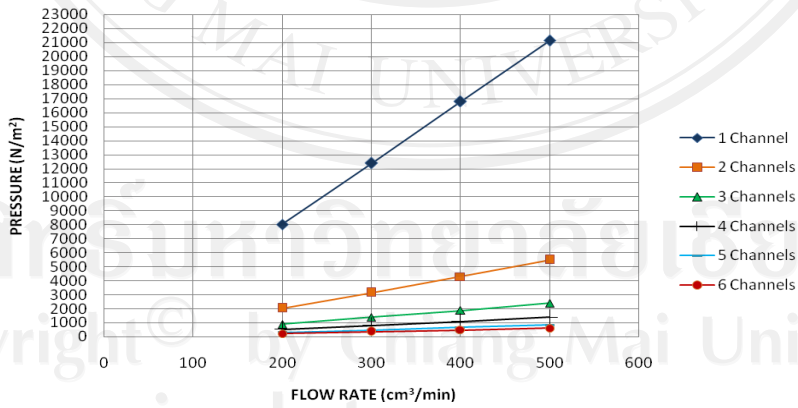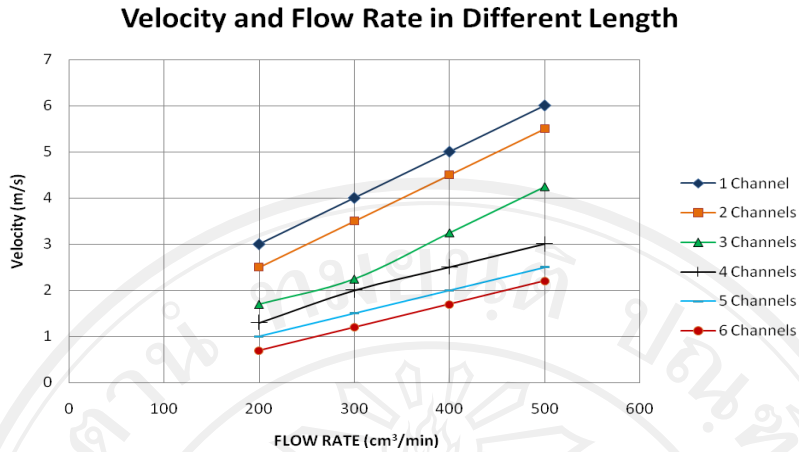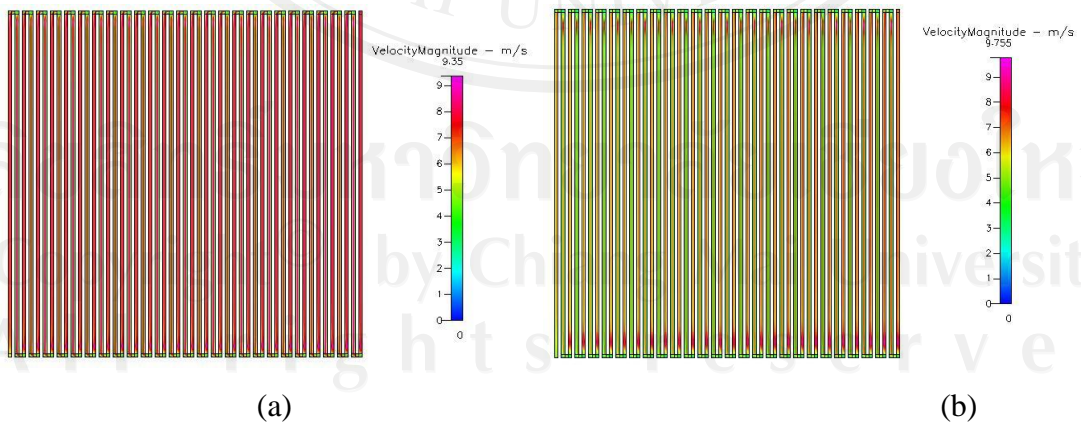

Fig.11. Velocity in different length

The velocities and pressure drop distribution in 1, 2, 3, 4, 5 and 6 serpentine channels at 300 cm^3/min. Figure 9 is shown 1 channel has average velocity approximate 4 m/s and pressure drop is 12,380 N/m^2. Gas distribution has uniform in serpentine pattern. Lower velocities distribution appears at channel curvatures and high velocities distribution at downstream of channel. The pressure drop has decreases along length channel. In 2 , 3, 4, 5 and 6 channels have a velocity approximate 3.5, 2.25, 2, 1.5 and 1.2 m/s, and pressure drop is 3,138, 1,385, 798.5, 489.4 and 359.5 N/m^2, respectively. The pressure drop and velocity in different length channels at all flow rates are shown in figs. 10. and 11. The 1 channel has highest pressure drop and velocity and 4, 5 and 6 channels have nearest pressure drop.

3.3 The effect of channel depth on flow field

(a)   (b)
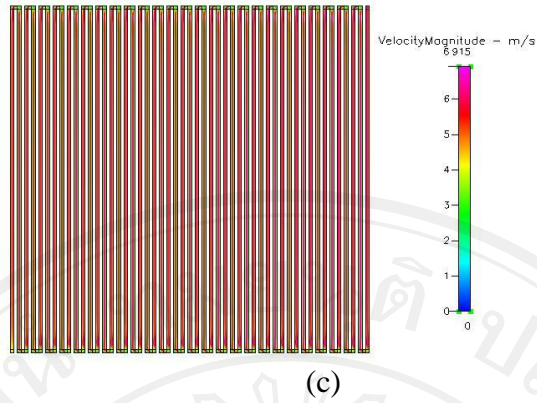
(c)

Fig.12. Velocity of flow field at 300 cm3/min (a) 0.8 mm. (b) 1.0 mm. (c) 1.2 mm.
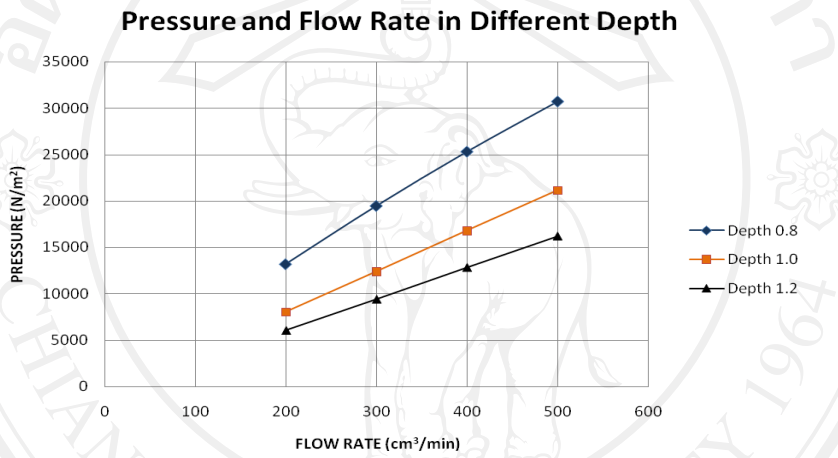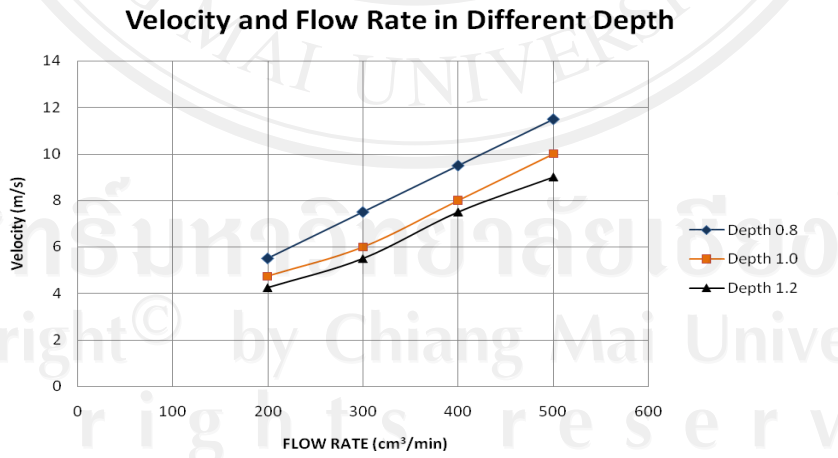

Fig.13. Pressure in different depth

Fig.14. Velocity in different depth

Figure 12 displays velocity of 3 depths channel at 300 cm^3/min. In 0.8 depth channel has velocity approximate 7.5 m/s and pressure drop is 19,470 N/m^2. In 1.0 and 1.2 depth channel have velocities approximate 6 and 5.5 m/s and pressure drop is 12,380 and 9,410 N/m^2, respectively. The pressure drop and velocity in different depth channels at all flow rates are show in figs. 13. and 14.
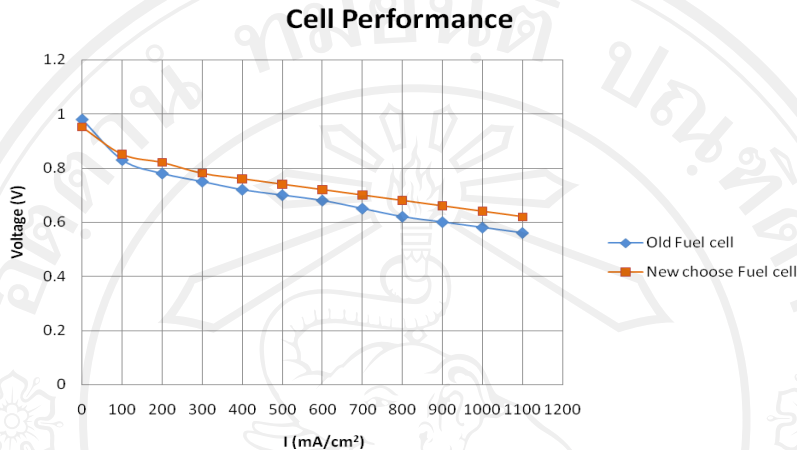

Fig.15. Comparisons between the old fuel cell and the new choose fuel cell

The performance of fuel cell predict from I-V curve. In fig. 15. show the experiment test between old fuel test and new choose fuel cell, the old fuel cell is 4 channels, smooth curve and depth 1 mm.. The new choose is 6 channels, sharp curve and depth 1 mm.. The new fuel cell has better performance than old fuel cell about 25%.

4. Conclusion

A 3-D numerical modeling to predict velocities distribution and pressure drop is presented in this research. The influence of channel length, channel curvature and channel depth is investigated. The best channel curvature from gas distribution is sharp curve and 6 channels serpentine because it has secondary flow and higher area of gas flow, high velocity and pressure drop when compare with channel length. From that result, the fuel cell with our flow field provides better performance. At the outlet, there is the distribution of gas regularly which releases the water from fuel cell. From the experiment results on 4 channels smooth curve and 6 channels sharp curve, there are found that the fuel cell has the density of electric power about 900 and 1,200 mA/cm^2 at 0.6 V, respectively. Flow field has 6 channel is 25% better than 4 channels. The study still continued in order to improve the fundamental knowledge on other geometric parameters. This information will be implied as a guideline for design an appropriate flow field for PEMFC.

Acknowledgements

We would like to extend our sincere thanks to Thailand Graduate Institute of Science and Technology (TGIST) and the authors gratefully acknowledge the contribution of Dr. Nirut Naksuk.
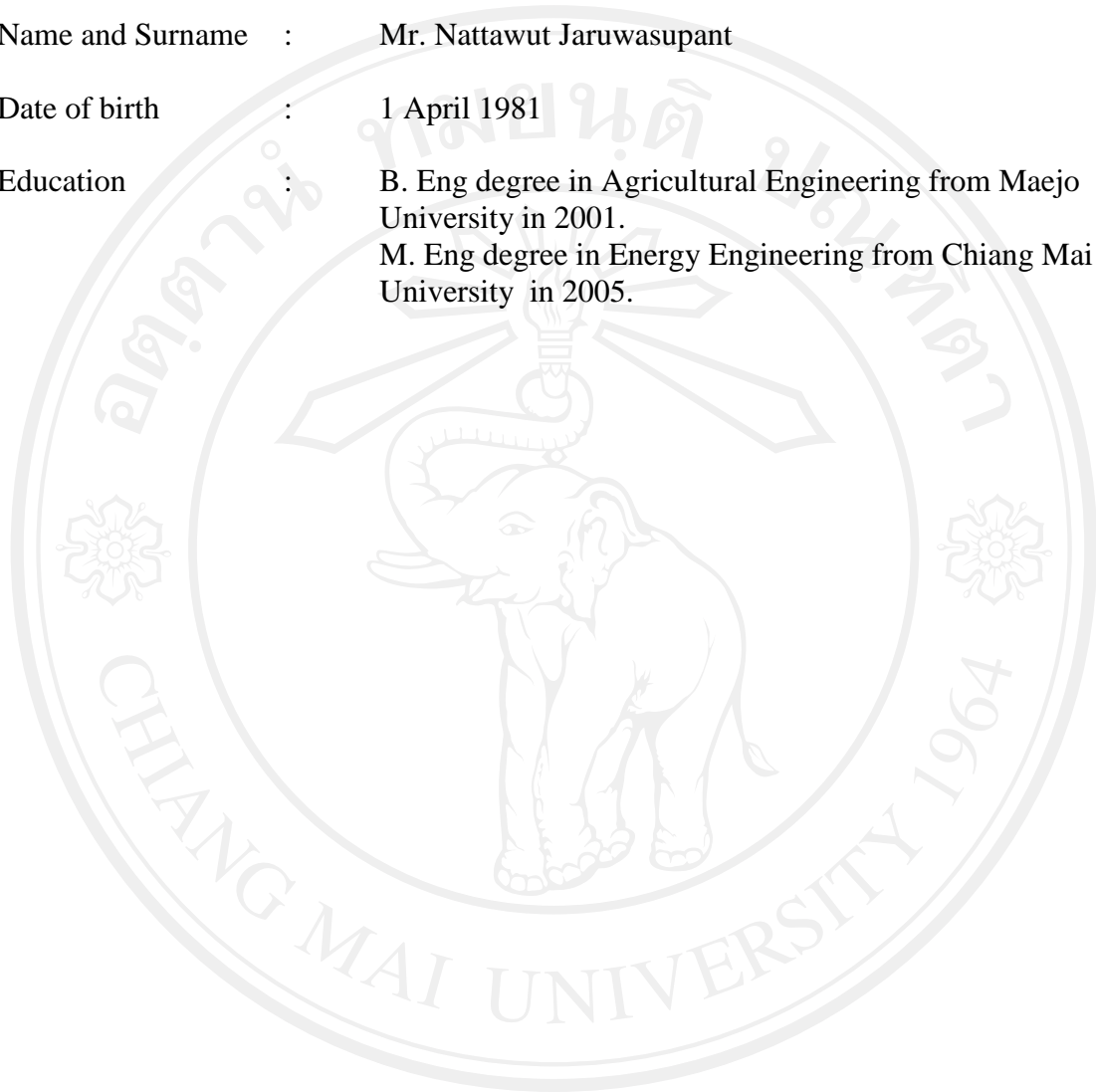
References

[1] Colleen Spiegel. PEM Fuel Cell Modeling and simulation Using MATLAB. Elsevier Academic Press ; 2008.

[2] Fang-Bor Weng, Ay Su, Guo-Bin Jung, Yen-Chiao Chiu and Shih-Hung Chan. 2005. Numerical prediction of concentration and current distributions in PEMFC, Journal of Power Sources, 145 : 546–554.

[3] Frano Barbir. PEM FuelCell : Theory and Practice. Elsevier Academic Press ; 2005.

[4] Jaruwasupant, N. and Khunatorn, Y. 2004. Numerical Modeling of Gas Flow in Proton Exchange Membrane Fuel Cell, paper presented in the the first symposium on engineering and architecture for sustainable development in the greater Mekong sub-region, 13-14 January. Lao.

[5] Jaruwasupant, N., Khunatorn, Y., Vorayos, N. and Wongsuwan, V. 2005. Study of Gas Flow and Pressure Distribution in Proton Exchange Membrane Fuel Cell : Numerical Modeling, paper presented in the Mechanical Engineering Network of Thailand the 19th Conference, pp. 158, 19-21 October. Thailand.

[6] Mennola, T. 2000. Design and Experimental Characterization of Polymer Electrolyte Membrane Fuel Cells, Licentiate's thesis, Department of Engineering Physics and Mathematics, Helsinki University of Technology, Finland.

[7] Sukkee, U and Wang,C.V. 2000. Three Dimensional Analysis of Transport and Reaction in Proton Exchange Membrane Fuel Cells, Department of Mechanical and Nuclear Engineering, Pennsylvania State University, USA.

[8] Kordesch,K. and Simader,G. (1996), Fuel Cell and their applications., Weinheim, Federal Replubic of Germany.

[9] Su, A., Chiu, Y.C. and Weng, F.B. (2005), The impact of flow field pattern on concentration and performance in PEMFC., Department of Mechanical Engineering, Yuan Ze University, Chung-Li, Taiwan, 29, pp. 409-425.

CURRICULUM VITAE

Name and Surname : Mr. Nattawut Jaruwasupant

Date of birth : 1 April 1981

Education : B. Eng degree in Agricultural Engineering from Maejo
University in 2001.
M. Eng degree in Energy Engineering from Chiang Mai
University in 2005.